THESIS SUBMITTED FOR DOCTOR OF PHILOSOPHY (PhD)

The Role of Matrix Metalloproteinases in Leukocyte Migration and Collagen Degradation in Tuberculosis

Tarangini Sathyamoorthy

Imperial College London, Department of Infectious Diseases and Immunity
2013

DECLARATION OF AUNTHENTICITY:
I hereby declare that the work presented in this thesis is my own

ABSTRACT

Tuberculosis (TB) causes disease worldwide and multi-drug resistance is rising. Matrix metalloproteinases (MMPs) cause immunopathological lung matrix destruction, which results in transmission, morbidity and mortality. Collagen is the primary structural fibril of the lung and I primarily studied two collagenases: secreted MMP-8, and membrane bound MMP-14, and also the stromelysin MMP-10, which activates not only MMP-8 but another collagenase MMP-1.

Human monocyte and macrophages were stimulated with *Mtb* H37Rv, BCG, ESAT-6 peptides or Conditioned Media from *Mtb* infected monocytes (CoMTb). MMP concentrations were measured by Luminex bead array and ELISA. Gene expression was quantified by RT-PCR. Immunohistochemistry was performed on biopsies. Flow cytometry quantified MMP-14 expression. Fluorescent microscopy detected MMP-14 and monocyte driven fluorescent collagen degradation. Monocyte migration was measured by the agarose spot assay.

MMP-8 was increased in the plasma in TB compared to both respiratory symptomatics and controls (both $p<0.001$). MMP-10 was increased in the respiratory secretions of patients with TB compared to controls ($p<0.05$). *Mtb* drove up to a 31.5 fold increase in MMP-10 secretion from macrophages (both $p<0.001$). *Mtb* caused 3.5 fold more MMP-10 secretion from macrophages than BCG ($p<0.001$) and a specific peptide from ESAT-6 drove MMP-10 secretion from macrophages. In induced sputum, MMP-14 mRNA was increased 3.3-fold in TB compared to controls and positively correlated with infiltration on chest radiograph (both $p<0.05$).

Macrophages of TB granulomas in biopsies stained strongly positive for MMP-14. *Mtb* increased monocyte MMP-14 surface expression 31.7-fold ($p<0.05$) and CoMTb 17.5-fold ($p<0.01$). *Mtb* infected monocytes degraded collagen, with co-localised MMP-14 surface expression. Monocytes migrated to the edge of CoMTb impregnated agarose drops, expressing MMP-14 on migration. Inhibition of MMP-14 activity with a neutralising antibody, decreased *Mtb* driven collagen degradation by 73% ($p< 0.001$) and CoMTb driven monocyte migration by 44% ($p<0.001$).

These data shows that, MMP-1, -8, -10 and -14 cause immunopathology and regulate leukocyte migration in TB.

CONTENTS

ABSTRACT 2
CONTENTS 4
LIST OF TABLES 8
LIST OF FIGURES 9
ACKNOWLEDGMENTS 11
1. INTRODUCTION 12
1.1 The Global Tuberculosis Epidemic 12
1.2 The Pathogen 13
1.3 The Host Immune Response 14
1.3.1 Innate immune response 14
1.3.2 Adaptive immune response 14
1.3.3 Progression to latent or active tuberculosis 15
1.4 The Clinical Disease 17
1.4.1 Presentation 17
1.4.2 Diagnosis 17
1.4.3 Antimicrobial therapy and drug resistance 18
1.5 The Negative Sequelae of Lung Damage 20
1.5.1 Transmission 20
1.5.2 Morbidity and mortality 21
1.5.3 Treatment failure and drug resistance 22
1.6 Tissue Destruction in Tuberculosis 24
1.7 Matrix Metalloproteinases 26
1.8 Matrix Metalloproteinases and Emphysema 32
1.8.1 Matrix metalloproteinase 1 33
1.8.2 Matrix metalloproteinase 9 34
1.8.3 Matrix metalloproteinase 12 34
1.9 Matrix Metalloproteinases and Tuberculosis 35
1.9.1 Pulmonary tuberculosis 35
1.9.2 Central nervous system tuberculosis 39
1.9.3 Granuloma formation 40
1.10 Regulation of Matrix Metalloproteinase Expression 41
1.10.1 Cytokines and chemokines 42
1.10.2 Pathogen related factors 44
1.10.3 Mitogen-activated protein kinase signalling 45
1.10.4 NF-κB, AP-1 and STAT-3 transcription factors 46

1.11 Matrix Metalloproteinase 14 50
1.11.1 Cell migration in granuloma formation and mycobacterial dissemination 50
1.11.2 Matrix metalloproteinase 14 and cell migration 52
1.12 Matrix metalloproteinase 10 56
1.13 Matrix metalloproteinase 8 58
1.13 Hypothesis 60
1.14 Objectives and aims 60
2. METHODS 61
2.1 Mtb and BCG culture 61
2.2 Cell culture 61
2.2.1 Monocyte purification 61
2.2.2 Maturation of monocytes to macrophages 62
2.2. 3 Normal human bronchial epithelial cell culture 63
2.2.4 Cell infection protocol 63
2.2.5 Preparation of conditioned medium from *Mtb* infected monocytes 63
2.2.6 Chemical inhibitors 64
2.2.7 ESAT-6 peptides 64
2.2.8 Harvesting of cell culture supernatants 65
2.3 Enzyme-linked Immunosorbent Assay 68
2.4 Luminex Bead Array 69
2.5 Confocal Microscopy 70
2.6 Flow Cytometry 71
2.7 Western Blotting 72
2.7.1 Total MMP-14 73
2.7.2 Phosphorylated and total p38/ERK /JNK 73
2.7.3 Total MMP-10 74
2.8 Real Time Polymerase Chain Reaction 74
2.8.1 RNA extraction 74
2.8.2 cDNA synthesis 75
2.8.3 Polymerase chain reaction 75
2.9 Fluorescent Collagen Degradation Assay 77
2.10 Agarose Spot Assay for Chemotaxis 78
2.11 Clinical Samples: Collection and Processing 79
2.11.1 Plasma 79
2.11.2 Induced sputum – supernatant and RNA extraction 80
2.11.3 Bronchoalveolar lavage 83
2.11.4 Lung Immunohistochemistry 83
2.12 Statistical analysis 84

3. ANALYSIS OF CIRCULATING MMPS INDICATES A DOMINANT ROLE FOR COLLAGENASES 85
3.1 Introduction 85
3.2 Results 86
3.2.1 Baseline patient characteristics 86
3.2.2 Plasma MMP-1 and MMP-8 are elevated in active pulmonary TB and MMP-8 is relatively TB-specific 88
3.2.3 Plasma collagenases are higher in males than females and elevated levels are present in active TB in males and females analysed separately 91
3.2.4 Principal component analysis demonstrates a distinction between TB and control patients but not between TB and respiratory symptomatics 95
3.2.5 Plasma MMP-8 may help differentiate patients with active pulmonary TB from symptomatic controls 97
3.2.6 Plasma MMP-8 negatively correlates with BMI in TB 99
3.3 Discussion 100
4. MMP-10 IS UPREGULATED BY THE *Mtb* VIRULENCE FACTOR ESAT-6 108
4.1 Introduction 108
4.2 Results 109
4.2.1 *Mtb* infection drives MMP-10 secretion from human MDMs 109
4.2.2 *Mtb* upregulates MMP-10 secretion from pulmonary epithelial cells via monocyte-dependent networks 110
4.2.3 MMP-10 is increased in the respiratory secretions of patients with pulmonary TB 113
4.2.4 MMP-10 secretion from *Mtb* infected MDMs is MAPK dependent but NF-κB independent 116
4.2.5 MMP-10 expression in MDMs is driven by *Mtb* but not by mycobacterial LAM or vaccine BCG 121
4.2.6 *Mtb* driven MMP-10 Secretion is dependent on a specific 15 Amino Acid Peptide Sequence in ESAT-6 124
4.3 Discussion 127
5. CELL SURFACE MMP-14 DRIVES COLLAGEN DEGRADATION AND LEUKOCYTE MIGRATION 135
5.1 Introduction 135
5.2 Results 136
5.2.1 MMP-14 is increased in the sputum of TB patients and correlates with lung infiltration 136
5.2.2 *Mtb* infection of primary human monocytes drives MMP-14 expression 140
5.2.3 MMP-14 causes pericellular collagen degradation in *Mtb* infected monocytes 143
5.2.4 MMP-14 is expressed in granulomas of patients with TB and is upregulated by *Mtb* induced intercellular networks 146
5.2.5 MMP-14 expression driven by *Mtb* induced intercellular networks is regulated by p38 and JNK but not ERK MAPK signalling 150
5.2.6 The components of *Mtb* induced intercellular networks 154
5.2.7 Signalling through Gi protein coupled pathways regulates monocyte MMP-14 expression driven by *Mtb* induced intercellular networks 158
5.2.8 Monocyte migration is driven by *Mtb* induced intercellular networks and regulated by MMP-14 160
5.3 Discussion 163
6. DISCUSSION 172
6.1 A model of synergistic MMP activity causing immunopathology in Mtb infection 172
6.2 MMPs and point of care TB diagnostics 175
6.3 Targeting TB immunopathology by MMP inhibition 176

6.4 Future work 177
6.4.1 Clinical samples 178
6.4.2 Cellular model 179
7. REFERENCES 182
8. FUNDING 197
9. ABBREVIATIONS 198

LIST OF TABLES

Table 1: MMP subdivisions by substrate specificity 30
Table 2: Chemical inhibitors used in tissue culture 66
Table 3: ESAT-6 peptide amino acid sequences 67
Table 4: ESAT-6 peptide pools matrix 68
Table 5: Plasma matrix metalloproteinase analysis - Characteristics of patient cohort 87
Table 6: Plasma MMP levels by patient group 89
Table 7: Plasma MMP levels for males and females separately by patient groups 92
Table 8: Induced sputum matrix metalloproteinase analysis - Characteristics of patient cohort 138
Table 9: Cytokines, chemokines and growth factors in 156
CoMCont and CoMTb 156
Table 10: Anopore *vs*. Millipore filtration of CoMCont and CoMTb 157

LIST OF FIGURES

Figure 1: MAPK signalling pathway 48
Figure 2: NF-κB signalling pathway 49
Figure 3: Chest Radiograph Scoring 82
Figure 4: Neutrophil collagenase MMP- 8 is specifically upregulated in the plasma in active pulmonary TB 90
Figure 5: Plasma MMP -1, -3, -8 and -9 are higher in males than females 93
Figure 6: Plasma MMP-1 and MMP-8 remain elevated in TB when analysed by gender 94
Figure 7: PCA demonstrates good discrimination between controls and TB, but not TB and respiratory symptomatics 96
Figure 8: Plasma MMP-8 discriminates TB from symptomatic controls with moderate accuracy 98
Figure 9: Plasma MMP-8 negatively correlates with BMI in TB 99
Figure 10: Direct *Mtb* infection drives MMP-10 expression in MDMs 111
Figure 11: *Mtb* induced intercellular networks drive MMP-10 secretion from human pulmonary epithelial cells 112
Figure 12: MMP-10 is elevated in the induced sputum of South African patients with active pulmonary tuberculosis (TB) 114
Figure 13: MMP-10 is elevated in the BALF of Indian patients with active pulmonary TB 115
Figure 14: MMP-10 expression is p38 and ERK MAPK dependent in *Mtb* infected MDMs 118
Figure 15:NF-κB does not regulate the transcription of MMP-10 in *Mtb* infected MDMs 120
Figure 16: Mycobacterial LAM is a poor stimulus for MMP-10 secretion from MDMs in comparison to *Mtb* 122
Figure 17: MMP-10 gene expression and secretion from MDMs is driven by *Mtb* but not vaccine BCG 123
Figure 18: A peptide pool of the entire ESAT-6 sequence drives MMP-10 secretion from MDMs 125
Figure 19: A single 15 amino acid peptide sequence from ESAT-6 drives MMP-10 secretion from MDMs 126
Figure 20: MMP-14 gene expression is increased in the sputum of patients with pulmonary TB and correlates with lung infiltration on chest radiograph 139
Figure 21: *Mycobacterium tuberculosis (Mtb)* infection of primary human monocytes drives surface MMP-14 expression 141
Figure 22: MMP-14 gene expression and total protein expression in monocytes is upregulated by direct *Mtb* infection 142
Figure 23: MMP-14 expression co-localises with collagen degradation driven by *Mtb* infected monocytes 144
Figure 25: MMP-14 is expressed in granulomas of patients with TB and is upregulated by *Mtb* induced intercellular networks 148
Figure 26: *Mtb* induced intercellular networks drive monocyte MMP-14 expression 149
Figure 27: *Mtb* induced intercellular networks drive p38, ERK and JNK MAPK phosphorylation in monocytes 152
Figure 28: Intercellular network driven monocyte MMP-14 expression is regulated by p38 and JNK but not ERK MAPK signalling 153

Figure 29: Signalling through Gi protein coupled pathways regulates monocyte MMP-14 expression driven by *Mtb* induced intercellular networks 159
Figure 30: *Mtb* induced intercellular networks induce monocyte migration and concurrent MMP-14 expression 161
Figure 31: MMP-14 regulates monocyte migration driven by *Mtb* induced intercellular networks.. 162
Figure 32: The interaction of MMP-1, -8, -10 and -14 in cell migration and extracellular matrix destruction in pulmonary TB 174

ACKNOWLEDGMENTS

I am very grateful to my supervisors Professor Jon Friedland and Dr Paul Elkington for giving great guidance and advice. Without the willingness of Professor Robert Wilkinson and Naomi Walker to accept me into the fold at the University of Cape Town the clinical arm of my MMP-14 study would not have happened. I would also like to thank Naomi, Shivani Singh and Gurj Sandhu for permitting me to analyse sputum, bronchoalveolar lavage fluid and plasma samples they had painstakingly collected and processed. Giving a detailed clinical history is time consuming and sputum induction and blood taking can be uncomfortable so a big thank you to all the study participants. Laura Stuttaford was the diligent BSc student who kick started the MMP-10 study and whose ability to learn quickly put me to shame! The list to come is very long but I feel everyone deserves a specific mention – Luisa Saraiva, Bernadette Pedersen, Catherine Ong, Rachel Moores, Lucinda Rand, Anna Ettore, Ian Teo, Rik Thomas, Basim Alshammari, Sara Brilha and Liku Tezera have all taught me laboratory techniques and/or provided technical advice which has been invaluable. Moreover, along with the bosses they have listened to me whinge with patience and a sense of humour and after nearly 4 years I consider them not only colleagues but good friends. My parents, my brother and his wife have been so supportive and caring through all my endeavours in life. But of course the final mention must be for my favourite people, Hemashri and Gauthami my adorable, cheeky nieces. My weekends would be very dull without them.....

1. INTRODUCTION

1.1 The Global Tuberculosis Epidemic

Tuberculosis (TB) is the second biggest killer among infectious diseases. The causative agent is *Mycobacterium tuberculosis (Mtb)*. In 2011 it caused 8.7 million new cases and 1.4 million deaths worldwide. This includes 310,000 cases of multidrug resistant TB (MDR-TB) and 84 countries reported extensively drug resistant TB (XDR-TB) [1]. Of great concern are the reports of "totally drug resistant TB" in Iran, India and South Africa [2-4]. In the UK there were 8693 new cases in 2011, with MDR cases rising from 0.6% in 2000 to 1.6% [5].

The majority of all TB occurs in low and middle income countries in Africa, Asia, Eastern Europe and Central/ South America [1]. In these resource challenged settings, it is difficult to implement the long treatment regimes. These stand at a recommended 6 months for drug sensitive and 18 - 24 months for drug resistant TB [6]. Treating drug resistant TB is expensive and complicated, involving drugs with serious side effects and limited efficacy [7]. Therefore there is an urgent need for new drugs which shorten treatment duration for both drug sensitive and resistant TB.

To develop new therapeutic approaches it is critical to understand underlying mechanisms of disease. Tissue destruction is characteristic of tuberculosis and is a consequence of immunopathology driven by the host response to *Mtb*. Within the

lungs pulmonary extracellular matrix (ECM) breakdown causes cavitation, which leads to morbidity, mortality and increased transmission. Research within our group and in my thesis has focussed on the roles of a group of enzymes known as matrix metalloproteinases (MMPs) in tissue destruction and immunopathology in TB.

1.2 The Pathogen

Mycobacterium tuberculosis (Mtb) was identified as the causative agent of tuberculosis in 1882 by the German scientist Robert Koch. It is a member of the *Mycobacterium tuberculosis* complex of organisms which cause human disease and bovine tuberculosis. This also includes *Mycobacterium africanum*, *Mycobacterium bovis*, *Mycobacterium microti*, and *Mycobacterium canetti*. *Mtb* is an obligate intracellular pathogen and humans are the main host. It is an aerobic bacteria that replicates more easily in the lungs apices, potentially because oxygen content is high. Therefore most cases of TB are pulmonary, although it infects and causes disease in any organ. It has a characteristic mycolic acid rich cell wall which renders it resistant to decolourisation after staining or 'acid fast'. It divides extremely slowly once every 15-20 hours which is the reason for the long duration of antimicrobial therapy required [8].

Mtb has evolved mechanisms to evade intracellular killing including preventing phagosome maturation and acidification and inhibiting apoptosis while promoting necrosis. These have been important to the success of the organism [9].

1.3 The Host Immune Response

1.3.1 Innate immune response

Mtb is inhaled and phagocytosed by alveolar macrophages, dendritic cells, neutrophils and monocytes. A range of mycobacterial antigens activate these cells to produce cytokines and chemokines which play important roles in enabling the immune system to control infection [10, 11]. Tumour necrosis factor alpha (TNFα) is a key cytokine for macrophage activation and the control of acute *Mtb* infection. *Mtb* infection is rapidly lethal with an associated high bacterial burden in TNFα deficient mice [12]. Interleukin 12 (IL-12) is vital to the subsequent adaptive immune response by driving T helper 1 (TH1) cells to produce interferon gamma (IFNϒ). IL-12 deficient mice show an increased bacterial burden and reduced survival [13]. Humans with mutations in the IL-12 gene or IL-12 receptor gene show a reduced IFNϒ response and increased susceptibility to non tuberculous mycobacterial infections [14].

1.3.2 Adaptive immune response

The onset of adaptive cell mediated immunity is delayed in humans to approximately 42 days after infection. Infected dendritic cells migrate to draining lymph nodes, and present mycobacterial antigens to naive T-cells. These differentiate into *Mtb* antigen specific TH1 cells which migrate to the site of infection in the lungs. The TH1 cells are further activated by IL-12 secreted by macrophages and produce IFNϒ. IFNϒ is a vital cytokine for activating macrophage killing mechanisms and controlling

infection [10, 11]. IFNϒ deficient mice are highly susceptible to *Mtb* infection [15] and humans with mutations in the IFNϒ or IFNϒ receptor genes develop severe mycobacterial infections [14].

It is at this stage that the classical histopathological hallmark of tuberculosis forms. The granuloma has traditionally been considered to be a feature of the adaptive immune response. It has a central core of necrotic cells, surrounded by macrophages that have transformed into epithelioid cells, multinucleate giant cells and foam cells surrounded by a rim of T cells. Many other cell types including neutrophils, B cells, natural killer cells and fibroblasts are present and adjacent lung epithelial cells also participate in the immune response [16].

1.3.3 Progression to latent or active tuberculosis

This initial infection is known as 'primary tuberculosis' and after the onset of the adaptive immune response described above many humans will control but not eliminate the mycobacterial infection. These persons have latent TB and are asymptomatic and non-infectious. It is estimated that one third of the world's population harbours latent TB. In these individuals a Ghon complex can be identified in the lungs at post mortem with a subpleural calcified/ fibrotic focus of infection (the Ghon focus) and an associated lymph node. The status of the bacteria within macrophages in the Ghon complex during latency is unclear though they remain viable [9, 11].

Reactivation of latent TB to cause active symptomatic disease (‘post primary tuberculosis’) is highest in the first 9 years after infection especially in the 16-35 year age group with a strong tuberculin skin test response [17]. The reason for reactivation is generally considered to be waning immunity though the only clearly established examples are T helper cell defects in Human Immunodeficiency Virus (HIV) positive individuals and therapeutic neutralisation of TNFα with monoclonal antibodies . In some humans the initial immune response does not achieve control and acute active tuberculosis (‘primary progressive tuberculosis’) ensues straight away. This is more common in infants [11].

In both TB due to reactivation or acute active disease the innate and adaptive immune responses will continue responding to the multiplying *Mtb*, and play an important role in causing the clinical presentation of disease [10, 11].

A final necessary step for any microbe is to infect a new host. In active TB the *Mtb* bacilli achieve airborne transmission in respiratory droplets generated by coughing, which are then inhaled by the new host [11]. Cavity formation within the lungs greatly increases infectivity [18].

1.4 The Clinical Disease

1.4.1 Presentation

The symptoms are those due to the systemic inflammatory response including fever, night sweats and weight loss and those due to localised inflammation in the lung including productive cough, haemoptysis, dyspnoea and chest pain [8].

1.4.2 Diagnosis

Microscopy for acid-fast bacilli (AFB) in a sputum smear is the most widely used diagnostic method but sensitivity varies from 34–80% [19]. It is not specific as it does not distinguish *Mtb* from non-tuberculous mycobacteria. Sputum culture is much more sensitive and the current WHO recommendations are a liquid culture system which provides results within 4 to 13 days, including susceptibility testing to first line drugs. [20]. The *Mtb* gene amplification test (GeneXpert MTB/RIF) diagnoses pulmonary TB using sputum samples with a turnaround time of just 2 hours. It simultaneously gives a result for rifampicin resistance which is a surrogate marker for multidrug resistance [20, 21]. Much effort has been invested in identifying biomarkers that would be amenable to a simple dipstick test, providing an immediate result. Improving TB diagnostics remains a significant challenge and is a goal of the WHO STOP TB Strategy [22].

Though not diagnostic in themselves, radiographic findings are often highly characteristic, with disease preponderance at the lung apices or the apical segments

of the lower lobes. One series showed upper lobe infiltration in 86% and cavitation in 55% of cases of newly diagnosed TB on chest radiograph [23].

1.4.3 Antimicrobial therapy and drug resistance

Standard treatment for drug sensitive pulmonary tuberculosis is a 6 month regime consisting of 2 months of rifampicin, isoniazid, pyrazinamide and ethambutol followed by 4 months of rifampicin and isoniazid [6]. MDR-TB is defined as resistance to at least rifampicin and isoniazid, XDR-TB as resistance to rifampicin and isoniazid, any fluoroquinolone and one of the three injectable drugs, capreomycin, kanamycin and amikacin [1].

The reasons for the emergence of drug resistance are multi-factorial. The duration of the treatment regime, even for drug sensitive disease, is prolonged at 6 months. In resource poor countries, where TB is endemic, health policies, regulation and enforcement can be weak. This results in antituberculous drugs being obtained without prescription, incorrect prescribing and poor adherence to treatment. The HIV epidemic may have contributed to the development of drug resistance by problematic drug interactions, reduced adherence due to a large number of medications and malabsorption. It has also resulted in an increased pool of individuals who are likely to progress to active TB after the initial infection rather than achieve control [7]. The consequences of drug resistance in resource poor settings with a high prevalence of HIV infection are catastrophic. In a rural area of South Africa sputum culture and drug sensitivity testing showed XDR-TB in 53 of

15patients. All of these patients were HIV positive and 52 of 53 died with a median duration of 16 days, well before they had even been diagnosed as having drug resistant disease [24].

The recommended treatment for MDR-TB is pyrazinamide with four second line drugs including a fluoroquinolone, an injectable agent, ethionamide or prothionamide and either cycloserine or para-aminosalicylic acid. Twenty months of therapy is advised. The treatment of XDR-TB is even more complex with individual tailoring. These drugs have unpleasant and serious side effects which make tolerance a problem [6].

Identifying effective regimens of a shorter duration using existing drugs, and also producing agents with new mechanisms of action is therefore a priority. The REMox and OFLOTUB III trials compare the standard 6 month regimen to a 4 month regimen with moxifloxacin or gatifloxacin added. Bedaquiline (TMC207) is a mycobacterial ATP synthase inhibitor and Delamanid (OPC-67683) a nitroimidazole which inhibits mycolic acid synthesis. Both have been shown to improve sputum culture conversion at 8 weeks and are being considered for multidrug resistant disease [25].

1.5 The Negative Sequelae of Lung Damage

As this research pertains to tissue destruction in TB, it is important to discuss the background evidence which shows that pulmonary cavitation is deleterious.

1.5.1 Transmission

Analysis of a large cohort of smear positive TB cases and their contacts showed that intravenous drug use, cavitatory disease on chest radiograph and a young age were significantly associated with generating secondary active TB cases including microepidemics (≥ 2 cases of active TB caused by the same index case) and potentially many more cases of latent TB [26]. In one particularly well investigated outbreak an index case with cavitatory pulmonary TB had 97 regular contacts at a public house he frequented. Using chest radiographs, tuberculin skin testing and DNA fingerprinting on isolates it was shown that in 6 months he had apparently infected 42% of these contacts with 14 cases of active TB (11 of the culture isolates underwent DNA fingerprinting and all had same chromosomal DNA restriction pattern as the index case) and 27 cases of latent TB [18].

A key factor leading to the high infectivity of cavitatory TB is the high bacterial burden within a space which communicates directly with a bronchus [27]. A study measured pre-treatment sputum time to positivity (TTP) in pulmonary TB patients with a range of disease patterns. The BacT/ALERT 3D Mycobacteria detection liquid culture system was used, which is a semi quantitative measure of bacterial load with an inverse relationship between TTP and colony forming units. The presence of

cavitation on chest radiograph was associated with a significantly shorter TTP of 6.6 days median, compared to 15.4 days if cavities were not present. In a subgroup analysis using CT chest, those who had 4-6 cavities had a significantly shorter TTP of 5.15 days median compared to 14 days in those with 1-3 cavities [28].

A potential reason for this high bacterial burden was demonstrated by immunohistochemical analysis of resected lung in patients with treatment refractory TB. Cross sections showed numerous mononuclear cells at the luminal surface of cavities with large numbers of intracellular bacilli present when compared to enclosed granuloma. These mononuclear cells stained CD68 positive indicating that they were macrophages. CD3, CD4, and CD8 T cells were scarce at the luminal surface of cavities in comparison to enclosed granuloma where T cells and macrophages co-localised. The absence of T cell-macrophage interaction at the luminal surface of the cavity surface may result in impaired mycobacterial killing by macrophages [29].

1.5.2 Morbidity and mortality

The presence of extensive tissue destruction and cavitatory disease causes increased morbidity both during active infection and after resolution. In a group who underwent surgical treatment for tuberculosis related haemoptysis, cavitation on chest radiograph was present in 100% of massive haemoptysis cases and 92% of major haemoptysis cases, compared to only 21% of minor haemoptysis cases [30]. In an endemic area without surgical treatment or percutaneous embolisation, massive haemoptysis is difficult to control and can have a mortality rate approaching

50% [31]. The haemoptysis occurs because of a Rasmussen's aneurysm which is a bronchial artery aneurysm which forms within or next to the cavity [32].

Analysis of a large cohort of patients with lung tissue destruction secondary to previous TB showed an average forced expiratory volume 49% predicted and forced vital capacity 61% predicted with an obstructive pattern in 76.8%. These findings are probably a consequence of fibrosis causing airways stenosis and poor compliance with distal airway collapse. Treatment with inhaled bronchodilators and corticosteroids lead to only small improvements in spirometry. Patients experienced acute exacerbations of their obstructive airways disease requiring emergency department attendance [33].

Unsurprisingly cavitatory disease is also a risk factor for mortality. An analysis of predictors of poor outcome in HIV negative patients treated for XDR-TB was performed where poor outcome included death in its definition. Cavitatory disease was an independent risk factor poor outcome. In the poor outcome group 79% had cavitatory disease on chest radiograph compared to 54% in the favourable outcome group [34].

1.5.3 Treatment failure and drug resistance

Cavitatory disease is associated with slower response to treatment and an increased risk of treatment failure and relapse. A study of patients with pulmonary TB receiving directly observed therapy used weekly smear and a liquid mycobacterial sputum culture to enable accurate assessment of time to negativity. In patients with

cavitatory disease on chest radiograph the time to smear negativity was 48 days median, compared to 20 days in those without cavitatory disease. Culture time to negativity was 49 days median compared to 12. The use of culture was important as smear positivity may be caused by dead bacilli [35]. In a large cohort of HIV negative patients being treated for fully sensitive *Mtb*, treatment failure or relapse occurred in 9.5% of those with cavitatory disease on chest radiograph compared to 3.6% of those without cavitatory disease [36]. These findings may be due to the high bacterial burden present in cavitatory disease [28] and subtherapeutic drug penetration into the damaged and fibrotic tissue of the cavity wall [27].

There is interesting evidence from studies using resected tuberculous cavities that cavitatory disease promotes the emergence of drug resistance mutations. Resistance occurs because of spontaneous chromosomal mutations at a rate of 10^{-6} to 10^{-8} mycobacterial replications, therefore the high the mycobacterial load seen within cavities, has greater potential to drive resistance [37]. Again subtherapeutic drug penetration into the damaged and fibrotic tissue of the cavity wall may play a role [27]. In paired sputum and resected cavity tissue cultures in patients who underwent adjunctive surgical resection for MDR/XDR TB, additional drug resistance was found in the cavity in 37% of cases [38]. In an analysis of resected lung in patients with treatment refractory TB, sequence analyses revealed heterogeneity in the drug resistance patterns among *Mtb* isolates from different lung lesions in the same case. The additional mutations were seen in *Mtb* cultured from cavity surfaces where bacilli were numerous [29].

1.6 Tissue Destruction in Tuberculosis

The French physician Rene´ Theophile Hyacinthe Laennec performed a series of autopsies on patients who had died of TB in the early 19th century and carefully described their pulmonary lesions including cavities [39] .

"*Whatever the form in which the tuberculous matter develops, it begins as a grey, semi-transparent matter that little by little becomes yellow, opaque, and dense. Then it softens, and slowly acquires a liquidity like pus, and, when it is expelled through the airways, it leaves cavities, commonly called ulcers of the lung, that we will designate as tuberculous excavations*." [39]

Two centuries later, the exact mechanisms causing these cavities remain unclear, and are the subject of ongoing research and debate. One reason for this has been the lack of a suitable animal model of cavitatory pulmonary tuberculosis. Mice develop chronic fibrosis but do not develop caseous necrosis or cavitate. Guinea pigs and monkeys do develop caseous necrosis but this only variably leads to cavitation. Rabbits pre-sensitised with subcutaneous injections of heat killed *M. bovis* who then have *M.bovis* directly injected into the lungs reliably form cavities, but the same response is not seen with *Mtb* [40, 41].

It is clear that an immunopathological host response is at least partly responsible for cavitation. Patients with HIV have reduced numbers of T helper lymphocytes and a study showed that 32% of HIV positive patients had 1 or more zone with cavitation compared to 81% of HIV negative patients. The mean number of zones containing cavities was higher in HIV negative patients at 1.7 compared to 0.5 [42]. Reduced immune function is associated with aging and a meta-analysis of 12 studies that compared pulmonary TB in older subjects and younger subjects showed that radiological cavitation and haemoptysis were more frequent in patients under 60 [43]. Studies in the 1960s showed that the *M. bovis* induced cavity formation in rabbits was attenuated by immunosuppressive agents such as azathioprine [44].

Because the caseating granuloma is a pathognomonic feature of *Mtb* infection theories have centred on this. The dogma suggests that immune cells, cytokines and lipids driving necrosis in TB, with cavities forming when caseating granuloma enlarge, undergo liquefaction and erode into bronchi [45]. However histopathological analysis of more than 100 cases of tissue sections from patients with untreated pulmonary TB from the pre-antibiotic era challenges this paradigm. Caseating granuloma were found in primary TB as the Ghon complex with calcified granulomas in the lung and hilar lymph nodes. However the histopathological features of post primary TB were very different. The upper lobes were predominantly involved. There was initially a lipoid pneumonia phase with accumulation of foamy alveolar macrophages which degenerated to leave lipoid debris. This then proceeded to a caseous pneumonia phase with necrosis and swelling of the tissue involving the alveolar septa, vessels and bronchi. These areas then softened and fragmented and were coughed up to leave cavities. No caseating granuloma were observed in the lungs of any of the

cases, nor was there any evidence that cavities form by erosion of caseating granuloma into bronchi [27].

1.7 Matrix Metalloproteinases

When considering the histopathological findings in pulmonary TB, discussed in the previous section, the composition of lung tissue must be borne in mind. The lung has ECM components which support the alveoli, conducting airways and vascular tree. The most abundant macromolecules in the pulmonary ECM are Type I, II and III collagen and these are the primary structural fibrils of the lung. They have a fibrillar triple helical structure which provides the tensile strength of the lung. Second is elastin which is rubbery in nature and has a randomly oriented polymerised structure. It allows the lung to recoil after inspiration. Fibronectin and laminin are glycoproteins which are crucial in mediating the interactions between the alveolar epithelial cells, vascular endothelial cells, fibrillar collagens and elastin. They not only act as ligands for cell surface receptors, but also carry binding sites for the other ECM components. Laminin and the non-fibrillar type IV collagen are key components of the basement membrane. Proteoglycans are heavily glycosylated proteins which form large complexes binding together other extracellular matrix components [46].

It is apparent that proteolysis of all of the pulmonary extracellular components described above would be a necessary pre-requisite for the destruction of lung tissue that occurs in cavitation. This implicates a group of enzymes known as matrix metalloproteinases (MMPs), which are collectively able to degrade all components of

the ECM including the basement membrane. An aetiological role for MMPs in tissue destruction and cavitation in TB can therefore be predicted.

The MMPs are a family of zinc dependent proteolytic enzymes, which are either secreted or membrane bound. There are 23 MMPs in total in humans and they are classified based on domain organization and substrate preference, into collagenases, gelatinases, stromelysins, membrane-type (MT)-MMPs and others. They share common structural features. There is a signal peptide that targets them for secretion, a prodomain which interacts with the catalytic domain to maintain latency, and a carboxy terminal hemopexin domain which confers substrate specificity. The membrane bound MMPs have an additional transmembrane domain and cytosolic tail. An interaction between a zinc ion in the catalytic domain and a thiol group of a cysteine residue in the prodomain maintains the enzyme in the inactive state. For secreted MMPs activation occurs extracellularly by proteolytic cleavage of the prodomain or modification of the cysteine thiol residue ('cysteine switch'). For membrane bound MMPs, activation occurs intracellularly by furin like pro-protein convertases. They all have a furin recognition sequence RX[R/K]R at the C-terminus of the propeptide. They are therefore activated intracellularly and active enzymes are likely to be expressed on the cell surface [47, 48].

The MMPs and their many substrates are shown in Table 1. These include transmembrane proteins, latent cytokines, protease inhibitors and pro-MMPs in addition to ECM components [49-52]. The collagenases MMP-1, MMP-8, MMP-13 cleave triple helical interstitial collagens I, II and III. The gelatinases MMP-2 and MMP-9 cleave gelatin and digest the basement membrane type IV collagen, but

not the interstitial collagens I, II and III. The stromelysins MMP-3, MMP-10 and MMP-11 digest fibronectin, laminin, proteoglycans and the basement membrane type IV collagen, though not the interstitial collagens. MT-MMPs in humans include four type I transmembrane proteins MMP-14, -15, -16, and -24 and two glycosylphosphatidylinositol-anchored proteins MMP-17 and -25. All MT-MMPs, except MMP-17, cleave proMMP-2 to the active form. MMP-14 degrades interstitial collagens I, II, and III. Other MMPs fall into a miscellaneous group and include the matrilysin MMP-7 and macrophage metalloelastase, MMP-12 [47, 48].

MMPs play a range of physiological roles. For example, in tissue repair they are important in ECM remodelling and cell migration. In immunity, they are involved in cell migration, intercellular signalling and cleavage of chemokines and cytokines. However in excess they are pathological and are implicated in a range of disease involving uncontrolled ECM destruction and tissue remodelling, notably cancer and arthritis [47, 49].

Because of the potential for excessive activity to be pathological, MMPs are tightly regulated at many levels. Control primarily occurs at the level of gene expression, pro-enzyme activation and enzyme inactivation or compartmentalisation. Enzyme inactivation is mainly mediated by Tissue Inhibitor of Metalloproteinases (TIMPs). These bind MMPs in a one to one fashion and the ratio of MMPs to TIMPs plays a major role in the fine balance between physiological ECM turnover and the excessive degradation present in disease [49, 53]. There are four TIMPs -1, -2, -3 and -4. They contain an N-terminal and a C-terminal subdomain. The TIMPs inhibit all the MMPs, though TIMP-1 is a poor inhibitor for MMP-14, MMP-16, MMP-19 and

MMP-24. The TIMP molecule is wedge shaped and slots into the active site of the MMPs. The catalytic zinc atom is chelated by an N-terminal amino group of four residues: Cys1-Thr- Cys-Val4 and the carbonyl group of Cys1 displaces a water molecule that is bound to the zinc atom, rendering the MMP inactive [48].

A range of MMPs and TIMPs are expressed by cells of the monocyte/macrophage lineage, neutrophils, T-cells, pulmonary epithelial cells and pulmonary fibroblasts which are all cells present at the site of infection in pulmonary TB [53, 54]. Therefore, MMP expression may be both cell type and stimulus dependent.

Table 1: MMP subdivisions by substrate specificity

Enzyme	Other names	Substrates	Activates
Collagenases			
MMP-1	Collagenase-1 (Interstitial collagenase, fibroblast collagenase)	Collagen I, II, III, VII, VIII, X, gelatin, proteoglycans, L-selectin α2-macroglobulin, latent TNF	MMP-2
MMP-8	Collagenase-2 (Neutrophil collagenase)	Collagen I, II, III, VII, VIII, X, gelatin, proteoglycans, fibronectin, laminin α2-macroglobulin	ND
MMP-13	Collagenase-3 (Rat collagenase)	Collagen I, II, III, IV, IX, X, XIV, gelatin, proteoglycans, fibronectin, laminin	MMP-2, -9
Gelatinases			
MMP-2	Gelatinase A (72-kDa gelatinase)	Gelatin, collagen IV, V, VII, X, XI, XIV, proteoglycans, fibronectin, laminin, elastin α2-macroglobulin, latent TNF	MMP-9, -13
MMP-9	Gelatinase B (92-kDa gelatinase)	Gelatin, Collagen IV, V, VII, X, XIV, proteoglycans, fibronectin, elastin, fibrin α1-antitrypsin, α2-macroglobulin, latent TNF, latent TGF-β1, latent VEGF	ND
Stromelysins			
MMP-3	Stromelysin-1	Collagen IV, V, IX, X, gelatin, proteoglycans, fibronectin, laminin Latent TGF-β	MMP-1, -8, -9, -13
MMP-10	Stromelysin-2	Collagen III, IV, V, gelatin, proteoglycans, fibronectin, elastin	MMP-1, -7, -8, -9
MMP-11	Stromelysin-3	fibronectin, laminin α1-proteinase inhibitor	ND

Membrane type			
MMP-14	MT1-MMP	Collagen I, II, III, gelatin, preoteoglycans, fibronectin, laminin, fibrillin	MMP-2
MMP-15	MT2-MMP	Proteoglycans, fibronectin, laminin, fibrin	MMP-2
MMP-16	MT3-MMP	Gelatin, casein, fibrin Syndecan-1	MMP-2
MMP-17	MT4-MMP	Gelatin Latent TNF	ND
MMP-24	MT5-MMP	ND	MMP-2
MMP-25	MT6-MMP	ND	MMP-2
Others			
MMP-7	Matrilysin	Collagen IV, gelatin, stromelysins, fibronectin, laminin, elastin Pro-α defensins FAS ligand, latent TNF, syndecan-1, E-cadherin,	MMP-3
MMP-12	Metalloelastase	Collagen IV, gelatin, stromelysins, fibronectin, laminin, fibrillin, elastin, Latent TNF, α1-antitrypsin	ND

ND – not delineated

Modified from Parks et al[49], Kahari et al [50], Chandler et al [51] and Ashworth et al [52]

1.8 Matrix Metalloproteinases and Emphysema

Before discussing the existing evidence relating to MMPs in TB it is appropriate to discuss the evidence for their role in another tissue destructive pulmonary disease, emphysema. These studies lend weight to the data suggesting a role for MMPs in pulmonary TB, and findings from both animal and human studies are presented.

Emphysema is defined as the enlargement of peripheral air spaces of the lung, accompanied by destruction of the walls of these structures. The hypothesis that this process results from an imbalance of proteases and their inhibitors arose from the finding that severe alpha 1 antitrypsin (AAT) deficiency is associated with the development of emphysema in humans in the context of cigarette smoke exposure. AAT is the main inhibitor of neutrophil elastase and instillation of human

n neutrophil elastase into *ex vivo* canine lungs produced anatomical emphysema, supporting the hypothesis. Subsequent immunohistochemical staining of the lungs demonstrated the presence of this elastase within the connective tissue in close proximity to elastase fibres [55].

Subsequent animal and humans studies suggest a role for not only the elastolytic activity of MMP-9 and MMP-12, but also the collagenolytic activity of MMP-1, in the pathogenesis of emphysema.

1.8.1 Matrix metalloproteinase 1

Transgenic mice expressing human MMP-1 in their lungs developed histological changes very similar to human emphysema but the control littermates did not [56]. Further mice studies used three types of transgenic mice with differing temporal MMP-1 expression. Early MMP-1 expression from 14 days post conception resulted in emphysematous changes at 5 days of age. Delayed expression to between birth and 2 weeks of age caused emphysema from 4 weeks of age. A very low expression delayed the emphysema to 1 year of age. The emphysema was associated with decreased immunohistochemical staining for type III collagen [57]. Smoke exposure in guinea pigs caused emphysematous changes. Immunohistochemical analysis revealed MMP-1 in the macrophages, alveolar walls and interstitium. The emphysematous lungs showed increased collagenolytic activity and reduced collagen content compared to controls not exposed to smoke [58].

In human alveolar macrophages taken from patients with emphysema and maintained in vitro there was increased MMP-1 mRNA expression and increased collagenolytic activity in the supernatant compared to healthy controls [59]. Immunohistochemical analysis of human emphysematous lungs showed that MMP-1 was present in the macrophages and epithelial cells of the patients but not healthy smokers [60]. MMP-1 mRNA, protein and collagenolytic activity was identified in the lung of emphysema patients who had stopped smoking but not healthy controls. The MMP-1 protein was expressed in alveolar epithelial cells of the patients but not healthy smokers [61].

1.8.2 Matrix metalloproteinase 9

Transgenic mice expressing human MMP-9 in macrophages developed emphysema with a loss of alveolar elastin, but not control littermates [62].

Stimulation of alveolar macrophages from patients with emphysema with cigarette smoke resulted in greater MMP-9 secretion than in healthy smokers [63]. In alveolar macrophages taken from patients with emphysema and maintained *in vitro* there was increased MMP-9 mRNA expression and increased secretion in the supernatant compared to healthy controls [59]. Immunohistochemical analysis showed that MMP-9 was present in the neutrophils of human emphysematous lungs but not in healthy smokers [60]. In humans with AAT deficiency and emphysema, higher baseline plasma MMP-9 levels were associated with poorer lung function and exercise capacity. Baseline plasma MMP-9 levels also predicted the development of worsening emphysematous changes on computed tomography and air trapping on pulmonary function testing [64].

1.8.3 Matrix metalloproteinase 12

MMP-12 deficient mice did not develop emphysema in response to cigarette smoke exposure though wild type litter mates did [65].

MMP-12 levels were higher in the induced sputum of patients with emphysema than in healthy current and ex smokers [66]. A high proportion of patients with severe emphysema are homozygous for the A/A allele of rs652438 in MMP-12. In cells

transfected with rs652438 A and G alleles, mean MMP-12 activity was higher for the A allele than the G allele. Increased emphysematous changes on CT were present for A/A homozygotes compared to G/G homozygotes [67].

1.9 Matrix Metalloproteinases and Tuberculosis

Accumulating evidenced implicates MMPs in tissue destruction in TB, with this being the central theme of our group's work. Key data has come from studying both direct infection and the networking interactions between different cell types. The *Mtb* induced intercellular network is mimicked by stimulating cells with Conditioned medium from *Mtb* infected monocytes (CoMTb). The number of mycobacteria in granulomas is low [68] and interactions between cells via cytokine, chemokine and growth factor secretion are important to cellular activation within the granuloma. CoMTb is rich in this cytokine, chemokine and growth factor milieu as well as *Mtb* antigens, but not live *Mtb* bacilli.

1.9.1 Pulmonary tuberculosis

The first study of MMPs in TB was relatively small. It showed that lipoarabinomannan (LAM, a lipoglycan cell wall component and major virulence factor in *Mtb*) upregulated MMP-9 mRNA and increased MMP-9 secretion from monocytic THP-1 cells. LAM also upregulated MMP-1 mRNA in both THP-1 cells and peripheral blood monocytes. Bronchoalveolar lavage (BAL) on 2 patients with active *Mtb* showed that

MMP-9 mRNA was upregulated [69]. Research in this field has steadily grown since, and the published data will be discussed in detail.

Tissue destruction and cavitation are not a feature of pulmonary vaccine Bacillus Calmette-Guérin (BCG) infection, which causes a pulmonary pneumonitis with non caseating granulomas [70]. *Mtb*, but not BCG, significantly upregulated MMP-1 gene expression and secretion from human macrophages. Therefore only the pathogen which causes disease where collagen destruction is present drives expression of the collagenase MMP-1. TIMP-1 gene expression and secretion from macrophages was not upregulated by *Mtb*. Immunohistochemistry from lung biopsies of patients with active TB showed that macrophages express MMP-1 in areas adjacent to tissue destruction [71].

Macrophages are not the only key cells producing MMPs in TB, and stromal cells may be equally important. For example, CoMTb upregulated human pulmonary epithelial cell MMP-1 and MMP-9 gene expression and secretion. In lung biopsies of patients with active TB, MMP-9 was expressed in pulmonary epithelial cells adjacent to but not distant from granulomas [72, 73]. Fibroblasts are also important sources of MMPs, and CoMTb drives MMP-1 and MMP-3 gene expression and secretion from human pulmonary fibroblasts, and reduces TIMP-1 gene expression and secretion [74, 75].

From the cellular data and immunohistochemical findings, it can be proposed that *Mtb* drives a matrix degrading phenotype of MMP activity unopposed by TIMPs in

human pulmonary TB. This is both by direct infection of macrophages and by an *Mtb* induced intercellular network stimulating epithelial cells and pulmonary fibroblasts.

This proposal is further supported by more recent data from mouse and human studies. As discussed earlier animals do not provide good models for cavitatory TB, therefore studying patient samples is important. Mice do not express a pulmonary MMP-1 ortholog, therefore transgenic mice expressing human MMP-1 were studied. *Mtb* infected transgenic, but not *Mtb* infected wild type mice, showed alveolar wall destruction and collagen degradation in areas of macrophage infiltration [76]. MMP-1 and MMP-3 in bronchoalveolar lavage and induced sputum of patients with pulmonary TB were elevated in comparison to controls while TIMP-1 and TIMP-2 were suppressed. The MMP-1 in the sputum was proteolytically active on casein zymogram, and levels positively correlated with more extensive inflammation on chest radiograph. When Ro32-3555, a collagenase inhibitor of proven safety in man, was co-incubated with *Mtb* infected human macrophages, it abrogated MMP-1 activity on casein zymography completely [76]. This provides good evidence for MMP-1 as a central effector in matrix degradation in pulmonary TB and raises the possibility of a therapeutic role for Ro32-355.

To further elucidate the role of MMPs in driving tissue destruction in pulmonary TB *in vivo*, MMPs were measured in the induced sputum of a cohort of HIV negative and positive patients with pulmonary TB compared to controls. Comparing MMP levels in HIV negative and positive patients was considered an interesting line of investigation, as HIV positive patients with TB exhibit less tissue destruction and rarely develop cavities even in advance disease. MMP-1, -2, -3, -8 and -9 were elevated in TB

overall, but were lower in the HIV positive patients relative to HIV negative patients with TB. MMP-1 and MMP-2 correlated with the extent of tissue destruction on chest radiograph and were higher in patients with cavities. These findings further implicate MMPs in tissue destruction in pulmonary TB [77].

One interesting recent study suggests that a MMP-1 gene polymorphism is involved in the tissue destructive pulmonary TB phenotype. The -1607 MMP-1 allele 2G enhances expression of this gene in active TB. Hispanics expressing the 2 locus genotype MMP-1 2G/2G were more likely to have a tissue destructive pulmonary TB requiring surgical intervention, when compared to carriers of other genotype combinations that do not enhance MMP-1 gene expression to the same extent. They also had higher plasma levels of MMP-1 [78].

Other data supporting a role for MMPs in pulmonary TB pathogenesis comes from microarray studies in humans and non-human primates, which though not specifically researching MMPs in their hypotheses provide valuable information. Monocytes from asymptomatic, cured patients with pulmonary TB and highly exposed individuals with latent TB were matured to macrophages and stimulated with *Mtb* H37Rv whole cell lysate. MMP-1 gene expression was upregulated 257 times more in pulmonary TB relative to those with latent disease, suggesting that if an individual has a stronger macrophage MMP-1 gene expression response to *Mtb* this is associated with the outcome of active pulmonary disease [79]. Microarray analysis of human pulmonary caseating granulomas and granulomatous lesions

from the lungs of *Mtb* infected non-human primates have showed increased expression of MMP-1, -2, -7, -9, -10 and –14 compared to normal lung tissue [80, 81].

1.9.2 Central nervous system tuberculosis

Tissue destruction is not only observed in pulmonary TB. Central nervous system (CNS) TB is particularly severe in its manifestations with marked inflammatory and tissue destructive changes present [82]. A body of evidence implicates MMPs in CNS TB also.

CoMTb upregulated MMP-1 and MMP-3 gene expression and secretion in human microglia but did not alter TIMP-1 and downregulated TIMP-2 secretion. Immunohistochemical analysis of human brain biopsies showed MMP-1 and MMP-3 staining at the centre of granulomas from patients with CNS TB, but no staining in controls. Dexamethasone reduces mortality in CNS TB [83], and steroids are protocol in CNS TB treatment [6]. Therefore it is particularly interesting that dexamethasone inhibited CoMTb driven microglial MMP-1 and MMP-3, but not TIMP-1 or TIMP- 2 secretion [84]. MMP-9 gene expression and secretion in human astrocytes was driven by CoMTb, but TIMP secretion was not. MMP-9 was expressed more abundantly in astrocytes in human brain biopsies from patients with CNS TB than in controls. Again dexamethasone inhibited astrocyte MMP-9, but not TIMP-1 or TIMP-2 secretion in response to CoMTb [85]. *In vivo* investigation revealed MMP-9 concentration in cerebrospinal fluid in tuberculous meningitis to be significantly higher than that in bacterial or viral meningitis. TIMP-1 was not elevated in the CSF in tuberculous meningitis [86].

From these findings in a cellular model and patient samples it can be proposed that an *Mtb* induced network of cytokines and chemokines stimulates microglial cells and astrocytes to drive a matrix degrading phenotype of MMP activity unopposed by TIMPs in human CNS TB.

1.9.3 Granuloma formation

Evidence from diverse lines of investigation are now implicating MMPs in non tissue destructive aspects of TB pathogenesis. For example, in the zebrafish embryo model of granuloma formation, *M marinum* infected MMP-9 morpholinos formed fewer, smaller granulomas and had a lower bacterial burden. Morpholinos are synthetic antisense oligonucleotides which act to block initiation of translation or RNA splicing of the specific mRNA sequence [87]. This suggests that MMP-9 is important for macrophage recruitment in the wild type zebrafish. Region of difference 1 (RD1) is a region present in the genome of *Mtb* and *M.marinum* which encodes virulence factors [88]. MMP-9 expression was reduced with *M. marinum* RD1 deleted infection compared to wild type *M. marinum*, suggesting that such upregulation is RD1 virulence locus dependent [89].

1.10 Regulation of Matrix Metalloproteinase Expression

An understanding of the control of MMP expression in TB is important to the future development of therapeutics. MMPs are regulated in multiple ways, but alteration of mRNA expression is the major mechanism controlling MMP activity. MMPs have differing promoter structures and can therefore vary in their response to cues, though shared elements can lead to co-expression. The MMP promoters contain consensus binding sites to numerous transcription factors, but NF-κB, AP-1, STAT, TCF/LEF, GC and Ets are prominent. A range of stimuli such as cytokines, chemokines, growth factors, microbial antigens, phagocytosis and mechanical stress act as stimuli. Through receptor binding, signal transduction pathways are activated and transcription factor promoter binding ensues, with resultant altered gene expression [47, 90].

As MMP-1 was the first MMP discovered, the factors altering its gene expression have been studied in the most detail. The mitogen activated protein kinase (MAPK) signalling pathway involves p38 kinases, extracellular signal related kinases (ERK) and c-Jun-N-terminal kinases (JNK) as signal transducers and the transcription factors NF-κB, AP-1 and STAT, and has been highlighted as playing roles in response to varying stimuli in different cell types [47].

Cell/tissue specific activation would appear to relate to the presence of specific signalling proteins and transcription factors in some cells and not others. For example the RUNX-2 transcription factor binding site in the MMP-13 promoter is

essential for its expression. However RUNX-2 protein is primarily found in chondrocytes, therefore MMP-13 expression is normally limited to cartilage and bone [91].

The existing data on the control of MMPs in TB will be discussed, focusing not only on both extracellular stimuli and intracellular signalling cascades.

1.10.1 Cytokines and chemokines

Data showing that *Mtb* induced intercellular networks drive MMP secretion has been discussed. Cytokines and chemokines are key extracellular stimuli which activate the downstream signalling pathways which ultimately increasing mRNA levels. In an attempt to identify a 'master' regulatory cytokine or chemokine, neutralising antibodies, recombinant cytokines/chemokines and chemical inhibitors have been applied to the cellular models.

With respect to pulmonary TB, neutralisation of TNFα, but not IL-1β, decreased CoMTb and *Mtb* induced MMP-9 secretion from monocytes. Recombinant TNFα directly stimulated MMP-9 secretion from monocytes [92]. Recombinant Oncostatin M synergized with TNFα to stimulate human pulmonary fibroblast MMP-1 and MMP-3 secretion, while suppressing secretion of TIMP-1 and TIMP-2. Stimulating pulmonary fibroblasts with these recombinant cytokines individually had no effect [74]. TNFα neutralisation suppressed CoMTb driven human pulmonary epithelial cell MMP-1 secretion [72]. Similarly it was critical to upregulation of MMP-9 secretion

from pulmonary epithelial cells, but neutralisation of interleukin 1 beta (IL-1β) and interleukin 6 (IL-6) had no effect t [73].

Moving on to CNS TB, TNFα and IL-1β neutralisation in CoMTb, decreased MMP-9 secretion from astrocytes, but recombinant TNFα and IL-1β alone or in combination had no effect [85]. Neutralisation of TNFα and IL-1β in CoMTb decreased MMP-1 and MMP-3 secretion from human microglial cells [84]. Supplementing CoMTb with the critical T cell cytokine IFNɣ resulted in an increased secretion of MMP-9 and reduced TIMP-1 and -2 from astrocytes.

Chemokine signalling and MMP expression has only been investigated for pulmonary TB. Pertussis toxin (PT) is secreted by the organism *Bordetella pertussis* and inhibits signalling through Gi protein coupled pathways [93]. Downstream effects include inhibition of immune cell chemotaxis in response to chemokines [94], as well as reduced expression of the chemokines themselves [95]. However a range of other ligands signal through G protein coupled receptors, so the effects of PT are not specific to chemokines [93]. PT inhibited CoMTb driven MMP-9 secretion in THP-1 cells and enhanced the inhibitory effect of an anti-TNFα antibody. However investigation of the potential chemokines present in CoMTb causing this effect did not identify a specific mediator [92].PT significantly suppressed CoMTb driven MMP-1 secretion from human pulmonary epithelial cells. Cholera toxin (stimulator of G protein coupled receptor signalling) in combination with TNFα significantly upregulated MMP-1 secretion compared to TNFα alone. However, as previously,

investigation of the potential chemokines present in CoMTb causing this effect did not identify a specific mediator [72].

These findings can be explained by studies in mice deficient for individual chemokines. These have indicated a high degree of overlap in this system and the absence of individual chemokines does not result in adverse outcomes in murine *Mtb* infection. This is a consequence chemokines receptors binding multiple ligands [96].

Therefore it is apparent that the regulation of MMPs driven by *Mtb* induced intercellular networks is relatively complex and not mediated by a single cytokine or chemokine, but that they act in combination and synergistically.

1.10.2 Pathogen related factors

The manner in which *Mtb* drives lung pathology to spread to new hosts is not a central theme of research within the field, with comparison between strains focusing more on cytokine responses and genetic differences[97]. The finding that *Mtb* but not BCG drives MMP-1 secretion from human macrophages is of particular interest as it indicates that a specific factor present in *Mtb* but not BCG drives MMP-1 secretion**.** M bovis causes pulmonary infection rarely in comparison to Mtb but does cause cavitation [98], and as mentioned previously BCG may cause a pneumonitis but not cavitation [70]. It is possible that the pathogen specific factor is encoded in the RD1 region of the *Mtb* genome, which is absent in the BCG genome [99]. As

mentioned previously RD1 encodes virulence factors, specifically 6kDa early secretory antigenic target (ESAT-6) and 10kDa culture filtrate protein (CFP-10) [88].

1.10.3 Mitogen-activated protein kinase signalling

MAPKs are serine/threonine-specific protein kinases involved in cellular responses to a diverse extracellular stimuli regulating among many other responses gene expression. MAPKs are catalytically inactive until they undergo multiple phosphorylation events in their activation loops, conducted by specialised enzymes. *In vitro* and *in vivo* evidence indicates that activation of the MAPK pathway proteins by phosphorylation is a key cellular response to *Mtb* infection [100, 101]. This will lead to increased MMP expression by downstream transcription factor activation [47]. The MAPK pathways are schematically represented in Fig. 1.

In pulmonary TB, CoMTb drives p38 MAPK phosphorylation in human pulmonary epithelial cells. Chemical inhibition of p38 MAPK signalling results in decreased CoMTb driven MMP-1 secretion from the epithelial cells [72]. CoMTb stimulated human pulmonary fibroblasts show p38 and JNK MAPK phosphorylation, which is also induced by recombinant TNFα, IL-1β and Oncostatin M (cytokines present in CoMTb). Chemical inhibition of p38 MAPK signalling, leads to decreased CoMTb driven MMP-1 secretion from the fibroblasts [75]. *Mtb* infection drives p38 and ERK MAPK phosphorylation in human macrophages. In patients with pulmonary TB, immunohistochemical analysis shows p38 MAPK phosphorylation in macrophages surrounding granulomas. Chemical inhibition of p38 MAPK and ERK MAPK results in reduced MMP-1 secretion from *Mtb* infected macrophages [100].

With regard to CNS TB p38, ERK and JNK MAPK phosphorylation is stimulated in human astrocytes by CoMTb and reduced when IL-1β in the CoMTb is neutralised [102].

1.10.4 NF-κB, AP-1 and STAT-3 transcription factors

The transcription factors Nuclear factor kappa B (NF-κB), Activator protein 1 (AP-1) and Signal transducer and activator of transcription 3 (STAT3) are implicated as those which control MMP expression in TB by the research to date. AP-1 is a heterodimeric protein composed of subunits c-Fos, c-Jun, ATF and JDP families. STAT-3 is a monomeric protein. AP-1 and STAT-3 enter the nucleus and bind to promoters upon phosphorylation. NF-κB is a family of dimeric transcription factors made from monomers including RelA, RelB, c-Rel, p50 and p52. It binds the inhibitor of kappa B family (IκB). Translocation of NF-κB into the nucleus is controlled by phosphorylation and subsequent degradation of IκB by IκB kinase (IKK) [47, 103]. The NF-κB pathway is schematically represented in Fig. 2. The MAPK pathways have a clearly defined role in activating AP-1, but the mechanism of interaction with STAT and NF-κB signalling is less well defined [47].

With regard to pulmonary TB, CoMTb drives STAT-3 phosphorylation in human pulmonary fibroblasts. STAT-3 phosphorylation is observed in fibroblasts of lung granulomas from patients with TB. Chemical inhibition of STAT- 3 phosphorylation downregulates CoMTb driven MMP-1 secretion [75].

In CNS TB, CoMTb drives increased NF-κB and AP-1 DNA binding in human microglia. Chemical inhibition of NF-κB reduced CoMTb driven MMP-1 secretion. Immunohistochemical analysis of brain granulomas from patients with TB shows nuclear p65 NF-κB in the granuloma centre but not in control brain tissue. Deletion of the NF-κB and AP-1 binding site resulted in reduced CoMTb driven MMP-1 promoter activation [84].

Dissecting the transcriptional regulation of MMPs in TB therefore represents an area where much further work needs to be undertaken.

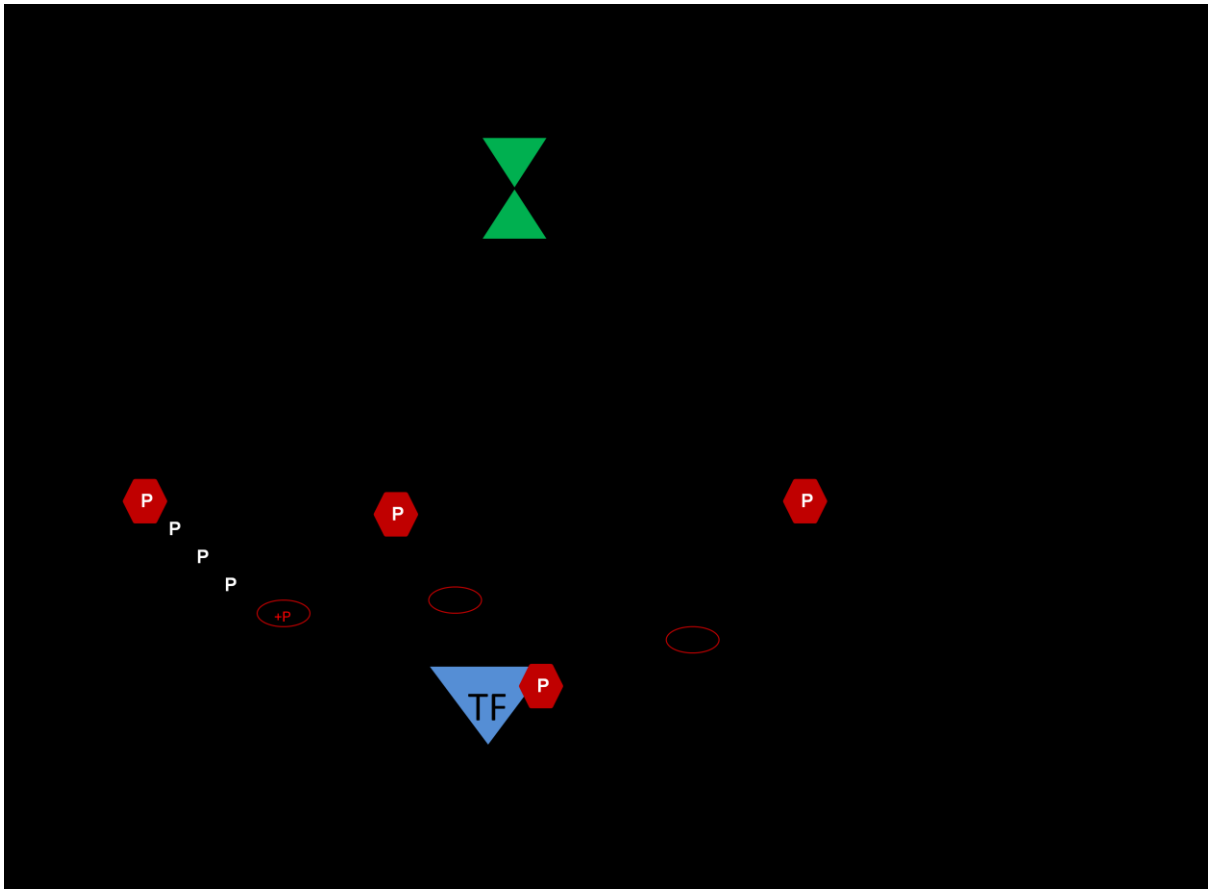

Figure 1: MAPK signalling pathway

Extracellular stimuli bind cell surface receptors and this triggers intracellular phosphorylation cascades. Separate cascades are responsible for the phosphorylation required for the activation of the p38, ERK and JNK MAPKs. In the final step the activated MAPKs phosphorylate substrates such as transcription factors (TF) in the cytoplasm. The phosphorylated transcription factor then enters the nucleus and initiates mRNA transcription.

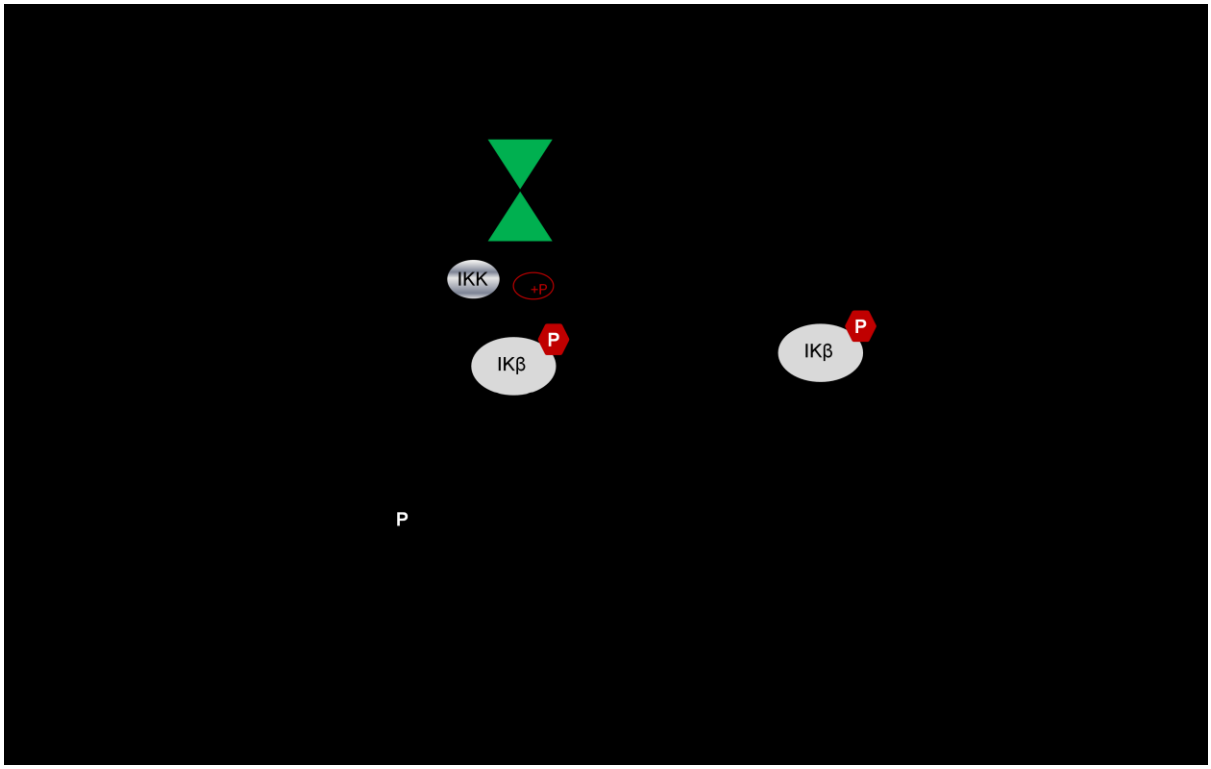

Figure 2: NF-κB signalling pathway

NF-κB is a family of dimeric transcription factors made from monomers including RelA, RelB, c-Rel, p50 and p52. Extracellular stimuli bind cell surface receptors and this triggers intracellular phosphorylation of IKK which phosphorylates IκB, causing it to dissociate from the NF-κB dimer. The NF-κB dimer can then enter the nucleus and initiate mRNA transcription.

1.11 Matrix Metalloproteinase 14

The studies outlined above have focussed on secreted MMPs. However, the membrane bound MMPs may also be of critical importance in TB and have possibly been overlooked due to the comparative difficulty in studying them. MMP-14, a membrane bound collagenase, is already implicated in TB. MMP-14 gene expression was upregulated in monocytes by direct *Mtb* infection [76] and in human lung TB granulomas [80]. Notably, MMP-14 has been shown to be critical to cell migration and invasion in the context of other disease processes [104-106].

1.11.1 Cell migration in granuloma formation and mycobacterial dissemination

The granuloma has traditionally been considered a feature of adaptive immunity. However a granuloma is at its simplest an organised aggregate of macrophages. Recent studies have indicated that these can not only form in the context of innate immunity but are highly dynamic structures which may play a role in bacterial expansion and dissemination, rather than being purely protective for the host. Monocyte/macrophage migration is a key feature of this phenomenon [16].

The optically transparent zebrafish embryo is a natural host for *M. marinum* infection, which is a close genomic relative of *Mtb*. The embryo lacks lymphocytes and an adaptive immune system but has macrophages. Using state of the art imaging, it is possible to visualise and monitor host-pathogen interactions in vivo [107]. Macrophages phagocytose *M marinum* immediately after injection and extravasate into tissues within 1 day, forming tight aggregates within 3 days. Infected and uninfected cells are present within the granuloma and have tightly opposed

membranes and indistinct cell boundaries indicating the formation of epithelioid and multinucleate giant cells [107].

An *in vitro* 2D granuloma model confirms that macrophages alone form early granulomas in humans. Septarose beads covalently coated with *Mtb* purified protein derivative were inoculated with healthy human peripheral blood mononuclear cells. Microscopy showed that monocytes were recruited from day 1 aggregating at the bead surface, then lymphocytes from day 4 [108].

Further work in the zebrafish embryo model demonstrated that macrophages are necessary for the initial control of mycobacterial infection but subsequently promote bacterial expansion and dissemination into deeper tissues. Wild type and pu 1 morphant embryos, which lack macrophages, were infected with *M marinum* into the hindbrain ventricle. Mycobacteria achieved higher burdens in pu.1 morphant embryos confirming the importance of macrophages in containing mycobacterial infection. However, while bacteria disseminated out of the hindbrain ventricle in more than half of the control morphants, none of the pu.1 morphants displayed any extraventricular bacteria. All extraventricular bacteria in the control morphants resided within macrophages. A significantly higher number of control embryos had extravascular bacteria compared to pu.1 morphants. All bacteria in the control embryos appeared to reside within phagocytes [109]. *M. marinum* infected macrophages in granulomas recruited uninfected macrophages. The newly arriving macrophages phagocytosed dying macrophages, allowing further bacterial growth. Some infected macrophages left the primary granuloma and seeded distal secondary granulomas [110].

Taken together, these experiments suggest that macrophage recruitment is a double-edged sword, necessary for initial control of infection, but also aiding proliferation and dissemination. However, the key regulators of cell migration into granulomas have not been fully defined.

1.11.2 Matrix metalloproteinase 14 and cell migration

MMP – 14 (or Membrane Type 1 Matrix Metalloproteinase) was the first membrane type MMP (MT-MMP) characterised. It was described as an activator of MMP-2, which was present on the surface of invasive lung carcinoma cells, and enhanced invasion of a reconstituted basement membrane in vitro [111]. Its main activity is as a collagenase degrading types I, II and III collagen, but it also degrades other components of the ECM including proteoglycans, fibronectin and laminin [112]. As with all MMPs, careful regulation of its activity is required. In addition to control at the level of gene expression and pro-enzyme activation, mechanisms of post translational modification involve inhibition by TIMP-2 in particular (but not TIMP-1), autodegradation [113], and internalisation via caveolae and clathrin coated vesicles with cycling back to the cell surface [114].

The ECM is a barrier to cell migration and must be degraded focally at the front of a cell if they are to migrate and propel forwards. The secreted MMPs exhibit a generalized rather than focal matrix resorptive activity. MMP-14 is unique because it is a membrane bound type I collagenase. By localising at the leading cell edge it can

breakdown ECM focally in the immediate pericellular environment thus promoting cell migration and invasion in a focussed manner [115]. Bearing this in mind, MMP-14 has been implicated not only in physiological processes such as wound healing but also diseases such as rheumatoid arthritis and malignancy. The evidence comes from both *in vitro* models and clinical samples.

In a seminal study, Madin-Darby Canine Kidney epithelial cells were cultured on a collagen matrix and were transfected to overexpress diverse MMPs. Only overexpression of MMP-14 caused significant acceleration of invasion of the cells into the matrix, with complete degradation of the collagen substratum, via a TIMP-2 sensitive process [116].

In another study, murine skin fibroblasts from specific MMP null mice were seeded on type 1 collagen. Subjacent collagenolysis was lost for only the MMP-14 null fibroblasts. Plasminogen restored subjacent collagenolysis to the MMP-14 null fibroblasts, by mobilizing secreted MMPs. However the MMP-14 null fibroblasts would not invade into a type 1 collagen gel even in the presence of plasminogen. This shows that MMP-14, rather than the secreted collagenases, serves a dual role of breaking down and promoting cell migration through collagen [117].

In a wound healing model of endothelial cell migration, which is required for angiogenesis, MMP-14 expression was present on the surface of migrating endothelial cells with localisation at motility associated structures. Neutralisation of MMP-14 activity inhibited endothelial cell invasion of collagen [118].

Local invasion of the joint cartilage by synovial pannus is a key finding in rheumatoid arthritis, and involves collagen degradation. Primary synovial cells were isolated from rheumatoid arthritis joints and specimens. Using western blotting and immunohistochemistry, it was shown that MMP-14 was highly expressed in primary synovial cells and the pannus cartilage junction. Synovial cell invasion into collagen matrix and cartilage was inhibited by TIMP-2 and adenoviral expression of a non-functional MMP-14 [104].

MMP-14 expression in a breast cancer cell line was knocked down by a retroviral ribozyme transgene causing reduced invasiveness *in vitro* compared to wild type cells [105]. Gastric carcinoma and fibrosarcoma cell lines were transfected with siRNA to knock down MMP-14 expression. Migration of these cells through matrigel was reduced compared to controls [106]. In those who died of breast cancer, significantly higher levels of MMP-14 mRNA were present in the tumour in comparison to patients who were disease-free 10 years after the initial operation [105]. In another study of breast cancer the highest MMP-14 mRNA expression was in specimens where lymph node metastasis and/or lymph vessel invasion was present [119].

Taken together, these studies all suggest a key role for MMP-14 in facilitating cell migration and invasion by matrix destruction at the leading edge of the cell.

Evidence from a zebrafish embryo model was presented earlier, which indicates that monocyte/macrophage migration may be key to bacterial expansion and dissemination in mycobacterial infection. For monocytes to migrate to the primary site of infection in pulmonary TB, they would have to transmigrate the endothelium, then traverse the basement membrane and pulmonary ECM by focal degradation of components along their migratory path. Pulmonary ECM degradation would similarly be necessary for monocytes/ macrophages to egress the primary granuloma. As type I collagen is the primary structural fibril of the lung focal, collagen degradation at the leading migratory edge of the monocyte would be required. A role for MMP-14 in this process can therefore be predicted.

Monocytes were first shown to express fully active MMP-14 on their surface in response to lipopolysaccharide stimulation [120]. Immunofluorescence microscopy showed that MMP-14 neutralisation with an antibody inhibited monocyte transmigration through endothelium and MMP 14 clustering was observed at motility associated protrusions of the monocytes [121]. Immature dendritic cells from wild type and MMP-14 null mice were cultured on cross linked gelatin. Using conventional and fluorescent light and electron microscopy it was shown that the dendritic cells formed protrusions into and degraded the gelatin matrix and that the gelatin degradation was MMP-14 dependent [122]. MMP-14 neutralisation with an antibody inhibited the migration human immature monocyte derived dendritic cells through Matrigel [123]. Therefore MMP-14 activity has already been implicated in the migration and invasion of cells of the monocyte/macrophage lineage.

This evidence raises the interesting possibility that MMP-14 may be involved two of the fundamental immunopathological processes in *Mtb* infection that are discussed above, namely cell migration and collagen destruction. The focal collagenolytic activity of MMP-14 expressed at the leading edge of migrating monocytes may be promoting migration of the cells, and therefore enhancing cellular recruitment, bacterial expansion and dissemination. But for cells that remain at a site of infection, MMP-14 expression throughout the monocyte/macrophage surface may be driving pericellular collagen breakdown and thus local tissue destruction. Therefore investigation of MMP-14 in TB is a potentially interesting new line of enquiry.

1.12 Matrix metalloproteinase 10

In a similar manner to MMP-14 being overlooked in TB due to relative difficulty of investigation, MMP-10 (stromelysin-2) may have not have been investigated due to lack of readily available reagents. It is a secreted MMP and a stromelysin with enzymatic activity for cleaving fibronectin, laminin and proteoglycans, but not triple helical collagens I, II and III. It shares 85% amino acid sequence homology with the much more extensively studied MMP-3 (stromelysin-1) through its catalytic domain and they are very similar in structure and substrate specificity [124]. However the MMP-3 and MMP-10 gene promoters differ in the binding sites present, resulting in differential transcriptional regulation and tissue expression [90, 125, 126]. Furthermore while MMP-3 has a higher proteolytic efficiency, MMP-10 binds TIMP-1 and TIMP-2 with much lower affinity [124]. Therefore the role of MMP-10 in physiological and pathological processes will differ from MMP-3 and it warrants investigation in its own right.

A feature of particular interest is that MMP-10 is able to cleave the pro-forms of MMP-1 and MMP-8 to the active forms [127-129]. MMP-3 also has this action and generates a form of MMP-1 with tenfold greater collagenolytic activity than serine proteases alone [130].

This action has been confirmed as being of potential importance in disease by *in vitro* models. Angiogenesis occurs within tumours and promotion of vascular regression is a potential therapy. In a model of capillary tube regression using endothelial cells (ECs) in three dimensional collagen matrices, the ECs were transfected to overexpress MMP-10. This increased activation of MMP-1 in a manner which temporally correlated with capillary tube regression and gel contraction. MMP-1 knockdown using small interfering RNA (siRNA) blocked the ability of MMP-10 overexpression to drive capillary tube regression and gel contraction [131], confirming the mechanism of MMP-10 activity being pro-enzyme activation of MMP-1. Malignant transformation of keratinocytes results in acquisition of a collagenolytic phenotype coincident with altered responsiveness to transforming growth factor (TGF) beta and epidermal growth factor (EGF). Neutralisation of active MMP-10 in supernatants of TGF-beta 1 and EGF stimulate keratinocytes lead to decreased conversion of pro MMP-1 to active MMP-1 and reduced keratinocyte invasion of a collagen gel [132].

The potential for MMP-10 to be playing a role in tissue destructive diseases *in vivo* has primarily been suggested by analysis of malignant biopsies. Using an *ex vivo* fluorescent assay, MMP-10 activity was detected in 80% of lung cancer specimens and only 20% of normal lung tissue samples [133]. High expression of MMP-10 was

frequently observed on immunohistochemical analysis of head and neck squamous cell carcinomas [134].

Strong evidence supporting a role for MMP-1 in a matrix degrading phenotype in TB has been presented, and an important role for MMP-8 is emerging (unpublished data). It can be proposed that MMP-10 is involved in driving matrix degradation in pulmonary TB, not only through its direct action on the pulmonary ECM, but by cleaving and activating proMMP-1 and proMMP-8. Therefore, assessment of MMP-10 in TB is a worthwhile and significant line of investigation.

1.13 Matrix metalloproteinase 8

An overview of MMP-8 is presented here because it emerges as potential mediator of tissue destruction in TB in one of the clinical studies undertaken for this thesis. Though there is a range evidence supporting a role for MMP-1 (collagenase-1) in tissue destruction in TB, MMP-8 (collagenase-2) has not been extensively studied. MMP-8 is primarily expressed in neutrophils and cleaves the triple helical collagens I, II and III as well as serine protease inhibitors and chemokines. It is also expressed in epithelial cells, macrophages, fibroblasts and T-cells [135].

In contrast to MMP-14 and -10 the role of MMP-8 in cancer progression is controversial. Some studies suggest that MMP-8 drives tumour progression, while others indicate that it is antimetastatic. Serum MMP-8 was elevated in squamous cell carcinomas of the head and neck and significantly correlated with tumour stage

[136]. In another clinical study MMP-8 protein was detected by immunohistochemistry in a malignant invading tumour cell islands, fibroblasts, neutrophils and plasma cells of squamous cell carcinomas of the head and neck [137]. However a mouse study showed that in breast cancer cell lines MMP-8 overexpression reduced metastasis, whereas knock-down increased metastasis [138].

.

Highly glycosylated forms of MMP-8 are stored in granules within neutrophils. Neutrophils are the first innate immune cells to influx at a site of inflammation. They degranulate after stimulation which results in extracellular release of MMP-8. Degradation of collagen driven by MMP-8 at the site of inflammation can influence disease outcome [135]. Bronchiectasis is characterized by chronic inflammation as a consequence of recurrent infection and permanent dilation of the bronchi ensues.

The bronchoalveolar lavage fluid from patients with bronchiectasis of varying severity was incubated with Type I collagen and densitometric analysis of collagen breakdown products performed. The collagenolytic activity was greater the more severe the bronchiectasis - using the differential inhibitory capacity of doxycycline it was confirmed that neutrophil derived MMP-8 was the predominant collagenase present [139].

Neutrophils are considered increasingly important in TB immunopathology and unpublished cellular and clinical data suggest a role for MMP-8 in collagen

destruction in TB. Therefore it is important to continue to study MMP-8 in clinical samples from TB patients.

1.13 Hypothesis

MMPs drive tissue destruction in human tuberculosis and diverse MMPs have unique roles in immunopathology, including regulating monocyte migration and augmenting tissue destruction.

1.14 Objectives and aims

1. To investigate the regulation of MMP-10 in a cellular model of human TB.

2. To assess the role of MMP-14 in monocyte migration and monocyte associated collagen destruction in a cellular model of human TB.

3. To measure MMP expression in clinical samples from patients with pulmonary TB including plasma, sputum and lung biopsies.

2. METHODS

2.1 Mtb and BCG culture

M.tuberculosis H37Rv (*Mtb*) and Pasteur vaccine Bacillus Calmette-Guérin (BCG) were cultured in Middlebrook 7H9 medium (BD Diagnostics, Oxford, UK) supplemented with 10% ADC enrichment medium (BD Diagnostics), 0.2% glycerol (Sigma, Poole, UK), 0.02% Tween 80 (Sigma) with agitation at 10rpm. Culture growth was monitored with a Biowave cell density meter (WPA, Cambridge, UK) and both were subcultured when the optical density was 1.00. The *Mtb* endotoxin level was measured by the amebocyte lysate assay (Associates of Cape Cod) and was <0.3 ng/ml LPS.

2.2 Cell culture

2.2.1 Monocyte purification

Monocytes were isolated from single donor leucocyte-enriched cones (NHS Blood and Transfusion, London, UK) or fresh peripheral blood from healthy human donors, by density gradient centrifugation and adhesion purification.

The blood was mixed with Hanks Balanced Salt Solution (HBSS, Gibco®, Life Technologies, Paisley, UK), and layered onto Ficoll (GE Healthcare Life Sciences, Little Chalfont, UK) before centrifugation at 1500rpm for 20-30mins. The leukocyte

cell layer was collected and washed repeatedly in HBSS by spinning at 1200 rpm for 5 minutes and resuspending the cell pellet. The total monocyte number was calculated by counting the adherent cells in a haemocytometer, after a 5 minute incubation at 37^{o}C. Monocytes were plated in RPMI 1640 (Gibco®), supplemented with 2mM glutamine (Invitrogen, Life Technologies, Paisley, UK) and 10µg/ml ampicillin (Sigma-Aldrich), at a density of 2.5 x10^{5} cells per cm^{2}. The monocytes were incubated at 37˚C for one hour to adhere and then washed three times in HBSS to remove non adherent lymphocytes.

Experiments were set up in RPMI 1640 supplemented with, 2mM glutamine (Invitrogen) and 10µg/ml ampicillin (Sigma-Aldrich), 10% heat inactivated fetal calf serum (FCS, Biowest, Nuaillé, France) . The monocytes were placed in a humidified incubator supplemented with 5% CO_2 at 37˚C for the duration of the experiment.

2.2.2 Maturation of monocytes to macrophages

Monocytes were isolated as above and matured to monocyte derived macrophages (MDMs) over 5 days in RPMI 1640, 2mM glutamine, 10µg/ml ampicillin and 10% heat inactivated FCS, supplemented with 10ng/ml of macrophage colony stimulating factor (R&D, Abingdon, UK)). Experiments were set up in Macrophage Serum Free Medium (Invitrogen). The MDMs were placed in a humidified incubator supplemented with 5% CO_2 at 37˚C for the duration of the experiment.

2.2. 3 Normal human bronchial epithelial cell culture

Normal human bronchial epithelial (NHBE) cells (Clonetics®, Lonza, Slough) were cultured in Bronchial Epithelial Cell Growth Medium (BEGM®, Clonetics®). The cells were subcultured at 80-90% confluence using trypsin-EDTA for 2min and neutralized with trypsin neutralizing solution (Clonetics®). For experiments, cells were seeded at a density of 40,000 per cm^2, rested overnight and experiments commenced at 80% confluence in BEGM.

.

2.2.4 Cell infection protocol

Monocytes were infected immediately after the completion of adhesion purification and macrophages after 5 days of maturation. *Mtb* or BCG at mid log growth at an optical density of 0.60 was used, which corresponds to 1 x 10^8 – 2 x 10^8 colony forming units (CFU) per ml and a multiplicity of infection (MOI) of 1.

2.2.5 Preparation of conditioned medium from *Mtb* infected monocytes

Monocytes were plated onto 60mm dishes in RPMI 1640 supplemented with 2mM glutamine and 10µg/ml ampicillin at a density of 2.5 x10^5 cells per cm^2. These were immediately infected with *Mtb* at an MOI of 1 (CoMTb) or 7H9 medium (CoMCont). The dishes were placed in a humidified incubator supplemented with 5% CO_2 at 37°C for 24 hours. The cell culture medium was aspirated and filtered through a

0.2μM Anopore membrane (Whatman, GE Healthcare Life Sciences, Little Chalfont, UK) [140]). The resulting cell culture supernatant is termed Conditioned Medium from Control Monocytes (CoMCont) or CoMTb as indicated.

CoMTb is rich in an *Mtb* induced intercellular network of cytokines, chemokines and *Mtb* antigens. CoMCont or CoMTb were used at a 1:5 dilution to stimulate monocytes or NHBE cells.

2.2.6 Chemical inhibitors

MDMs were pre-incubated with inhibitors for 2 hours prior to infection, monocytes for 1 hour prior to stimulation. The chemical inhibitors used are shown in Table 2.

2.2.7 ESAT-6 peptides

6kDa early secreted antigenic target (ESAT-6), a protein encoded by the RD1 virulence locus of *Mtb*, has the following amino acid sequence.

MTEQQWNFAGIEAAASAIQGNVTSIHSLLDEGKQSLTKLAAAWGGSGSEAYQGVQ
QKWDATATELNNALQNLARTISEAGQAMASTEGNVTGMFA

Peptides of 15 amino acid length with 10 overlapping amino acids (Pepceuticals, Enderby, UK) covering the entire sequence were used to stimulate MDMs. The sequences of these 17 peptides are shown in Table 3. Initially a pool of all ESAT-6

peptides was used a stimulus. Next overlapping pools containing 3-4 peptides as defined by the peptide matrix shown in Table 4 were used. Using the peptide matrix it was possible to deduce if there was a single 15 amino acid peptide sequence driving MMP-10 secretion from MDMs. The peptides were of >90% purity and time of flight mass spectrometry laser desorption for each showed a single peak only.

All the reagents used in cell culture were endotoxin free.

2.2.8 Harvesting of cell culture supernatants

Cell culture supernatants were harvested at 72 hours from MDMs, NHBEs and MRC-5 cells and 24 hours from monocytes. Where cells had been infected with live *Mtb* H37Rv the supernatants were filtered through a 0.2μm Durapore membrane (Millipore, Feltham, UK) [140].

Table 2: Chemical inhibitors used in tissue culture

Name	Target	IC_{50}	Supplier
SB203580 (SB): p38 MAPK		0.3-0.5 μM	Enzo Life Sciences, , Exeter, UK
PD98059 (PD): ERK MAPK inhibitor	MEK 1	4 μM	Calbiochem®
SP600125 (SP): JNK MAPK inhibitor	c-Jun	5-10 μM	Calbiochem®
SC-514: NF-κB inhibitor	IKK-2	3-12 μM	GE Healthcare Life Sciences,
Helenalin: NF-κB inhibitor	p65	N/A	Enzo Life Sciences
Pertussis Toxin (PT): G-protein coupled receptor inhibitor	G protein αi subunits	N/A	Calbiochem®

Table 3: ESAT-6 peptide amino acid sequences

Peptide no.	Amino acid sequence
1.	MTEQQWNFAGIEAAA
2.	WNFAGIEAAASAIQG
3.	IEAAASAIQGNVTSI
4.	SAIQGNVTSIHSLLD
5.	NVTSIHSLLDEGKQS
6.	HSLLDEGKQSLTKLA
7.	EGKQSLTKLAAAWGG
8.	LTKLAAAWGGSGSEA
9.	AAWGGSGSEAYQGVQ
10.	SGSEAYQGVQQKWDA
11.	YQGVQQKWDATATEL
12.	QKWDATATELNNALQ
13.	TATELNNALQNLART
14.	NNALQNLARTISEAG
15.	NLARTISEAGQAMAS
16.	ISEAGQAMASTEGNV
17.	QAMASTEGNVTGMFA

Table 4: ESAT-6 peptide pools matrix

Peptide pool number	5	6	7	8	9
1	P1	P2	P3	P4	P5
2	P6	P7	P8	P9	P10
3	P11	P12	P13	P14	P15
4	P16	P17			

2.3 Enzyme-linked Immunosorbent Assay

Enzyme-linked Immunosorbent Assay (ELISA) Duosets (R&D) were used to measure the levels of MMP-10 and TNF alpha in cell culture supernatants.

ELISA plates (Costar®) were coated with capture antibody (1µg/ml) overnight and blocked with 1% bovine serum albumin (BSA) for one hour. Next, standards and samples were incubated for 2 hours, followed by the detection antibody (100ng/ml) also for 2 hours. Streptavidin-Horse Radish Peroxidase (HRP) was added for 20 minutes. Washes in 0.05% Tween-20 (Sigma-Aldrich) in phosphate buffered saline (PBS, Sigma-Aldrich) were performed between each of these steps. Finally, the substrate Tetramethylbenzide (Sigma-Aldrich) was added, the colour change was monitored and after 2-3 minutes stopped using 2M sulphuric acid. The plate was read at 450nm with a reference wavelength of 540nm on a µQuant plate reader (Biotek Instruments Inc).

2.4 Luminex Bead Array

Luminex corp has developed a microparticle based multiplex immunoassay for the accurate quantification of a range of analytes in very small volumes in various sample types (serum, plasma and cell culture supernatants). This was used to quantify cytokine/ chemokines and growth factors (Invitrogen) in CoMCont and CoMTb and MMPs (R&D) in sputum, bronchoalveolar lavage and plasma.

Specific antibodies are pre-coated onto colour-coded microparticles or beads. Microparticles, standards, and samples were pipetted into a Luminex plate and agitated at 500rpm for 2 hours allowing immobilized antibodies to capture the analyte of interest. Biotinylated antibodies specific to the analyte were added and agitated for 1 hour. Next, streptavidin phycoerythrin (PE) is added with agitation for 30 minutes to generate a signal. Washes are performed between each step. Finally, the beads are resuspended and read using the Luminex® dual laser analyser (Bio-Rad Bio-Plex 200 System). One laser classifies the bead and determines the analyte which is being detected, the second laser determines the magnitude of the PE derived signal, which is in direct proportion to the analyte bound.

MMP beads (R&D systems. Abingdon UK) were used for MMP-1, -2, -3, -7, -8, -9, -10, -12 and -13. The lower level of detection of the assay was 1.1, 12.6, 7.3, 6.6, 16.6, 13.7, 3.2, 0.7 and 63.5 pg/ml respectively. Cytokine human 30-plex beads (Invitrogen) were used for CCL2 (MCP-1), CCL-3(MIP-1α), CCL-4 (MIP-1β), CCL-5

(RANTES), CXCL-8 (IL-8), CXCL-9 (MIG), CXCL-10 (IP-10), CCL-11 (Eotaxin), IFNα, IFNϒ, IL-1β, IL-1 receptor antagonist, IL-2, IL-2 receptor,IL-4, IL-5, IL-6, IL-7, IL-10, IL-12, IL- 13, IL-15, IL-17, TNFα, EGF, FGF, G-CSF, GM-CSF, HGF, VEGF.

2.5 Confocal Microscopy

Confocal microscopy was used to detect cell surface expression of MMP-14 by fluorescent immunostaining. Monocytes were stimulated on chamber slides (Nunc* Lab-Tek* II Chamber Slide* System, Thermo Scientific, Hemel Hempstead, UK). At 24 hours the cells were blocked with 5% human serum (Sigma-Aldrich)/1% BSA (Sigma-Aldrich) for 30 minutes and stained with either a mouse anti-human MMP-14 monoclonal primary antibody (MAB3328, Millipore) or a mouse isotype control antibody (ab18447, Abcam, Cambridge, UK) for 30 minutes. The cells were fixed in 2% paraformaldehyde (Sigma-Aldrich) for 1 hour, and stained with an Alexa647 conjugated secondary antibody (A-21235 goat antimouse IgG Alexa647, Invitrogen) for 30 minutes. Washes in PBS were performed between each step. The nucleus was stained with DAPI (Invitrogen) and a borosilicate glass cover slip (Fisher Scientific, Loughborough, UK) mounted.

Confocal microscopy was performed on a Leica TCS SP5 Confocal with the Leica Application Suite 2.6.2 software. Images were analysed using Image J software version 1.44p (NIH, USA).

2.6 Flow Cytometry

Flow cytometry was used to detect monocyte surface expression of MMP-14 by fluorescent immunostaining. It differs from confocal microscopy in that it is a quantitative method.

Monocytes were stimulated in 12 well plates. At 24 hours the cells were harvested using Cell Dissociation Buffer Enzyme Free (Invitrogen) at 37°C for 15 minutes and a cell scraper. Harvested cells were counted using a haemocytometer and equal cell numbers per condition transferred to FACS tubes. They were centrifuged at 1200 rpm for 5 minutes to pellet the cells and blocked with 10% heat inactivated human serum/1% BSA for 30 minutes on ice. The cells were pelleted and stained with either a PE-conjugated mouse anti-human MMP-14 primary antibody or an PE-conjugated mouse IgG2B isotype control (IC0041P, R&D) for 1 hour on ice, in the dark A final wash in 1% BSA was performed. If cells had been infected with *Mtb* they were also fixed in 2% paraformaldehyde for 1 hour.

Flow cytometry was performed immediately after staining on a FACSCalibur (BD Biosciences, Oxford, UK) machine which was calibrated regularly using FACS CaliBRITE (BD Biosciences) beads. The baseline Forward Scatter, Side Scatter and FL2H settings were adjusted using an unstained, unstimulated sample of cells. Cell viability was assessed using propidium iodide (PI, Sigma-Aldrich) staining. Flow Jo software (Version 7.6.2) was used for data analysis.

2.7 Western Blotting

Western blotting was used for chemiluminescent detection of total MMP-14 and -10, and phosphorylated and total p38/ERK /JNK as detailed below.

Proteins were separated on the basis of weight by gel electrophoresis. The samples were defrosted and heat inactivated at 70°C and an appropriate volume loaded into the wells of a NuPAGE® 4-12% Bis-Tris Gel (Invitrogen) in an XCell *SureLock* Mini-Cell (Invitrogen), filled with the appropriate running buffer (MES buffer for proteins <60kDa, MOPS buffer for proteins >60kDa, Invitrogen). A full range rainbow protein molecular weight marker (GE Healthcare Life Sciences) was also loaded. The samples were separated on the gel by electrophoresis at 200V for 50 minutes. The gel was removed and placed with a nitrocellulose membrane (Amersham Hyobond – ECL, GE Healthcare Life Sciences) in an X-Cell II Blot Module (Invitrogen) soaked in Transfer Buffer (Invitrogen) with 20% methanol (Sigma-Aldrich)/0.6% SDS (Sigma-Aldrich). Proteins were electro-transferred to the membrane at 30V for 90 minutes. The membrane was blocked with 0.1% Tween-20, 5% non-fat milk in Tris- buffered saline (Sigma-Aldrich) prior to staining with primary antibodies overnight. The membranes were then stained with HRP conjugated secondary antibodies for 1 hour. Washes with 0.1% Tween-20 in Tris- buffered saline were performed between each step. The membranes were then placed in chemiluminescent substrate (Amersham ECL Plus /Prime Western Blotting Detection System, GE Healthcare Life Sciences) for 1 to 2 minutes. They were exposed to chemiluminescence film (Amersham

Hyperfilm ECL, GE Healthcare Life Sciences) and this was developed, showing the protein of interest as a dark band.

2.7.1 Total MMP-14

Monocytes were stimulated in 6 well plates and at 24 hours were scraped into SDS lysis buffer (62.5mM Tris, 2% SDS, 10% glycerol, 50mM DDT, 0.01% Bromphenol blue, Sigma-Aldrich). Beta- actin (β-actin) was used as the loading control. The primary antibodies were rabbit anti-human polyclonal anti-MMP-14 antibody (AB6004, Millipore) and mouse anti-human monoclonal anti-β-actin (A1978, Sigma-Aldrich). The secondary antibodies were HRP -conjugated goat anti-rabbit IgG (7074, Cell Signalling Technology, Boston, USA) and HRP-conjugated goat anti-mouse IgG (115-035-062, Jackson ImmunoResearch Europe Ltd, Newmarket, UK).

2.7.2 Phosphorylated and total p38/ERK /JNK

Monocytes were stimulated in 60mm dishes and at 30 minutes were scraped into SDS lysis buffer. The primary antibodies were rabbit polyclonal phospho-p38/ total p38 (9211/9212), phospho-ERK/ total ERK (9101/9102) and phospho- JNK/ total JNK (9251/9252), (Cell Signalling Technology). The secondary antibody was HRP-conjugated goat anti-rabbit IgG (7074, Cell Signalling Technology). The membrane was stripped with Restore Plus western blot stripping buffer (ThermoScientific) for consecutive probing of phosphorylated and total forms on the same membrane.

2.7.3 Total MMP-10

Cell culture supernatants harvested from macrophages at 72 hours were loaded with 2x loading buffer. The primary antibody was Rabbit polyclonal to MMP-10 (ab38930, Abcam) and secondary HRP-conjugated goat anti-rabbit IgG (7074, Cell Signalling Technology).

The densitometry of bands was measured using Image J software version 1.44p (NIH, USA).

2.8 Real Time Polymerase Chain Reaction

Real time polymerase chain reaction (RT-PCR) was used to measure MMP-10 mRNA levels in macrophages and MMP-14 mRNA levels in monocytes.

2.8.1 RNA extraction

Total RNA was extracted from cells using phenol chloroform extraction and the Purelink RNA Mini Kit (Invitrogen) which is a column based nucleic acid purification kit.

Monocytes or macrophages were stimulated in 6 well plates and after 6 or 24 hours scraped into 1ml TRIzol (Sigma-Aldrich). Samples were stored at -80 ºC for a maximum of 1 month. They were defrosted, chloroform (Sigma-Aldrich) added then centrifuged at 12 000 g for 5 minutes. The colourless upper phase (containing RNA)

was added to an equal volume of 70% ethanol. The RNA was then extracted onto the silica membrane of a spin column by a series of washes with buffers from the kit. The extracted RNA was finally eluted into 30µl RNAse free water and stored at -80 ºC. The samples were defrosted and RNA concentration and quality determined on the NanoDrop ND-1000 spectrophotometer prior to cDNA synthesis.

2.8.2 cDNA synthesis

cDNA was synthesized using the Quantitect Reverse Transcription Kit (Qiagen,Manchester, UK). The final reaction volume was 20 µl. For each sample a volume of RNA equivalent to 50ng, 200ng, 500ng or 1µg was diluted up to 12µl with RNase-free water. 2µl of genomic DNA wipeout buffer was added and heated at 42 ºC for 2 minutes. A 6 µl mastermix containing random primers, reverse transcriptase and dNTPs was added and heated at 42ºC for 15 minutes, with primer annealing and strand extension occurring within the same reaction. The reaction was terminated by heating at 95 ºC for 3 minutes. The synthesized cDNA was stored at -20˚C.

2.8.3 Polymerase chain reaction

The final PCR reaction volume was 25µl in nuclease fee water (Gibco®). It contained diluted cDNA or standard, 1x Brilliant II Taq polymerase (Agilent Technologies, Wokingham, UK), 1x primers/probe for the gene of interest (MMP-14 or MMP-10, Applied Biosystems, Manchester, UK) and a reference gene (β-actin). Applied Biosystems do not provide the end user with the primer/ probe sequences.

RT-PCR was performed in a Framestar 96 well PCR plate (4titude, Wotton, UK) on a Stratagene Mx3000Pro machine with an initial 10 minute denaturation step at 95˚C (Taq polymerase activation) followed by 40 cycles at 95˚C for 30 seconds (cDNA denaturation) then 60˚C for 1 minute (annealing of primers and probes/extension). Gene expression was normalised to 18S or β-actin. This reference genes was chosen for the stability of its expression across different experimental conditions.

For MMP-14 and β-actin a plasmid standard was kindly synthesized by Dr Catherine Ong. Serial dilutions were used to generate a standard curve with a known number of gene copies. A plasmid standard was not available for MMP-10 therefore a standard curve was generated using the serial dilutions of the sample with the highest expected expression of the gene of interest and 'quantities' were assigned.

The cycle threshold for the gene of interest and reference gene was extrapolated from the standard curve to give an amount. The gene of interest was then normalized to the reference gene. The unstimulated sample was chosen as the 'calibrator' sample and all others expressed as a fold change compared to this.

2.9 Fluorescent Collagen Degradation Assay

A fluorescent collagen degradation assay was used to investigate monocyte driven collagen destruction in *Mtb* and the role of MMP-14 in the process.

Chamber slides (PAA Laboratories Ltd,, Yeovil, UK) were coated briefly with 0.005% poly-L-lysine (Sigma-Aldrich) to create a substratum to improve cell adherence, then 0.5% glutaraldehyde (BDH) to non-covalently couple the substratum to the fluorescent collagen. Fluorescein isothiocyanate (FITC) conjugated type I collagen, from bovine skin (Sigma-Aldrich) was diluted to 100µg/ml in 0.1M acetic acid, vortexed and a volume equating to 15µg/cm^2 added to each chamber. The collagen solution was left to adhere to slides for 2 hours at room temperature with gentle agitation. Washes with sterile PBS (HyClone, Thermo Scientific) to remove all residual reagents were performed between each step, and all solutions were made using sterile PBS or Cell Culture Grade Water (HyClone, Thermo Scientific) to ensure the slides were suitable for tissue culture. The slides were stored at 4˚C overnight.

Monocytes were adhered to commence an experiment as previously described. After 24 hours incubation the chamber was removed. The slide was washed gently in PBS, stained and fixed as per the MMP-14 fluorescent immunostaining protocol above. Collagen degradation was indicated by absence of the green FITC signal on fluorescent microscopy.

Confocal microscopy was performed on a Leica TCS SP5 Confocal with the Leica Application Suite 2.6.2 software. Images were processed and quantified using Image J software version 1.44p (NIH, USA).

2.10 Agarose Spot Assay for Chemotaxis

This assay was used to investigate monocyte migration towards CoMTb employed as a chemotactic agent rather than a direct stimulus. It is a modification of a previously described assay [141].

A 0.5% agarose, low gelling temperature (Sigma-Aldrich) solution in sterile PBS was boiled and then allowed to cool to 40˚C on a hot block. RPMI 1640 or CoMTb was added to the agarose solution at a 1:10 dilution. Using cut tips 10µl of the solution was pipetted onto cover glass bottom chamber slides (PAA-Laboratories) pre-coated with type I collagen as above. This created a 'spot' on the surface of the slide with the agarose acting as a media through which chemoattractants in the CoMTb can diffuse. Two spots per condition were pipetted. The slide was then left at 4˚C for 5 minutes for the agarose to set.

Monocytes were adhered immediately to commence an experiment. After 24 hours incubation the slide (with the chamber in situ) was washed gently in PBS and stained and fixed as per the MMP-14 fluorescent immunostaining protocol above except DAPI staining and cover slip placement were excluded. Images were taken using an

Olympus E-620 camera attached to the Olympus CK2 light microscope. Images were processed and quantified using Image J software version 1.44p (NIH, USA).

2.11 Clinical Samples: Collection and Processing

2.11.1 Plasma

These samples had been collected previously by Dr Gurjinder Sandhu [142]. The study was ethically approved by Universidad Peruana Cayetano Heredia (Lima, Peru) and Imperial College London (London, United Kingdom). Written informed consent was obtained in all cases.

Participants were recruited over a 2 year period from 16 community TB clinics serving the shantytown of Ventanilla in Lima, Peru. All patients provided four consecutive sputum samples for microscopy and culture. Patients with active TB were recruited on the basis of positive sputum microscopy with subsequent confirmation by culture. Symptomatic controls were those who had symptoms suspicious of TB (persistent cough and 2 or more from fever, weight loss, decreased appetite or haemoptysis) but in whom active TB was subsequently excluded by sputum microscopy and culture. Healthy controls were recruited from randomly selected households in the community where patients with active TB were not resident.

A 4 ml blood sample was obtained from each participant in an EDTA tube and transferred to the laboratory on ice. The plasma was separated (3500 rpm, 10

minutes) aliquotted and frozen at -70°C for subsequent analysis [142] . Prior to Luminex bead array analysis the samples were defrosted at 4°C and multiple 50µl aliquots were placed in 96 well plates before refreezing at -70°C. This minimized freeze thaw cycles of the samples prior to measurement of MMPs.

2.11.2 Induced sputum – supernatant and RNA extraction

The induced sputum samples from which the supernatant was analysed had been collected previously by Dr Naomi Walker [77]. The induced sputum samples from which the RNA was extracted and analysed were collected prospectively by Dr Tara Sathyamoorthy. The studies were ethically approved by the University of Cape Town (UCT) Research Ethics Committee. Written informed consent was obtained in all cases.

Adult participants were recruited from Ubuntu clinic in the township of Khayelitsha, Cape Town, South Africa.

TB patients met at least one inclusion criteria from:

- Sputum smear positive for AFB on microscopy *or* sputum Gene Xpert positive *or*
- Sputum culture positive for *Mtb or*
- Clinical features highly suggestive of TB with diagnostic features on chest radiograph and started on TB treatment by a clinician

Control patients were asymptomatic individuals who presented voluntarily. Only patients within 72 hours of commencing treatment and HIV negative cases were included.. A brief clinical history and examination were performed, followed by a chest radiograph. Chest radiograph infiltration was scored using a previously developed modified system on a scale of 0 – 10 according to the number of segments involved (Fig. 3) [143].

Sputum induction was performed in designated, well ventilated, isolated areas using nebulised 5% saline. 1ml of RNA later (Qiagen) was added on site to the samples which would be processed for RNA extraction. Two samples were sent for microbiological investigation (smear microscopy and culture) and one sample was transported to UCT BSL3 laboratory on ice.

Mucolysis was performed by adding an equal volume of 0.1% Dithiothreitol (Sigma-Aldrich) and agitating gently at room temperature for 20 minutes. In the case of samples processed for supernatant collection they were then centrifuged at 1600rpm for 5 minutes and the supernatant was aspirated and sterile filtered through a 0.2μM Durapore membrane (Millipore) [140] to remove *Mtb*. The filtrates were aliquotted and frozen at -20°C for subsequent analysis [77]. In the case of samples to be processed for RNA extraction the mucoid layer was filtered off by passing through 100μM pore size strainer (BD) then the sample was centrifuged at 500g for 10 mins. The cell pellet was aspirated and 1.5ml of cold TRI reagent added before vortexing. The TRI reagent kills the *Mtb*. The samples were stored at minus 80 ^{o}C until RNA extraction.

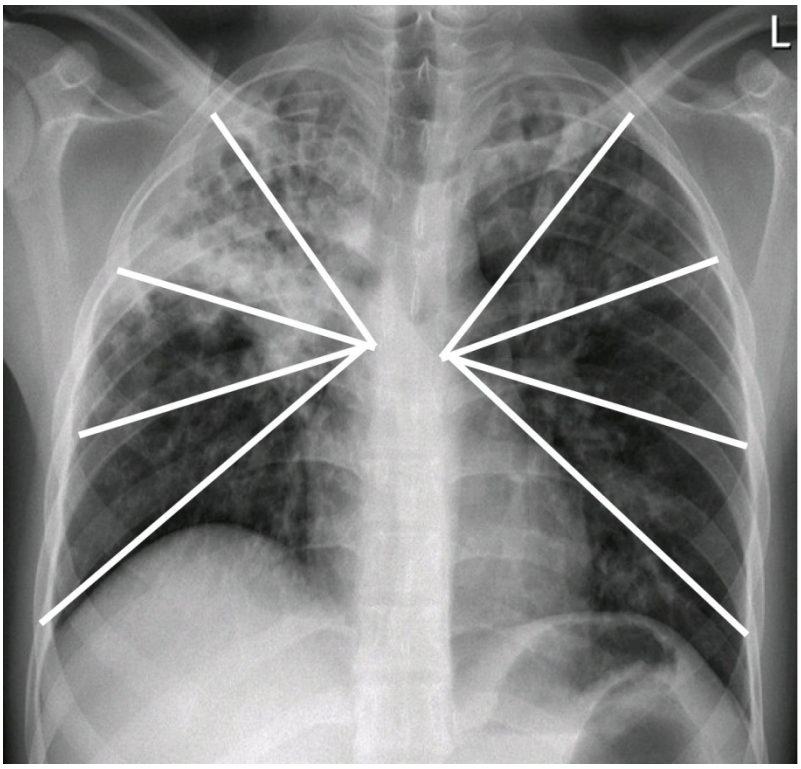

Figure 3: Chest Radiograph Scoring

Chest radiograph infiltration was scored using a previously developed modified system on a scale of 0 – 10 according to the number of segments involved. The white lines shown on the chest radiograph here delineate the ten segments.

2.11.3 Bronchoalveolar lavage

These samples had been previously collected by Dr Shivani Singh [144]. The study was ethically approved by the Nalanda University Hospitals Research Ethics Committee. Written informed consent was obtained in all cases. Participants were recruited over a 1 year period at Nalanda University Hospitals, Patna, India.

BAL was performed on patients being investigated for respiratory symptoms. Patients with active TB were those with positive bronchoalveolar lavage microscopy with subsequent confirmation by culture. Control patients were those respiratory symptomatics in whom active TB was excluded by sputum microscopy and culture. Flexible bronchoscopes were used and the procedure was performed between two bronchoscopists.

The samples were centrifuged at 1600rpm for 5 minutes. The supernatant was aspirated and sterile filtered through a 0.2μM Durapore membrane (Millipore) [140]. The filtrates were aliquotted and frozen at -20°C for subsequent analysis.

2.11.4 Lung Immunohistochemistry

This project was approved by the Hammersmith and Queen Charlotte's Research Ethics Committee. Lung biopsy blocks taken from patients investigated for lung cancer but with a final diagnosis of tuberculosis were studied, along with control patients whose biopsies showed normal lung tissue. The blocks were deparrafinized and then rehydrated prior to antigen retrieval. The anti MMP-14 primary antibody (ab77965, Abcam) was applied, followed by a post primary HRP conjugated polymer.

Finally the diaminobenzedine substrate was added. The block was then haemotoxylin costained. Washes were performed between each step. The slides were reviewed with a histopathologist and images were taken using a Zeiss Askiospop 2 with Askioscan camera.

2.12 Statistical analysis

Statistical analysis was performed using GraphPad Prism 5 by Student's t-test, Mann Whitney U test or One Way Analysis of Variance (ANOVA) with Tukey's post hoc analysis. ROC curves were generated using R version 2.15.2 using the package pROC [145]. We have used Youden's index to calculate and optimal cut off threshold in each case [146]. Principal component analysis was conducted using Qlucore Omics Explorer 2.2 (Qlucore). Clinical data and plasma MMPs were analyzed firstly for correlation by principal component analysis, and then the divergence between patient groups was studied.

3. ANALYSIS OF CIRCULATING MMPS INDICATES A DOMINANT ROLE FOR COLLAGENASES

3.1 Introduction

There has been a growing interest in analysis of biomarkers in TB, both as a diagnostic marker and also to monitor the efficacy of treatment. However, analysis of plasma and serum inflammatory mediators, such as cytokines and chemokines, to better understand disease pathogenesis has generally not shown major differences between patients with TB and control groups [147]. Studies in small patient cohorts have shown higher levels of plasma MMP-8 and MMP-9 in patients with TB compared to controls [148-150]. However, a comprehensive analysis of circulating MMPs in a well-powered clinical cohort has not been previously performed. Therefore in this study we investigated the hypothesis that MMPs are key drivers of TB immunopathology by analysing the plasma levels of MMP-1, -2, -3, -7, -8, -9 and -10 in a set of prospectively collected samples from 380 patients with active tuberculosis, symptomatic controls (symptoms suspicious of TB but active disease excluded) and healthy controls. These samples had been collected as part of a proteomic study [142] and I was able to study them with a hypothesis-driven approach.

3.2 Results

3.2.1 Baseline patient characteristics

120 healthy controls, 109 symptomatic controls and 151 patients with active pulmonary TB were recruited (Table 5). The healthy and symptomatic groups were well matched for age, but the TB group was significantly younger than the symptomatic group (median TB 28.5 years *vs*. symptomatic 32 years, $p<0.05$). There were a higher proportion of females in the healthy and symptomatic controls group (66% for both) and a higher proportion of males in the active TB group (56%). This may reflect a difference between the sexes in health seeking behaviour, as females tend to attend clinics more regularly than males [151]. All the patients with active TB were either smear or culture positive with 92% both smear and culture positive. All symptomatic controls were smear and culture negative. There was a lower proportion of patients with past TB in the healthy controls (3%) but similar proportion in the symptomatic controls (17%) and active TB (23%). Patients with active TB had a lower body mass index (BMI) at enrolment compared with symptomatic controls and healthy controls (TB 21.66 *vs*. symptomatic 24.15 and healthy 25.86 respectively, $p<0.001$ for both), consistent with the diagnosis of pulmonary TB [152]. Symptomatic controls and patients with active TB had overlapping clinical symptoms though the duration was longer in the TB group (median TB 7 days *vs.* symptomatic 2 days, $p<0.001$).

Table 5: Plasma matrix metalloproteinase analysis - Characteristics of patient cohort

Patient characteristics	Healthy		Symptomatic		TB		
	n	%	n	%	n	%	
Total number of patients	120	31	109	29	151	40	p<0.05 Symptomatic vs. TB
Median age (IQR) years	31 (23-40)		32 (24.5 - 47.5)		28.5 (22-38)		
Sex ratio Male: Female	41:79	34:66	37:72	34:66	85:66	56:44	
Smear:							
Positive	n/a		0	0	139	92	
Negative	n/a		109	100	7		
Culture:							
Positive	n/a		0	0	139	92	
Negative	n/a		109	100	8		
Past TB	4	3	19	17	34	23	
Mean BMI (SD)	25.86 (4.33)		24.15 (4.67)		21.66 (2.97)		p<0.001 Healthy or Symptomatic vs. TB
Symptoms:							
Cough	42	35	109	100	151	100	
Haemoptysis	2	2	28	26	71	47	
Fever	17	14	52	48	93	62	
Weight loss	40	33	72	66	123	81	
Appetite loss	23	19	57	52	109	72	
Median symptom duration (IQR) days	0		2 (1-10)		7 (1-30)		p<0.001 Symptomatic vs. TB

3.2.2 Plasma MMP-1 and MMP-8 are elevated in active pulmonary TB and MMP-8 is relatively TB-specific

MMP-1, -2, -3, -7, -8, -9 and -10 were profiled in the plasma of all patients by Luminex multiplex array. Samples from the archived cohort were defrosted in the cold room and aliquotted onto 96 well plates. In preliminary studies, MMP-12 and MMP-13 were not detected in plasma and so were not included in this analysis of circulating MMPs. MMP-2 was detected but was excluded from statistical analysis as many values fell out of range above the standard curve.

MMP - 1 was increased in both active pulmonary TB and symptomatics compared to healthy controls ($p<0.001$ and 0.01 respectively), but there was no difference between active TB and symptomatics (Fig. 4A). The concentration of MMP-8 was specifically increased in the plasma of patients with active TB compared to both symptomatics as well as healthy controls (Fig. 4D both $p <0.001$). There was no difference between symptomatics and healthy controls. MMP - 7 was increased in both active pulmonary TB and symptomatics compared healthy controls (p 0.01 for both), but there was no difference between active TB and symptomatics (Fig. 4C). However the median MMP-7 value in respiratory symptomatics was higher at 66pg/ml compared to 20.1 pg/ml in both active pulmonary TB and healthy controls, suggesting that plasma MMP-7 is elevated in a small proportion of patients with TB only. MMP-9 was increased in active TB only compared to healthy controls (Fig. 4E, $p<0.05$). There was no statistically significant difference in MMP-9 between active TB and symptomatic controls or symptomatic controls and healthy controls. MMP-3 and MMP-10 showed no difference between any of the groups (Fig. 4B and 4F). Therefore the MMPs that were elevated in TB were MMP-1, -7, -8 and -9, but MMP-8

was the most TB specific as it was elevated compared to respiratory symptomatics. Median values and interquartile ranges for all MMPs are provided in Table 6.

Table 6: Plasma MMP levels by patient group

	Healthy	Symptomatic	TB
MMP-1	1.55 (1.55-90.9)	223.9 (52.36 - 71.1)	229.2 (71.1 - 593.6)
MMP-3	6059 (3949 - 10656)	5956 (4097 - 9708)	7296 (4469 - 11386)
MMP-7	21 (21 - 21)	66 (21 - 222)	21 (21 – 147)
MMP-8	3236 (2244 - 6379)	3547 (2099 - 6259)	8359 (4471 - 16069)
MMP-9	58234 (39489 - 88224)	59853 (37009 - 97915)	73181 (47367 - 114444)
MMP-10	512 (363 – 711)	584 (372 – 894)	539 (384 – 759)

Median levels and interquartile ranges (in brackets) in pg/ml

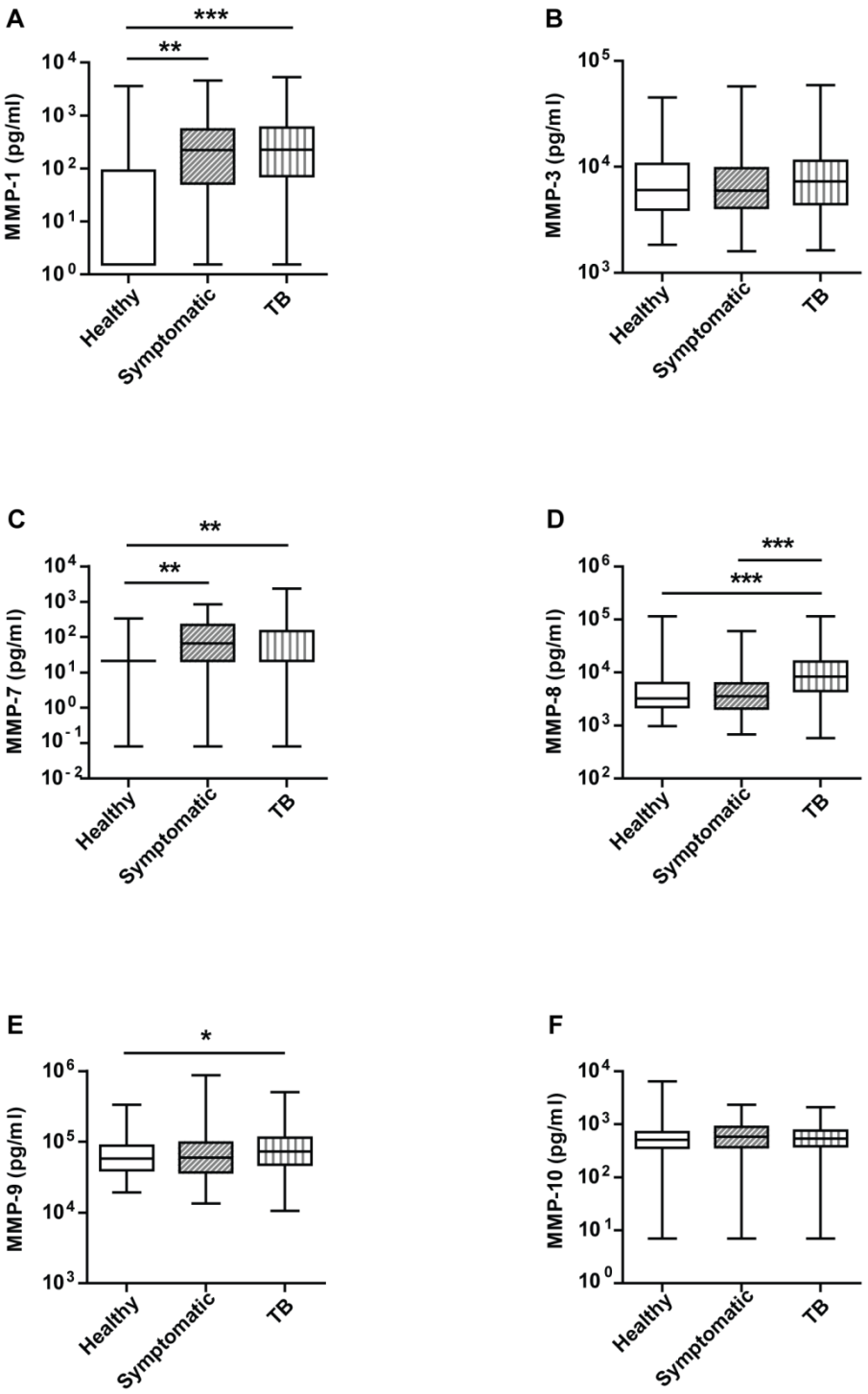

Figure 4: Neutrophil collagenase MMP- 8 is specifically upregulated in the plasma in active pulmonary TB

Plasma samples were collected prospectively from patients in Lima, Peru. **A,** MMP-1 was increased in both active TB and symptomatic controls compared to healthy controls. **B,** MMP-3 showed no difference between the groups. **C,** MMP-7 was increased in both active TB and symptomatic controls compared to healthy controls. **D,** MMP-8 was specifically increased in active TB only compared to symptomatic controls and healthy control. **E,** MMP-9 was increased in active TB only compared to healthy controls. **F,** MMP-10 showed no difference between the groups. MMP concentrations were measured by Luminex bead array. Statistical analysis was performed using a one way ANOVA with Tukey's post hoc test (***p<0.001, **p<0.01, *p<0.05). Each box represents the 25th to 75th centiles, the central line the median, and the whiskers the minimum and maximum values.

3.2.3 Plasma collagenases are higher in males than females and elevated levels are present in active TB in males and females analysed separately

It has previously been shown that MMP-3, -8 and -9 are higher in males than in females [153]. In the cohort analysed above, MMP-1, -3, -8 and -9 were similarly higher in males (Fig. 5A to D and Table 7, MMP-1 $p<0.05$, MMP-8 $p<0.001$, MMP-3 and MMP-9 $p<0.0001$).

The active TB group had a higher percentage of males and the symptomatic control group more females. Therefore MMP-1, -3, -8 and -9 levels were analysed separately for each sex to ensure that the elevated levels observed were not artefactual. With sex-dependent analysis, MMP-1 remained increased in both active TB and symptomatics compared to healthy controls in males (Fig 6A, $p<0.01$ and 0.05 respectively). However in females, it was only increased in active TB compared to healthy controls (Fig 6B, $p<0.01$). MMP-8 remained increased in active TB compared to symptomatics and healthy controls in both males (Fig. 6C $p< 0.05$ and 0.01 respectively) and females (Fig 6D, $p < 0.01$ and 0.05 respectively). MMP-3 and MMP-10 shows no significant differences between the three clinical groups for the sexes when analysed separately. The median values and interquartile ranges for MMP-1, -3, -8 and -9 for the sexes separately and across the three clinical groups are provided in Table 7.

Table 7: Plasma MMP levels for males and females separately by patient groups

		All	Healthy	Symptomatic	TB
MMP-1	Male Female	204 (9- 540) 83 (9-317)	7 (4-84) 10 (6-94)	344 (81-635) 202 (36-467)	287 (83-598) 178 (29-594)
MMP-3	Male Female	10134 (7302-14111) 4848 (3352 - 6774)	10603 (7063 - 14968) 5177 (3344 - 7517)	10725 (7836 - 14327) 4978 (3440 - 6774)	9640 (7181 - 13789) 4702 (3273 - 6508)
MMP-7	Male Female	34 (20 – 116) 3 (19 – 108)	N/A	N/A	N/A
MMP-8	Male Female	6277 (3201 - 12381) 4094 (2214 - 7725)	3413 (2409 - 6368) 3125 (2040 - 6427)	4069 (2363 - 6889) 3374 (2021 - 5722)	10622 (5381 - 17359) 7043 (3909 - 13404)
MMP-9	Male Female	75150 (50272- 111266) 55631 (38356 - 92406)	64786 (48935 - 107322) 52659 (34556 - 82052)	77247 (46492 - 109487) 53285 (35007 - 88313)	80411 (53645 - 117600) 63861 (42572 - 108639)
MMP-10	Male Female	543 (376 – 788) 526 (364 – 764)	N/A	N/A	N/A

Median levels and interquartile ranges (in brackets) in pg/ml

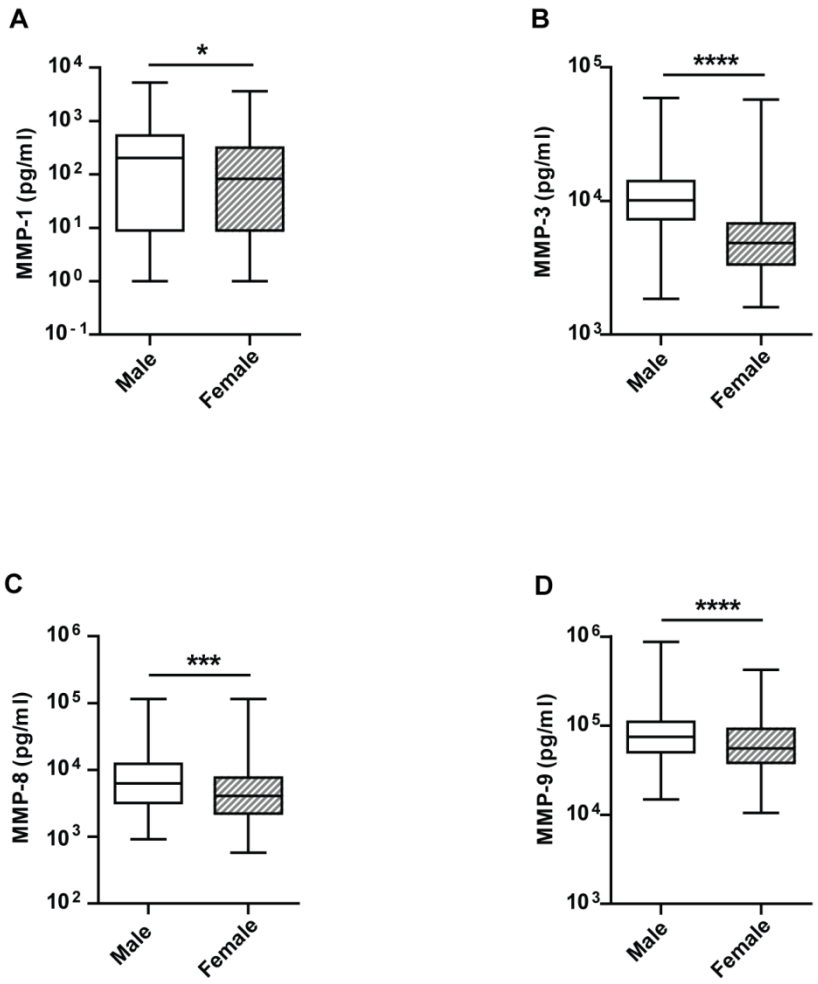

Figure 5: Plasma MMP -1, -3, -8 and -9 are higher in males than females

All the plasma MMPs measured were analysed separately by gender across the entire cohort. **A,** MMP-1 **B,** MMP-3 **C,** MMP-8 and **D,** MMP-9 were all higher in males than females. MMP concentrations were measured by Luminex bead array. Statistical analysis was performed using a one Mann-Whitney U Test (****p<0.0001, ***p<0.001, *p<0.05). Each box represents the 25th to 75th centiles, the central line the median, and the whiskers the minimum and maximum values.

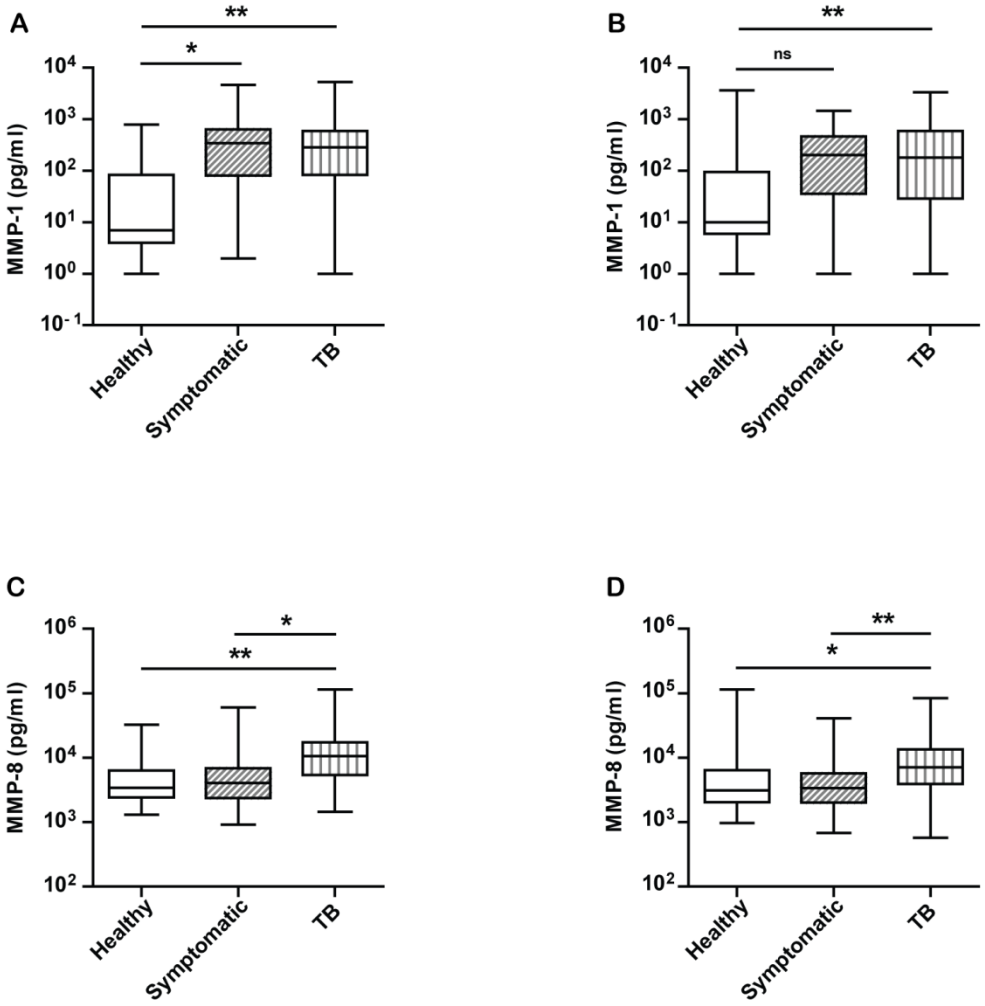

Figure 6: Plasma MMP-1 and MMP-8 remain elevated in TB when analysed by gender

Across the entire cohort MMP-1 and MMP-8 were higher in men than women. As there was a higher proportion of women in the healthy control and symptomatic control groups MMP-1 and MMP-8 in the clinical subgroups were analysed individually for males and females. **A,** In males MMP-1 was increased in TB and symptomatics compared to healthy controls. **B,** In females MMP-1 was only increased in TB compared to healthy controls. **C,** In males MMP-8 was specifically increased in TB only compared to symptomatic controls and healthy controls. **D,** Similarly in females MMP-8 was specifically increased in TB only compared to symptomatic controls and healthy controls ($p<0.01$ and 0.05 respectively). MMP concentrations were measured by Luminex bead array. Statistical analysis was performed using a one way ANOVA with Tukey's post hoc test (**$p<0.01$, * $p<0.05$). Each box represents the 25^{th} to 75^{th} centiles, the central line the median, and the whiskers the minimum and maximum values.

3.2.4 Principal component analysis demonstrates a distinction between TB and control patients but not between TB and respiratory symptomatics

Next, the association between selected clinical features and plasma MMPs was investigated, using Principal Component Analysis (PCA). PCA is a mathematical algorithm, which is used to identify patterns in large data sets and reduces the dimensionality of the data while expressing it in a manner that highlights similarities and differences. The dimensionality of the data is reduced by looking for directions along which the variation is maximal, known as principal components [154]. Individual points on the plot generated represent a single analyte or patient. The distance between points reflect their Pearson correlation coefficient, whereby a short distance demonstrates close correlation.

Utilising the Qlucore multivariate analysis software, I analysed the relationship between circulating MMPs and clinical characteristics such as cough, body mass index (BMI), past TB, sex, sputum smear result, tuberculin skin test (TST) and IFNγ release assay (IGRA) (Fig. 7A). MMP-1, -7, -8 and -9 were included in the analysis as they were elevated in TB. The variables that associated most closely were TST and IGRA, consistent with both depending on the host immune response to *Mtb*, and MMP-8 and MMP-9, suggesting that both have a common source, consistent with them being co-secreted by neutrophils. Further analysis using all the variables demonstrated a relatively good separation between healthy controls and TB patients (Fig. 7B). However, when the same analysis was performed for TB against respiratory symptomatics, there was relatively greater overlap between the groups (Fig. 7C), suggesting that the utilisation of these 11 variables to differentiate TB from respiratory symptomatics may be of limited applicability.

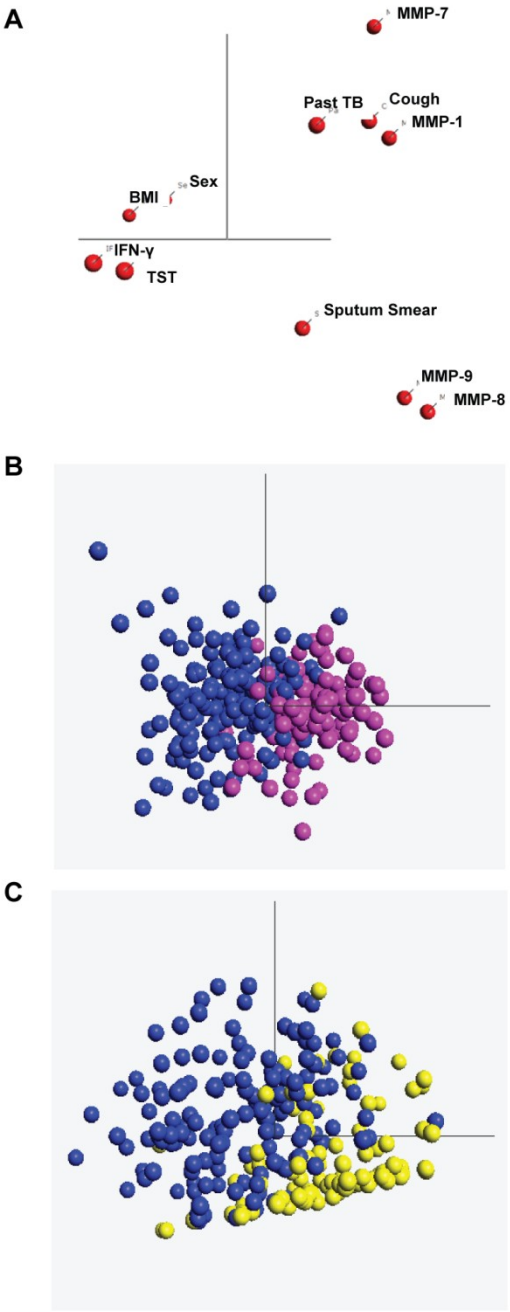

Figure 7: PCA demonstrates good discrimination between controls and TB, but not TB and respiratory symptomatics

A, Three dimensional network principal component analysis plot demonstrating the association between different analytes. Individual points represent a single analyte, and the distance between points reflect their Pearson correlation coefficient, whereby a short distance demonstrates close correlation. **B, C,** Three dimensional network PCA plot generated using key parameters that differed between patients with TB and controls: cough, BMI, past TB, sex, sputum smear result, TST and IGRA, MMP-1, -7, -8 and -9. Each point represents one patient. Control patients are purple, TB patients are blue and respiratory symptomatics are yellow. Divergence is demonstrated between controls patients and TB patients **(B)** but there is greater overlap between respiratory symptomatics and TB patients **(C).**

3.2.5 Plasma MMP-8 may help differentiate patients with active pulmonary TB from symptomatic controls

Next, receiver operating characteristic (ROC) analysis was performed utilising MMP-8 as a single variable to determine if it helped differentiate active TB from symptomatics (symptoms suspicious of TB but active disease excluded), because this was the most highly discriminatory analyte of all MMPs measured. The area under the curve (AUC) was 0.765 (Fig. 8A) with a Youden's criteria for optimal cut-off of MMP-8 = 6600 pg/ml with a specificity of 77.3% and sensitivity of 64.3%.

When ROC curves were plotted separately for males and females they showed that plasma MMP-8 has a greater predictive ability for active TB in men compared to women (Fig. 8B and 8C). For men the AUC was 0.798 with a Youden's criteria of 6967 pg/ml and a higher specificity (80.8%) and sensitivity (68.2 %.) For women the AUC was 0.721 with a Youden's criteria of 3780 pg/ml and a lower specificity (57%) though a higher sensitivity (79.7%) than the ROC curve for the sexes combined or men alone.

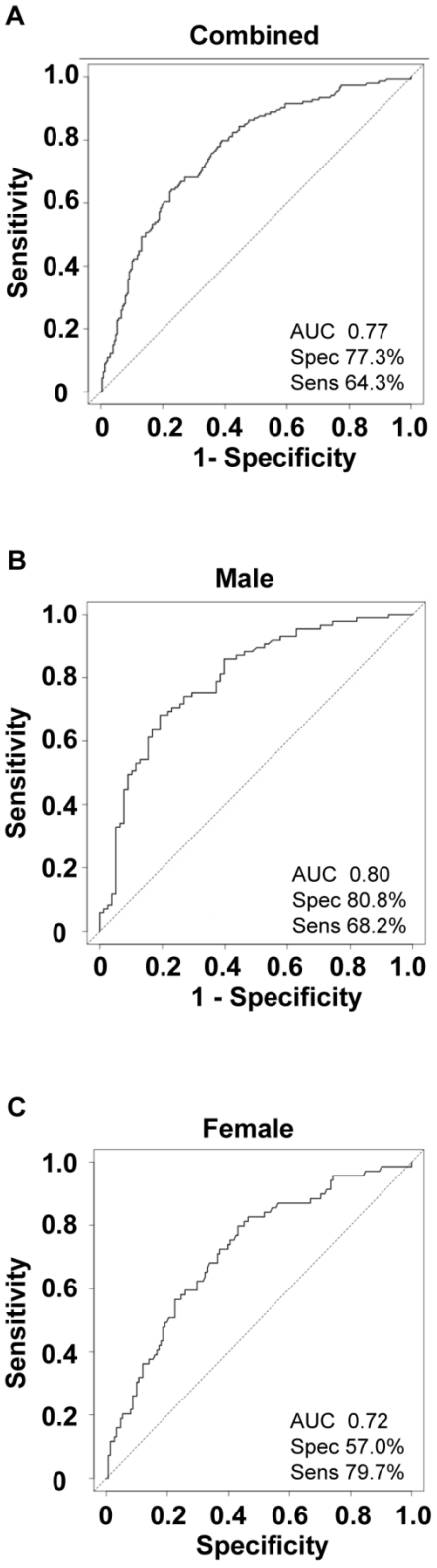

Figure 8: Plasma MMP-8 discriminates TB from symptomatic controls with moderate accuracy

ROC curves were plotted to investigate the ability of MMP-8 to discriminate TB from symptomatic controls (symptoms suspicious of TB but active disease excluded). **A,** For the entire cohort the AUC was 0.77 indicating moderate accuracy as a discriminator, optimal cut off MMP-8= 6600 pg/ml, specificity 77.3%, sensitivity 64.3%. **B,** For males separately the AUC) was 0.80 indicating good accuracy as a discriminator, optimal cut off MMP-8= 6967 pg/ml, specificity 80.0%, sensitivity 68.2%. **C,** For females separately the AUC was 0.72 indicating moderate accuracy as a discriminator, optimal cut off MMP-8= 3780 pg/ml, specificity 57%, sensitivity 79.7%.

3.2.6 Plasma MMP-8 negatively correlates with BMI in TB

Finally, as it was noted that patients with active TB had a lower BMI at enrolment, the relationship between BMI and plasma MMP-8 levels was assessed for this subgroup. Low BMI is a marker of poor nutritional status and is a risk factor for developing TB [152], relapse after treatment [155] and death [156]. A negative correlation between plasma MMP-8 and the BMI of TB patients was identified (Fig. 9 r= - 0.460; **** p<0.0001). Though I was unable to find published data indicating a negative correlation between BMI and extent of cavitation, underweight patients with cavities have been identified as particularly high risk for relapse [155]. Therefore the negative correlation between BMI and MMP-8 supports a role for this collagenase in driving tissue destruction in TB patients

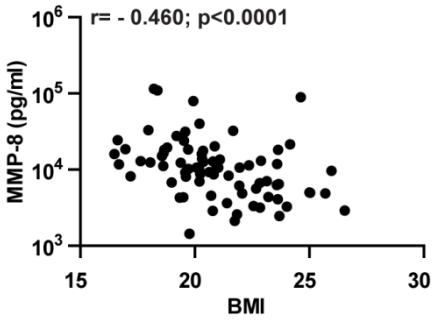

Figure 9: Plasma MMP-8 negatively correlates with BMI in TB

Plasma MMP-8 negatively correlated with the BMI of patients with TB by Spearman correlation coefficient (r= - 0.460; **** p<0.0001).

3.3 Discussion

A cohort of 380 patients with active pulmonary TB, respiratory symptomatics (symptoms suspicious of TB but active disease excluded) and healthy controls was prospectively recruited and carefully characterised. The first comprehensive analysis of circulating MMPs comparing healthy controls, patients with pulmonary TB and respiratory symptomatics was performed. Two collagenases, MMP-1 and MMP-8, were elevated in active TB, but MMP-8 was specifically upregulated in TB compared to both symptomatics and healthy controls. MMP-1, -3, -8 and -9 were higher overall in males than females. Analysis of the sexes separately confirmed that MMP-8 was increased in active TB compared to symptomatic and controls, and MMP-1 was increased in both active TB and symptomatic controls. Consequently, the results were not being falsely skewed by the higher number of female symptomatics and healthy controls. The ROC curve for MMP-8 showed that it may help discriminate active pulmonary TB from symptomatics.

Previous studies have assessed MMPs at the primary site of disease rather than in the circulation, by analysis of sputum and lung biopsies. An early study showed that in two patients with active TB compared to a single control, MMP-9 mRNA measured by northern blot was elevated [69]. Immunohistochemical analysis showed MMP-1 expression both in the macrophages of TB granulomas and adjacent epithelial cells [71, 72]. MMPs -1, -2, -3 and -8 were increased in the induced sputum of patients with pulmonary TB [77]. MMP-1 and MMP-2 correlated with the extent of infiltration on chest radiograph and were higher in those patients with cavitation [76, 77]. The

MMP-1 in the sputum was shown to be proteolytically active by casein zymography [76]. A longitudinal study of induced sputum MMP concentrations at diagnosis and then at the second week, eighth week and end of TB treatment showed that MMP-1,-2,-3,-8 and -9 were increased in pulmonary TB compared to healthy controls at diagnosis. MMP-1 and -3 were associated with higher TB severity scores. Treatment resulted in a rapid reduction of MMP-1, -3 and -8 levels [157].

Therefore, in this study of circulating MMPs, where the collagenases MMP-1 and MMP-8 were elevated, there is some consistency with the induced sputum studies but there are also differences in sampling the two compartments. MMP-1 seems predominant in the sputum, whereas MMP-8 is the best marker in the plasma, suggesting that analysis of plasma does not completely reflect events in the lung interstitium. It is interesting to note that two collagenases were elevated in plasma, as collagen is the primary structural fibril of the pulmonary ECM and our findings support the hypothesis that excessive collagenolytic activity is of particular importance to the tissue destruction seen in pulmonary TB.

Plasma MMPs in tuberculosis have previously been investigated in TB. The first study compared plasma MMP-2 and MMP-9 levels in 20 patients with active tuberculosis and 20 healthy controls in Poland, using quantitative zymography. Elevated MMP-9 but not MMP-2 levels were identified in TB. The MMP-9 levels correlated with radiological disease severity as measured by computed tomography [149]. More recently plasma MMP-1, MMP-7, MMP-8 and MMP-9 levels were measured in 28 patients with tuberculous pleural effusions and 16 patients with non-tuberculous effusions in India, who were all HIV seronegative, using ELISA. Plasma

MMP-8 only was significantly elevated in TB compared to non-TB. Plasma MMP-1 and MMP -9 but not MMP-7 showed a trend towards being higher in TB, though statistical significance was not achieved [148].

Two studies that investigated plasma MMPs in TB were published in 2013, indicating growing interest in the area. One study measured plasma MMP-8 levels in patients with active pulmonary TB and healthy controls in South Africa, of mixed HIV seroprevelance, using Luminex bead array. Plasma MMP-8 was elevated in TB compared to healthy controls. In this study, Procollagen III N-terminal peptide (PIIINP) was also measured, which is released during the synthesis and breakdown of Type III Collagen. Plasma levels of PIIINP were also elevated in the TB group. ROC analysis combining plasma PIIINP and MMP-8 differentiated pulmonary TB from healthy controls with an AUC of 0.832, a sensitivity of 89.5% and specificity of 65% [150]. The second study used an unbiased approach of DNA aptamers for proteomic profiling of paired serum of TB patients at enrolment and after 8 weeks of quadruple antituberculous chemotherapy. MMP-1 fell after the treatment period in all 39 patients and MMP-9 fell in 36 patients, where as MMP-2 was increased in 38 patients [158].

The results of these studies are supportive of our findings and show that plasma MMP-8 is elevated in TB patients in different geographical locations with varying HIV seroprevalence. The study we have performed differs in two main ways. Firstly it includes a much larger number of participants and secondly and more importantly has a respiratory symptomatic control group. This allows conclusions about plasma MMPs in TB specifically compared to other respiratory infections to be drawn.

Of the MMPs studied, MMP-8 emerges as being specifically upregulated in the plasma in active TB only compared to other respiratory infections, while MMP-1 is non-specifically upregulated in respiratory infection. It could initially be considered surprising that MMP-1 is elevated almost equally in the plasma of active TB and symptomatic controls, given the previous published data on MMP-1 in induced sputum in TB. However the symptomatic controls had symptoms consistent with pulmonary infection, though TB was not the final diagnosis. MMPs have a range of non tissue destructive roles which are important in the innate immune response. Their ability to cleave host defence proteins such as toll like receptors, cytokines and chemokines, has effects such as promoting leukocyte recruitment to the site of infection, activating inflammatory cells, initiating inflammatory signalling cascades and augmenting microbicidal activity [49, 159].

The elevated plasma MMP-1 in the context of symptomatics, who do not have a tissue destructive pulmonary pathology, may reflect a role in innate immunity rather than matrix degradation. For example, incubation of LPS stimulated monocytes with the broad spectrum MMP inhibitor BB-94 resulted in decreased secretion of the active form of TNFα as analysed by Western blot, and this was not due to reduced mRNA levels. Incubation of recombinant proTNFα with individual recombinant MMPs alone and in the presence of BB-94, with the mixtures subsequently analysed by Western blot showed that MMP-1 was able to convert proTNFα to the active form [160]. Therefore, the effect of MMP-1 may be more diverse than matrix destruction alone.

Elevated MMP-8 in active TB implies the presence of excessive neutrophil activity in these patients. Neutrophils are the main cellular source of MMP-8, though it may be expressed by other cell types [135]. MMP-8 and MMP-9 are stored in granules within neutrophils with their release occurring on cellular activation and degranulation [161]. In our study the close association of MMP-8 with MMP-9 by Principal Component Analysis, suggests that neutrophils are the primary source of MMP-8 in the plasma of TB patients. This is consistent with an emerging concept of dysregulated neutrophil activity driving pathology in pulmonary TB [162].

For example, a higher percentage of neutrophils compared to macrophages were found in the sputum and bronchoalveolar lavage fluid of patients with active pulmonary TB. The neutrophils contained more intracellular bacteria than the macrophages [163]. A mouse strain that are highly genetically susceptible to TB showed a large influx of neutrophils to lung tissue within 1 week of infection, which persisted to 3-4 weeks, and was associated with a higher number of mycobacteria phagocytosed by neutrophils and higher bacterial burden overall compared to a less susceptible mouse strain [164]. Both studies suggest in their concluding remarks that neutrophils may represent a permissive site for mycobacterial growth, and that the neutrophil activation and degranulation which ensues would cause damage to lung tissues. MMP-8 would be among the products released into lung tissue on neutrophil degranulation.

Whole blood genome profiling in a large training and validation set, which specifically compared patients with active pulmonary TB to other inflammatory diseases and

bacterial infections, identified an interferon inducible neutrophil driven 86 gene transcription signature specific to TB. The module with the largest number of transcripts changing within it related to type I interferon alpha-beta inducible signalling. Separation of white blood cells show that these transcripts were mostly overexpressed in neutrophils, and to a lesser extent monocytes though not T-cells [162].

Previous investigation of plasma MMPs in other respiratory infections has focussed on the measurement of MMP-9 in isolation in community acquired pneumonia (CAP). Three studies have shown that plasma MMP-9 levels measured by ELISA and/ or activity measured by gelatin zymography were elevated compared to healthy controls and that levels returned to normal after antibiotic treatment [165-167]. However, a comprehensive analysis of MMPs in diverse infectious conditions has not been performed.

While it is interesting to note that plasma MMPs are elevated in respiratory infections other than TB, CAP is largely a non tissue destructive respiratory infection, with cavitation rarely occurring except in severe cases. Therefore the immunological importance of MMP-9 in CAP may relate to roles such as activating chemokines and cytokines, promoting leukocyte migration to the site of infection and promoting bacterial killing that have been mentioned previously. However the causative micro-organisms in hospital acquired pneumonia (HAP) differ from CAP and pulmonary tissue destruction is a more common feature. One study measured MMP-8 and MMP-9 by ELISA and showed that they were elevated in both the bronchoalveolar lavage fluid and plasma of patients with HAP compared to healthy controls [168].

The finding of elevated plasma MMPs in a non tuberculous respiratory infection associated with tissue destruction is complementary to our data.

We observed gender differences in circulating MMPs within our cohorts. It is recognised that men mount a greater and often more damaging inflammatory response to infection compared to women. A proposed mechanism is that male sex hormones are damaging and female sex hormones are protective [169]. For example in sepsis the mortality rate of men can be as high as 70% compared to 26% in women, and men have higher levels of pro-inflammatory TNFα, but lower levels of the immunosuppressive IL-10 [170]. Female neutrophils have been found to express decreased MMP-9 and TNFα during the period of the menstrual cycle when oestrogen levels are higher [171]. With specific reference to mycobacteria, *M marinum* infected male mice showed numerous granulomatous inflammatory lesions and a high bacterial burden in their lungs at 3 weeks post infection, where as female mice had few small lesions with comparatively health lung parenchyma and a lower bacterial burden. The findings in male and female mice were more similar if the males were castrated and reverted to the original pattern if the castrated males were administered testosterone [172].

Men have a higher reported incidence, retreatment rate and mortality in TB as well as greater infiltration on chest radiograph and more frequent haemoptysis [173]. Elevated plasma MMPs in men compared to women has been previously identified [153] and was confirmed in this study for MMP-1, MMP-3, MMP-8 and MMP-9. The higher plasma MMP-8 levels we identified in men with TB are consistent with the studies discussed above which describe a greater pro-inflammatory response to

infection in males. This may in part be responsible for the more severe tissue destruction and poorer outcome exhibited in men.

In summary, I demonstrated that plasma MMP-1 and MMP-8 are elevated in active pulmonary TB and implicate excessive collagenase activity in tissue destruction in TB. The increased plasma MMP-8 is specific to TB patients and is not elevated in respiratory symptomatic controls with other respiratory infections. As MMP-8 is largely derived from neutrophils, this finding is consistent with neutrophils having an important role in driving TB immunopathology.

My plasma analysis suggests critical importance of collagenolytic MMPs in tissue destruction in TB. These MMPs are secreted as zymogens, requiring proteolytic cleavage, and so I was interested in the possibility that the other MMPs that were not elevated in the plasma in active TB were still playing an important role at the site of disease. My attention was specifically drawn to MMP-10 because it can proteolytically activate MMP-1 and MMP-8 [129] and is upregulated in *Mtb* infected macrophages [71], but has been little investigated in any disease process. MMP-10 (Stromelysin-2) is a stromelysin which cleaves proteoglycans, laminin and type IV collagen, but unlike MMP-1 and MMP-8 does not directly cleave the triple helical collagens. Therefore MMP-10 may indirectly promote breakdown of triple helical collagens, the primary structural fibrils of the lung, by activating the collagenases. I therefore proceeded to investigate MMP-10 expression and regulation in a macrophage based cellular model of human TB and in patients with pulmonary TB.

4. MMP-10 IS UPREGULATED BY THE *Mtb* VIRULENCE FACTOR ESAT-6

4.1 Introduction

MMP-10 (Stromelysin-2) has been less studied in TB compared to other MMPs for which reagents are widely available. MMP-10 directly cleaves proteoglycans, laminin and type IV collagen within ECM, but does not cleave the triple helical collagens [47]. However, MMP-10 is able to cleave the pro-form of the collagenases MMP-1 and MMP-8 to the active form [129] . Therefore MMP-10 may be involved in promoting tissue destruction in pulmonary TB, not only through its direct action on proteoglycans, laminin and type IV collagen within the pulmonary ECM, but by indirectly augmenting degradation of triple helical collagen, the primary structural fibrils of the lung. MMP-10 driven activation of MMP-1 has been found to be of importance in disease in models of angiogenesis [131] and malignant keratinocyte invasion [132].

To date there are no studies investigating MMP-10 in TB or in any other human infection in detail. However, preliminary data do suggest that MMP-10 may be implicated in TB pathogenesis. Unbiased gene profiling studies analyzing all MMPs found that *Mtb* drove MMP-10 gene expression in human macrophages and monocytes [71, 76]. MMP-10 gene expression was 14 fold higher in human TB granulomas compared to normal lung tissue on microarray analysis of tissue excised at time of surgery for TB [80]. Furthermore, the active metabolite of vitamin D

reduced *Mtb* induced MMP-10 mRNA expression in peripheral blood mononuclear cells and monocytes [174].

Therefore, these diverse data implicating MMP-10 in TB led me to investigate the hypothesis that MMP-10 is a driver of tissue destruction in TB. My approach was to investigate MMP-10 expression and regulation in a macrophage based cellular model of human TB and in patients with pulmonary TB.

4.2 Results

4.2.1 *Mtb* infection drives MMP-10 secretion from human MDMs

First, MMP-10 secretion from MDMs directly infected with *Mtb* was investigated. *Mtb* at an MOI of 0.1, 0.5 and 1 caused a dose dependent upregulation of MMP-10 of 1.3, 20.2 and 29 fold with mean levels of 481±108, 7462±2074 and 10719±1713 pg/ml respectively compared to 370±331pg/ml from uninfected MDMs at 72 hours incubation (Fig. 10A, MOI 0.1 not significant, $p<0.001$ for MOI 0.5 and 1). Kinetics studies showed *Mtb* infection had no effect at 24 hours compared to uninfected MDMs, but a 5.1-fold upregulation of MMP-10 secretion occurred at 48 hours rising to 31.5-fold at 72 hours (Fig. 10B, $p<0.01$ and $p<0.001$ respectively). Western blotting confirmed the ELISA findings, showing MMP-10 as a dark band at 54kDa in the supernatant from *Mtb* infected but not uninfected MDMs (Fig. 10C). The growth medium used to culture Mtb, 7H9 alone, had no greater effect on MMP-10 secretion than no stimulus.

Mtb upregulated MMP-10 mRNA gene expression (normalized to β-actin),182-fold compared to uninfected MDMs at 24 hours (Fig.10D, p< 0.0001). This shows that the increased MMP-10 secretion seen in *Mtb* infected MDMs is secondary to increased mRNA accumulation.

4.2.2 *Mtb* upregulates MMP-10 secretion from pulmonary epithelial cells via monocyte-dependent networks

Next, we investigated the effects of local monocyte dependent networks in driving MMP-10 secretion from pulmonary epithelial cells. CoMTb increased MMP-10 secretion 4.5-fold from epithelial cells with levels of 2525±209pg/ml from unstimulated cells compared to 11250±286 pg/ml from stimulated cells at 72 hours (Fig. 11A, p<0.0001). In a separate experiment CoMTb increased MMP-10 secretion 16.6-fold from epithelial cells compared to CoMCont, with levels of 5649±226 pg/ml compared to 340±56 pg/ml respectively at 72 hours (Fig. 11B, p<0.0001).

CoMTb was prepared by filtering the supernatants of infected monocytes through a Whatman Anopore filter, which binds MMPs [140] and consequently CoMTb itself at the dilutions used to stimulate cells contained MMP-10 levels in the range of 380 to 2220 pg/ml, significantly lower than that detected after 72 hours of cellular stimulation.

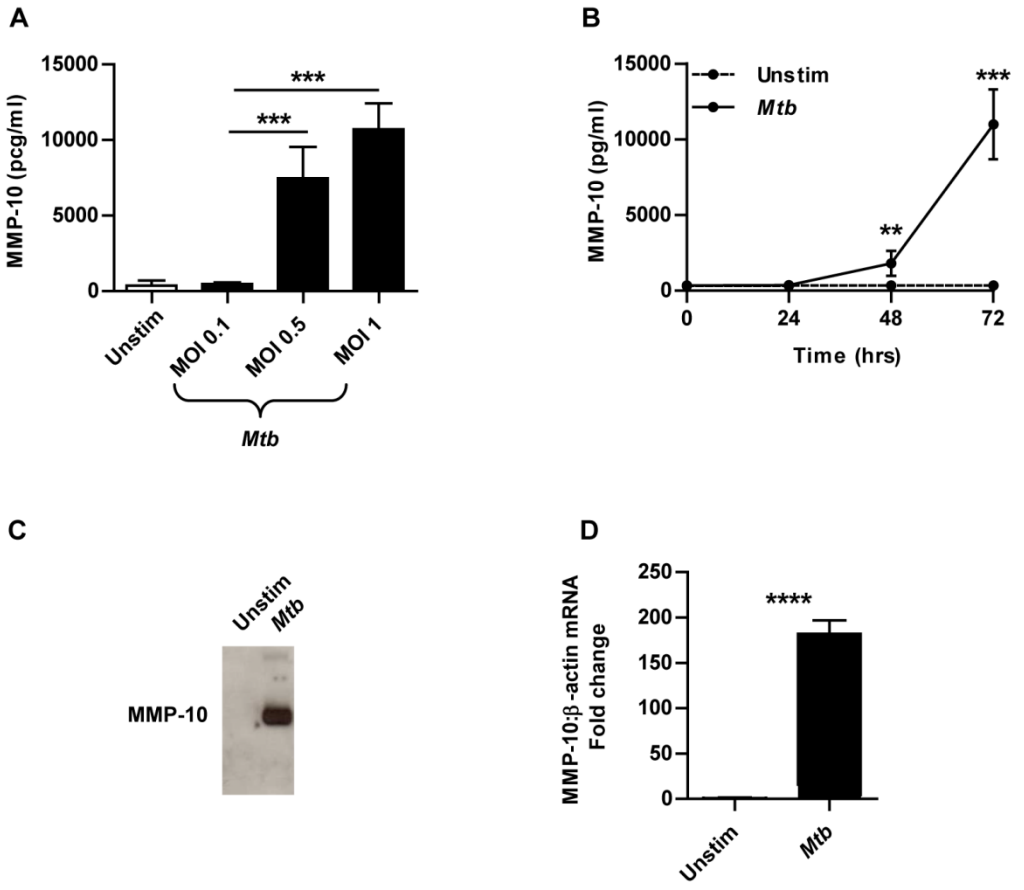

Figure 10: Direct *Mtb* infection drives MMP-10 expression in MDMs

A, MMP-10 secretion from MDMs infected with increasing MOI of *Mtb*. Increased MMP-10 was secreted as the MOI for *Mtb* increased from 0.1 to 1. **B,** Kinetics of MMP-10 secretion from *Mtb* infected MDMs. *Mtb* (MOI 1) caused a gradual increase in MMP-10 secretion from 24 hours through to 72 hours. MMP-10 concentration in MDM supernatants was measured by ELISA and is expressed as pg/ml. **C,** Western blot analysis of MMP-10 secretion from *Mtb* infected MDMs. Increased MMP-10 secretion from *Mtb* infected (MOI 1) MDMs at 72 hours was confirmed by Western blot analysis using an MMP-10 specific antibody. MMP-10 was detected in MDM supernatants as a dark band at 54kDa. **D,** MMP-10 gene expression in *Mtb* infected MDMs. *Mtb* (MOI 1) upregulated MMP-10 gene expression (normalised to β-actin) at 24 hours. MMP-10 and β-actin gene expression were measured by RT-PCR. Statistical analysis was performed using a one-way ANOVA with Tukey's post hoc test or a Student's unpaired t-test (** $p < 0.01$, *** $p < 0.001$, **** $p < 0.0001$).

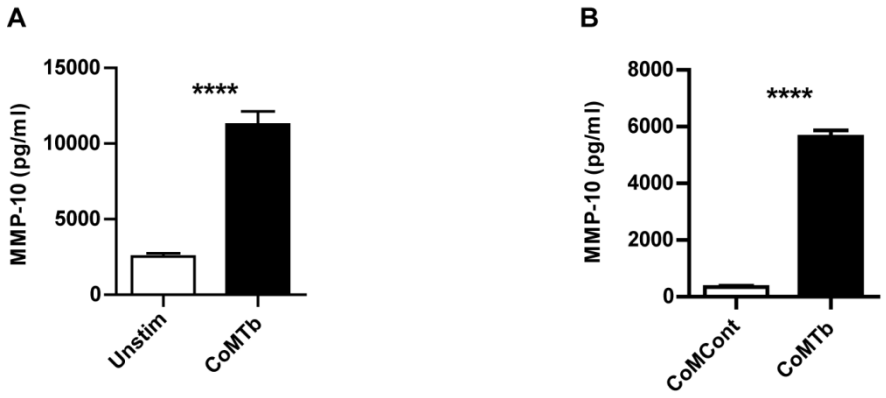

Figure 11: *Mtb* induced intercellular networks drive MMP-10 secretion from human pulmonary epithelial cells

MMP-10 secretion from CoMTb stimulated pulmonary epithelial cells. CoMTb (1:5 dilution) increased MMP-10 secretion from pulmonary epithelial cells at 72 hours in comparison to both **A,** unstimulated cells and **B,** CoMCont stimulated cells. MMP-10 concentration in cell culture supernatants was measured by ELISA and is expressed as pg/ml. Mean +/- SD for an experiment performed in triplicate are shown and are representative of two independent experiments. Statistical analysis was performed using Student's unpaired t-test (**** $p < 0.0001$)

4.2.3 MMP-10 is increased in the respiratory secretions of patients with pulmonary TB

To investigate the relevance of the cellular findings on increased MMP-10 secretion to clinical disease, we measured MMP-10 levels in the respiratory secretions of two separate patient cohorts. The first was in the induced sputum of patients with TB (n=21) and a mixture of healthy and respiratory symptomatic controls (n=21) from Khayelitsha Township, South Africa. The second was in the BALF of TB patients (n=17) and control patients with non-tuberculous respiratory disease (n=14) from Calcutta, India. The final diagnoses in these control patients were asthma, pneumonia, carcinoma, sarcoidosis, foreign body aspiration and pulmonary vasculitis [144]. The characteristics of the patient cohorts are detailed in the references indicated [77, 144].

MMP-10 was increased in patients with TB compared to controls groups for both the induced sputum and BALF cohorts (Fig. 12 and 13, $p<0.05$). In the induced sputum study in South African patients, median MMP-10 concentrations were 5067 pg/ml (interquartile range 1440 – 19077) in TB patients compared to 2648 pg/ml (797 – 5914) in controls. For the BALF study in Indian patients, MMP-10 concentrations were median 6531 pg/ml (interquartile range 637 -11929) in TB patients compared to 783 pg/ml (76-5473) in controls. These data show that MMP-10 concentrations are higher present at the site of disease in pulmonary TB.

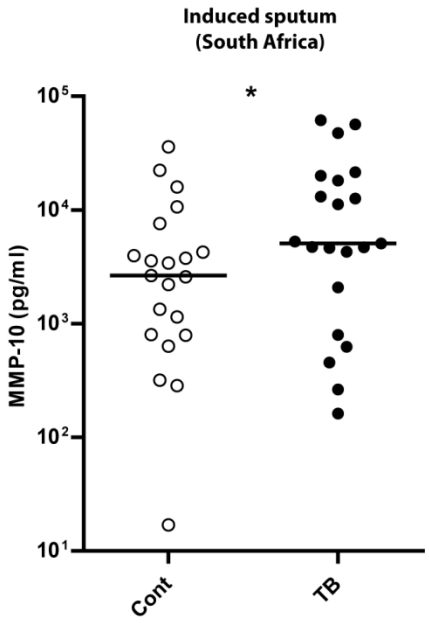

Figure 12: MMP-10 is elevated in the induced sputum of South African patients with active pulmonary tuberculosis (TB)

Induced sputum samples were collected prospectively from patients with active pulmonary TB and a mixture of healthy and respiratory symptomatic controls in Cape Town, South Africa. MMP-10 was increased in induced sputum in active pulmonary TB (n=21) compared to controls (n=21). MMP-10 concentrations were measured by Luminex bead array and are expressed as pg/ml. Each circle represents one patient and the horizontal line the median value. Statistical analysis was performed using a Mann Whitney U test (* $p < 0.05$).

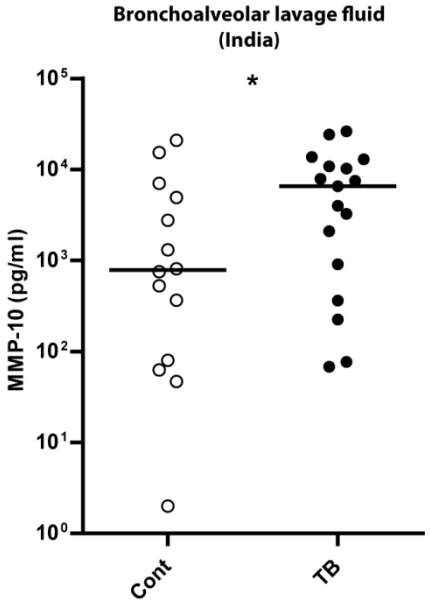

Figure 13: MMP-10 is elevated in the BALF of Indian patients with active pulmonary TB

BALF samples were collected prospectively from patients with active pulmonary TB and control patients with other pulmonary diseases in Patna, India. MMP-10 was increased in BALF in active pulmonary TB (n=17) compared to controls (n=14) with other pulmonary diseases. MMP-10 concentrations were measured by Luminex bead array and are expressed as pg/ml. Each circle represents one patient and the horizontal line the median value. Statistical analysis was performed using a Mann Whitney U test (* $p < 0.05$).

4.2.4 MMP-10 secretion from *Mtb* infected MDMs is MAPK dependent but NF-κB independent

Next, we investigated the role of key signalling pathways in the control of *Mtb* driven MMP-10 secretion using specific chemical inhibitors. The signalling pathways that regulate MMP-10 are poorly defined, but it has previously been demonstrated that the MAPK pathways regulate MMPs in other inflammatory conditions[47]. The MAPK and NF-κB pathways are briefly illustrated in Fig. 1 and 2. *Mtb* infection drives phosphorylation of the signalling molecules p38 and ERK MAPK in MDMs [100].

To assess the role of p38 MAPK signalling, chemical inhibition was undertaken using SB203580 (SB). SB inhibits the activation of MAPKAP kinase 2 by p38 MAPK by binding to the ATP-binding pocket, and thus inhibiting phosphorylation of downstream proteins [175]. SB caused a dose dependent decrease in *Mtb* driven MMP-10 secretion from MDMs at 72 hours of 75% at 1μM and 92% at 10μM (Fig. 14A, $p<0.01$ and 0.001 respectively). ERK MAPK inhibition using PD98059 (PD), which binds to inactive forms of ERK thus preventing their activation [176], decreased MMP-10 secretion by 15% at 1μM (not significant) and 33% at 10μM (Fig. 14B, $p<0.01$). Blockade of the p38 and ERK MAPK pathways using 10μM of each inhibitor downregulated *Mtb* driven MMP-10 gene expression (normalized to β-actin) by 82% and 91% respectively (Fig. 14C, $p<0.01$ for both). This shows that *Mtb* driven MMP-10 secretion in MDMs is regulated by the p38 and ERK MAPK signalling pathways acting at the level of gene expression. The JNK MAPK inhibitor SP600125 caused excessive cell death and therefore this pathway was not assessed further.

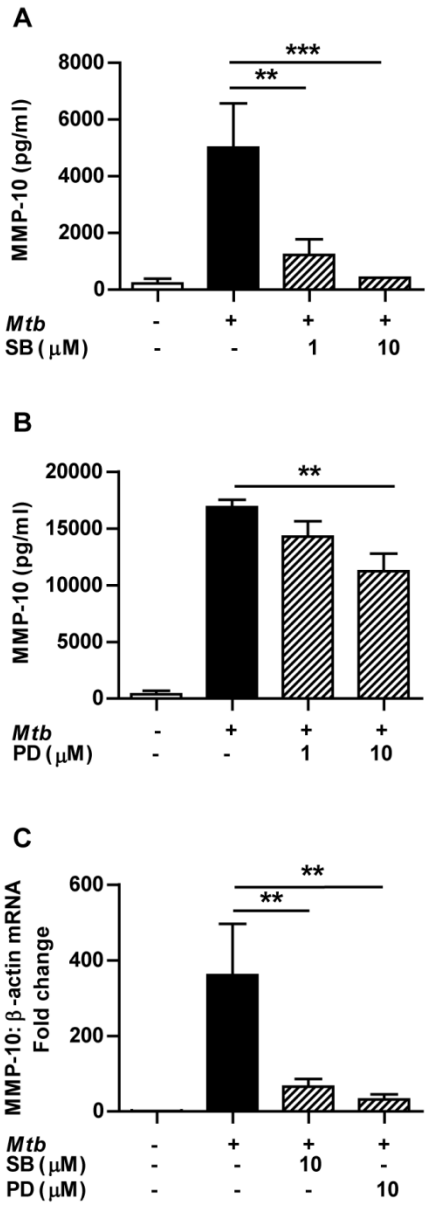

Figure 14: MMP-10 expression is p38 and ERK MAPK dependent in *Mtb* infected MDMs

MMP-10 gene expression and secretion from *Mtb* infected MDMs with chemical inhibition of p38 and ERK MAPK signalling. MDMs were pre-incubated with the p38 MAPK inhibitor SB203580 (SB) or the ERK MAPK inhibitor PD98059 (PD) at 1μM or 10μM for 2 hours prior to *Mtb* infection (MOI 1). **A,** SB and **B,** PD caused a dose dependent reduction in *Mtb* driven MMP-10 secretion from MDMs at 72 hours. MMP-10 concentration in MDM supernatants was measured by ELISA and is expressed as pg/ml. **C**, SB and PD caused a reduction in *Mtb* driven MMP-10 gene expression normalised to β-actin at 24 hours. MMP-10 and β-actin gene expression were measured by RT-PCR. Mean +/- SD for an experiment performed in triplicate are shown and are representative of two independent experiments. Statistical analysis was performed using a one-way ANOVA with Tukey's post hoc test (* $p<0.05$, ** $p<0.01$, *** $p<0.001$).

NF-κB is considered a critical transcriptional regulator in innate immunity [103], but MMP-10 does not have a consensus NF-κB binding site in its promoter [90], However using chromatin immunoprecipitation in human fibroblasts, non-canonical binding was shown in the promoter of the related stromelysin MMP-3, with modulation of MMP-3 gene expression as a result [177]. The promoter regions of MMP-3 and MMP-10 share many similarities. Therefore we proceeded to investigate if this critical transcription factor was regulating MMP-10 expression in *Mtb* infection.

Chemical inhibition of NF-κB signalling using SC-514 and Helenalin was performed. SC-514 binds to the ATP-binding pocket of IKKβ, thus inhibiting its activity. IKKβ normally activates NF-κB by phosphorylating its inhibitor IκB which then dissociates [178]. NF-κB is composed of a p50 and p65 subunit, and Helenalin has been shown to alkylate and inhibit the p65 subunit as well as reduce its expression[179]. Neither SC-514 or Helenalin altered *Mtb* driven MMP-10 secretion from MDMs (Fig. 15A and B, not significant). The MMP-1 promoter carries a consensus NF-κB binding site [90]. Therefore to assess if these chemical inhibitors regulated expression of a gene with the clear potential to be under the control of NF-κB, we measured MMP-1 in the same supernatants. We found that SC-514 reduced *Mtb* driven MMP-1 secretion by 6% at 1μM (not significant) and 51% at 10μM (Fig 15C, $P<0.001$). Helenalin reduced MMP-1 secretion by 45% at 0.25μM (not significant) and 63% at 0.5μM (Fig. 15D, $P<0.05$). These data show that MMP-10 secretion from MDMs in *Mtb* infection is not transcriptionally regulated by NF-κB, but that the chemical inhibitors were functioning as predicted as they suppressed MMP-1 secretion.

No cell death was observed with the concentrations of inhibitors used. Dimethyl Sulfoxide (DMSO), the carrier for the inhibitors, had no effect on *Mtb* driven MMP-10 secretion when used at equivalent concentrations alone.

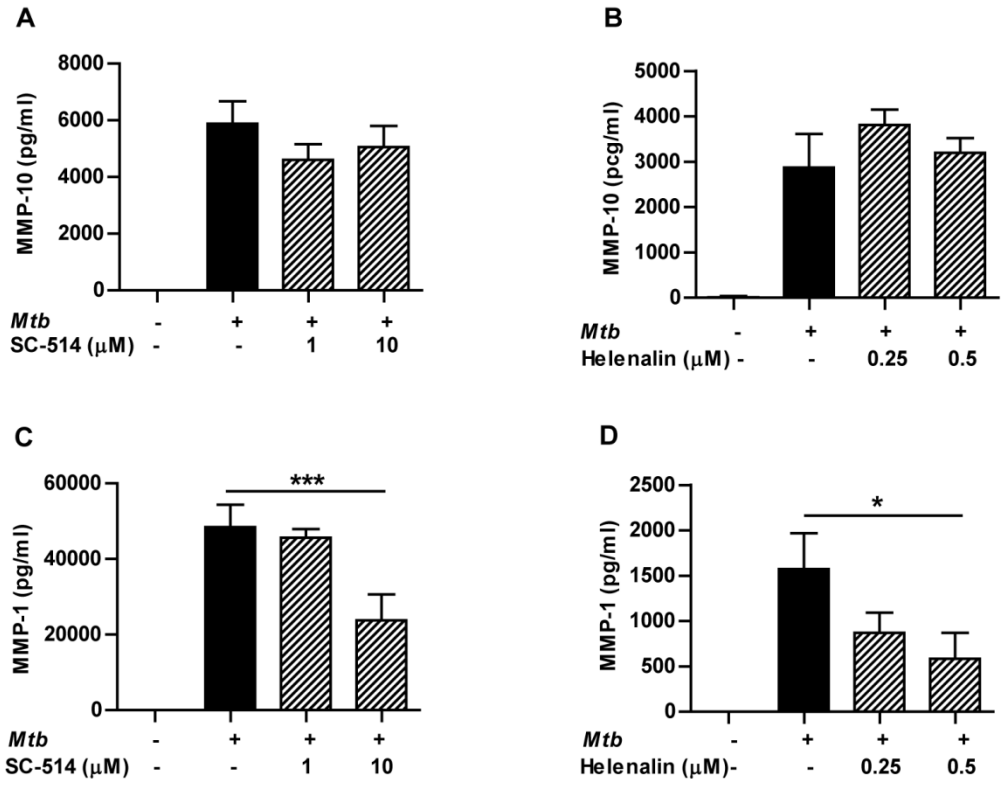

Figure 15:NF-κB does not regulate the transcription of MMP-10 in *Mtb* infected MDMs

MMP-10 and MMP-1 secretion from *Mtb* infected human MDMs with chemical inhibition of NF-κB mediated signalling using SC-514 and Helenalin. MDMs were pre-incubated with SC-514 at 1μM or 10μM and Helenalin at 0.25μM or 0.5μM for 2 hours prior to *Mtb* infection (MOI 1). **A,** SC-514 and **B,** Helenalin had no effect on *Mtb* driven MMP-10 secretion from MDMs at 72 hours. **C,** SC-514 and **D,** Helenalin caused a dose dependent downregulation of MMP-1 secretion from MDMs at 72 hours. MMP-10 and MMP-1 concentrations in MDM supernatants was measured by ELISA and is expressed as pg/ml. Mean +/- SD for an experiment performed in triplicate are shown and are representative of two independent experiments. Statistical analysis was performed using a one-way ANOVA with Tukey's post hoc test (* $p<0.05$, *** $p<0.001$).

4.2.5 MMP-10 expression in MDMs is driven by *Mtb* but not by mycobacterial LAM or vaccine BCG

LAM is a mycobacterial cell wall component that has been implicated in driving TB pathogenesis and principally a Toll-like receptor 2 (TLR-2) agonist known to be important in inflammatory responses to *Mtb* [101]. Stimulation of MDMs with LAM resulted in MMP-10 secretion which was 5% of that observed with direct *Mtb* infection (Fig. 16A, $p<0.001$). MMP-1 secretion and TNFα secretion were measured in the same supernatants. LAM upregulated proportionately higher MMP-1 secretion at 30% of that driven by direct *Mtb* infection (Fig. 16B), while TNFα secretion was equal (Fig. 16C). This shows that LAM is not a critical *Mtb* derived factor in driving MMP-10 secretion from MDMs, even when cellular activation (as measured by TNFα secretion) is equal.

To further investigate the relationship between MMP-10 and TB pathogenic factors, we compared upregulation by *Mtb* and the vaccine strain *M. bovis* BCG. Tissue destruction is not a feature of pulmonary infection with the vaccine strain *M. bovis* BCG [70], and the primary attenuation is the loss of a secretion system entitled RD1 (region of difference 1).

MMP-10 secretion after BCG infection of MDMs was 586 ± 97 pg/ml compared to 2048 ± 347 pg/ml from *Mtb* infected MDMs at 72 hours (Fig. 17A, $p<0.001$). *Mtb* infection drove MMP-10 gene expression (normalized to β-actin) that was 4 fold higher than that cause by BCG infection (Fig. 17B, $p< 0.001$) of MDMs at 24 hours. This indicates that the divergent effects of BCG and *Mtb*, with respect to MMP-10

secretion, are transcriptionally regulated. Measurement of TNFα in the same supernatants showed that *Mtb* and BCG stimulated similar levels of TNFα secretion (Fig. 17C, no significant differences between the conditions). The *Mtb* and BCG cultures used for infection were plated on agar, and colony counting performed after 2 weeks incubation. This confirmed that an equal number of CFUs of *Mtb* and BCG were used to infect the MDMs in these experiments (Fig. 17D). These data show that a factor present in *Mtb* but not BCG is responsible for driving MMP-10 secretion from MDMs.

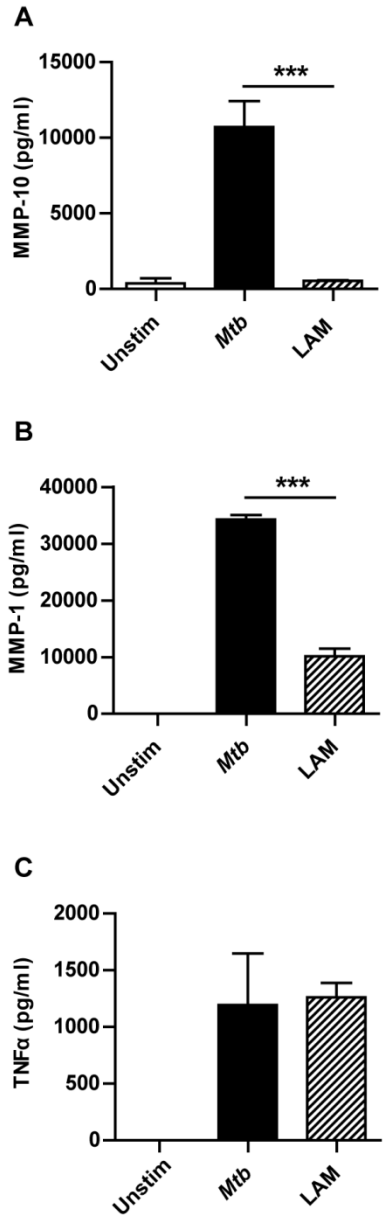

Figure 16: Mycobacterial LAM is a poor stimulus for MMP-10 secretion from MDMs in comparison to *Mtb*

MMP-10, MMP-1 and TNFα secretion from MDMs in response to *Mtb* infection (MOI 1) and stimulation with mycobacterial LAM (10 μg/ml). **A**, *Mtb* drove twenty times greater MMP-10 secretion than LAM from MDMs at 72 hours. **B**, *Mtb* drove three times greater MMP-1 secretion than LAM from MDMs at 72 hours. **C**, *Mtb* and LAM produced equal TNFα secretion from MDMs at 72 hours**.** MMP-10 and TNFα concentrations in MDM supernatants were measured by ELISA and are expressed as pg/ml. Statistical analysis was performed using a one-way ANOVA with Tukey's post hoc test (*** $p < 0.001$).

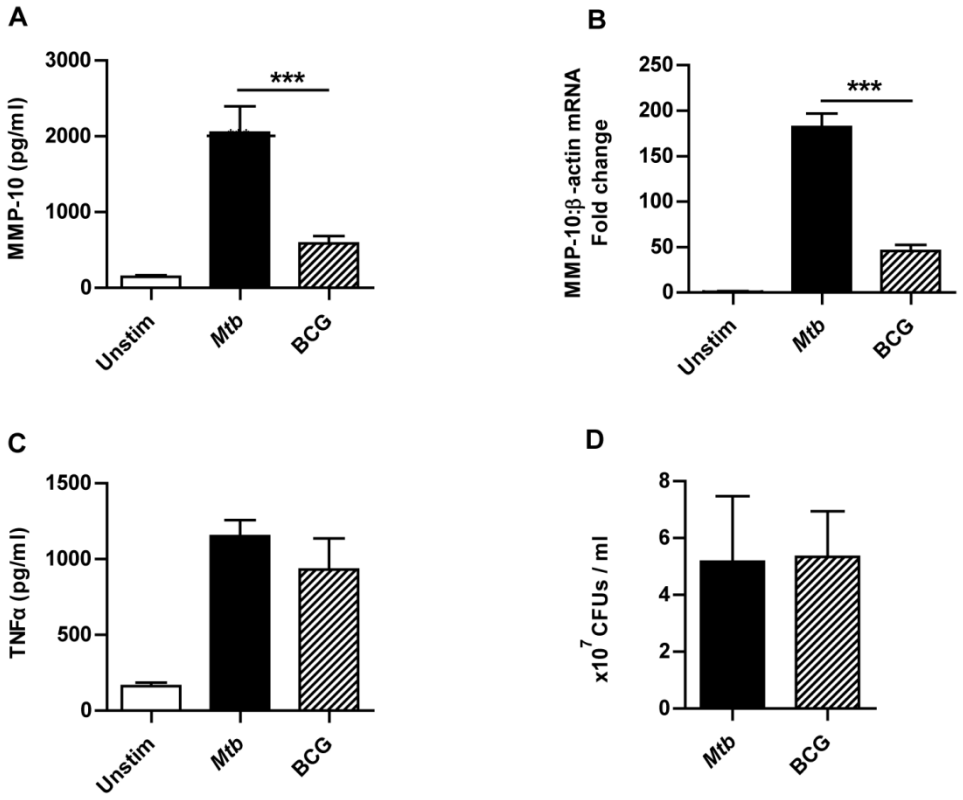

Figure 17: MMP-10 gene expression and secretion from MDMs is driven by *Mtb* but not vaccine BCG

MMP-10 gene expression and secretion and TNFα secretion from *Mtb* infected (MOI 1) MDMs compared to BCG infected (MOI 1) MDMs. **A**, *Mtb* drove greater MMP-10 secretion from MDMs than BCG at 72 hours. **B**, *Mtb* drove greater MMP-10 gene expression (normalised to β-actin) in MDMs than BCG) at 24 hours. **C**, *Mtb* infection and BCG infection produced equal levels of TNFα secretion at 72 hours. **D,** CFUs produced by *Mtb* and BCG cultures. Equal volumes of *Mtb* and BCG cultures of an optical density of 0.6 produced equal numbers of colony forming units when plated and grown on agar for 2 weeks. MMP-10 and TNFα concentrations in MDM supernatants were measured by ELISA and are expressed as pg/ml. MMP-10 and β-actin gene expression were measured by RT-PCR. Statistical analysis was performed using a one-way ANOVA with Tukey's post hoc test (*** $p < 0.001$).

4.2.6 *Mtb* driven MMP-10 Secretion is dependent on a specific 15 Amino Acid Peptide Sequence in ESAT-6

Since BCG did not drive MMP-10 secretion and lacks the RD1 region in its genome [99], we investigated ESAT- 6, a protein encoded by the RD1 region. It is implicated in *Mtb* virulence [180, 181] and modulation of the host immune response [182, 183]. Furthermore, ESAT-6 has been implicated in driving MMP-9 secretion from epithelial cells [89].

MDMs were stimulated with a series of short linear peptide sequences from ESAT-6 set up as a series of peptide pools (Table 3). Stimulation of MDMs with the total pool of all ESAT-6 peptides at a concentration of 10 μg/ml caused a 3.7 fold increase in MMP-10 secretion of 137.2 ± 56.5pg/ml compared to 36.3 ± 25.9 pg/ml with stimulation by the ESAT-6 peptides at 1 μg/ml at 72 hours. (Fig. 18,$p<0.001$). Unstimulated MDMs secreted for this donor secreted 7.8 ± 7.9 pg/ml.

Next overlapping pools containing 3-4 peptides at a total concentration of 10 μg/ml, as defined by the matrix shown in Table 4, were used to stimulate MDMs. This is a method to identify key immunostimulatory peptides with the minimal number of experimental variables. Pools 1 and 8 were the only pools that caused significantly higher MMP-10 secretion at 72 hours than that from unstimulated MDMs, with a 5.2 fold and 3.9 fold upregulation respectively (Fig. 19A, $p<0.001$ and $p<0.01$ respectively). It can be deduced from the matrix in Table 4 that the single peptide common to both these pools is ESAT-6 peptide 4 which has the amino acid sequence SAIQGNVTSIHSLLD (Table 3). Stimulation of MDMs with ESAT-6 peptide

4 (10 µg/ml) alone drove 3.8 fold higher MMP-10 secretion of 66.7 ± 11.7 pg/ml) compared to 23.3 ± 4.9 pg/ml with ESAT-6 peptide 13 at 72 hours (Fig. 19B $p<0.001$). ESAT-6 peptide 13 was chosen as the negative control peptide because it was present in the non-stimulatory peptide matrix pools 3 and 7. Unstimulated MDMs for this donor secreted 17.3 ± 0.6 pg/ml. These data suggest that the amino acid sequence SAIQGNVTSIHSLLD within ESAT-6 is a specific *Mtb* derived factor which drives MMP-10 secretion.

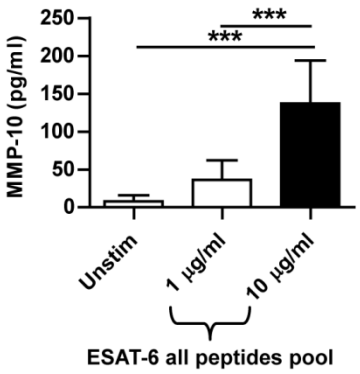

Figure 18: A peptide pool of the entire ESAT-6 sequence drives MMP-10 secretion from MDMs

MMP-10 secretion from MDMs stimulated with a pool of 17 overlapping ESAT-6 peptides spanning the entire protein sequence at concentrations of 1 µg/ml and 10 µg/ml (see METHODS Table 2). The ESAT-6 peptide pool drove MMP-10 secretion from MDMs in a dose dependent manner. MMP-10 concentrations in MDM supernatants were measured by ELISA and are expressed as pg/ml. Mean +/- SD for two experiments performed in triplicate are shown. Statistical analysis was performed using a one-way ANOVA with Tukey's post hoc test (*** $p<0.001$).

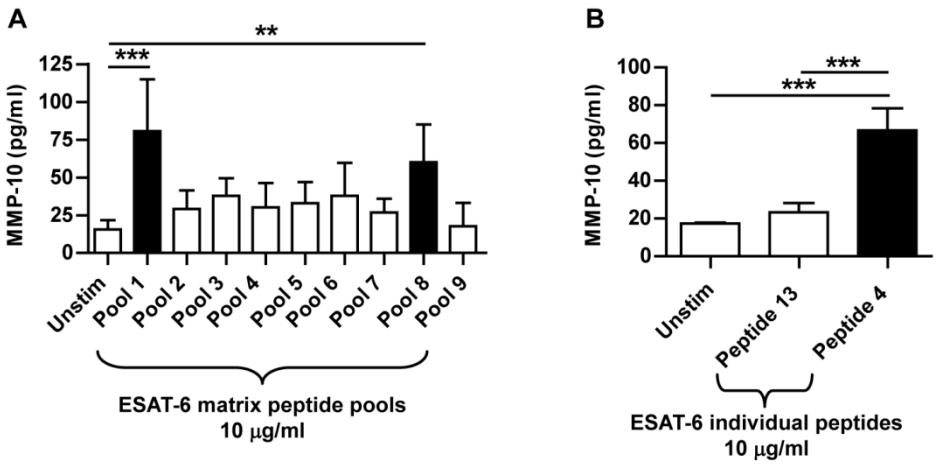

Figure 19: A single 15 amino acid peptide sequence from ESAT-6 drives MMP-10 secretion from MDMs

To identify if an individual peptide from the 17 peptides in the ESAT-6 pool was stimulating the MMP-10 secretion from MDMs, a peptide matrix was used (see METHODS Table 3). **A**, MMP-10 secretion from MDMs stimulated with the smaller ESAT-6 peptide pools (10μg/ml) from the peptide matrix table. Pools 1 and 8 drove greater MMP-10 expression than the other pools, indicating that ESAT-6 peptide 4 was stimulating the MMP-10 secretion. **B**, MMP-10 secretion from MDMs stimulated with ESAT-6 peptide 4 and ESAT-6 peptide 13 (10μg/ml) individually. ESAT-6 peptide 4 alone stimulated greater MMP-10 secretion that ESAT-6 peptide 13. ESAT-6 peptide 13 was used as a negative control peptide as it was present peptide matrix pools 3 and 7 which did not stimulate MMP-10 secretion from MDMs. MMP-10 concentrations in MDM supernatants were measured by ELISA and are expressed as pg/ml. Mean +/- SD for two experiments performed in triplicate are shown. Statistical analysis was performed using a one-way ANOVA with Tukey's post hoc test (** $p<0.01$, *** $p<0.001$).

4.3 Discussion

Mtb upregulated MMP-10 secretion from MDMs in a time and dose dependent fashion. *Mtb* induced local monocyte networks drove MMP-10 secretion from human pulmonary epithelial cells and fibroblasts. Elevated levels of MMP-10 were identified, at the site of disease in the respiratory secretions of patients with pulmonary TB compared to controls in two separate cohorts from South Africa and India. MMP-10 secretion from *Mtb* infected macrophages was under the control of the p38 and ERK MAPK pathways but not dependent on NF-κB signalling. *Mtb* drove greater MMP-10 secretion from macrophages than LAM and vaccine BCG. A specific 15 amino acid sequence peptide within the virulence factor ESAT-6, which is specifically secreted by *Mtb* but not BCG, stimulated MMP-10 secretion from macrophages. These data support our hypothesis that MMP-10 plays a role in driving tissue destruction in pulmonary TB and is upregulated by *Mtb* to facilitate tissue destruction and hence transmission.

Macrophages are the main cell type involved in the immune response to *Mtb,* but pulmonary epithelial cells and fibroblasts are also present adjacent to the site of infection. Though these cells do not directly phagocytose *Mtb,* they participate in the immune response by way of paracrine signalling. *Mtb* infected macrophages in the lungs secrete cytokines, chemokines and growth factors which modulate the activity of these adjacent cells. The finding that MMP-10 is secreted both in response to direct *Mtb* infection of MDMs and by epithelial cells and fibroblasts exposed to local *Mtb* induced networks is consistent with previous data for MMP-1. Direct *Mtb*

infection drove MMP-1 gene expression and secretion in MDMs and CoMTb upregulated pulmonary epithelial cell and fibroblast MMP-1 gene expression and secretion [71, 72, 75]. The data also suggest that MMP-10 present at the site of infection may come from diverse cellular sources and potentially achieve high concentrations.

Our cell culture studies were supported by the finding of increased levels of MMP-10 in the induced sputum and BALF of patients with TB compared to controls. This shows that this increased MMP-10 gene expression identified in human TB granulomas [80] translates to the presence of a protein which is potentially functionally active and therefore important to clinical disease. It should also be noted that both control groups contained patients with non tuberculous respiratory disease, therefore the result indicates some specificity of increased MMP-10 expression to pulmonary TB, a disease which is particularly tissue destructive in its nature.

Increased MMP-10 in respiratory secretions was present across two racially and geographically distinct patient cohorts, that are likely to have been infected with genetically different *Mtb* strains. For example a study of the London immigrant population suggested that the CAS strain predominates in the Indian subcontinent and the LAM strain in Southern Africa [184] This shows that MMP-10 secretion is a preserved feature of the immune response in *Mtb* infection.

There are multiple intracellular signalling pathways involved in the innate immune response to *Mtb* infection and the MAPK signalling pathways are considered particularly important [101]. These pathways have been shown to regulate MMP expression in *Mtb* infection. Analysis of multiple signalling molecules by phosphoarray has shown that *Mtb* infection results in much greater phosphorylation of the signalling molecules p38 and ERK MAPK in MDMs than other molecules such as JNK, MSK and AKT [100]. Chemical inhibition of the p38 MAPK and ERK MAPK signalling pathways reduced MMP-1 secretion, from *Mtb* infected MDMs, as a consequence of reduced gene expression [100].

To our knowledge, the role of p38 and ERK MAPK signalling in controlling MMP-10 expression in *Mtb* infection has never been investigated. Considering the paucity of data in this area and the existing knowledge in relation to their role in control of MMP-1 expression, it seemed interesting to investigate their role in controlling MMP-10 expression. We showed that MMP-10 secretion is also controlled by the p38 and ERK MAPK pathways in *Mtb* infected MDMs and that the regulation occurs predominantly at the level of gene expression. The secretion data would suggest that the p38 pathway is more critical in regulation than the ERK pathway, but the gene expression data showed equal suppression. This may be due to differing importance of each pathway in individual donors, or the p38 pathway having additional effect on the mRNA which prevents subsequent protein translation, such as mRNA stabilisation [185].

The stimulation of TLRs by mycobacterial components acting at the surface of macrophages is considered a critical aspect of the innate immune response to *Mtb*. [101], The transcription factor NF-κB is considered an important downstream signalling component for the TLR2 signalling, which activates NF-κB via Myd88. This drives TNFα expression which in turn further activates NF-κB [186]. Chemical inhibition and promoter analysis showed that NF-κB regulated CoMTb driven MMP-1 expression from CNS microglial cells [84]. Despite the absence of a consensus NF-κB binding site in the MMP-10 promoter, the critical importance of the TLR-2 and NF-κB signalling in the innate immunes response to *Mtb*, and the finding of non-canonical binding of NF-κB to the promoter of close related MMP-3 prompted us to investigate this further. However we found that MMP-10 secretion in *Mtb* infected MDMs was not NF-κB dependent. It is likely that the minimal MMP-10 secretion driven by mycobacterial LAM is a consequence of the absence of NF-κB as a regulator, as the TNFα levels showed that the *Mtb* infected and LAM stimulated cells were equally activated. This theory is supported by the data showing that LAM was a more potent stimulator of MMP-1 secretion by MDMs, which was NF-κB dependent unlike MMP-10 secretion. It is possible that the independence of MMP-10 expression from the NF-κB /TLR2 signalling pathway may be part of a regulatory network to limit inflammation, as less MMP-10 at the site of disease may prevent excessive tissue destruction.

Potential candidates for the transcription factors activating MMP-10 gene expression are AP-1 and STAT, both of which have consensus binding sites in the MMP-10 promoter [90] . In cardiomyocytes, siRNA knock down of AP-1 and STAT-3

expression reduced CRP driven MMP-10 secretion, measured by Western blotting. [187], and so future studies studying these transcription factors may be more fruitful

Tissue destruction and cavitation are a feature of pulmonary TB. Intravesical BCG treatment for bladder transitional cell carcinoma can occasionally cause systemic infection in the context of immunocompromise. This presents as a pneumonitis with non caseating granuloma and cavitation is absent [70]. It is known that BCG does not drive MMP-1 secretion from MDMs as potently as *Mtb*, and this is an interesting finding considering that TB is a tissue destructive disease while BCG is not. We therefore decided to investigate MMP-10 secretion from MDMs in response to *Mtb* and BCG infection. We found that *Mtb* drove greater MMP-10 secretion, secondary to increased gene expression, from MDMs than the vaccine strain BCG. Both mycobacteria drove similar levels of TNFα secretion, therefore reassuring me that the difference was not purely a consequence of poorer pro-inflammatory stimulation of the cells by BCG or a lower infectious dose. This suggests that specific factors present in *Mtb* but not BCG are responsible for driving MMP-10 expression, and these are likely to be related to pathogenicity.

Region of difference 1 (RD1) is a region absent in the genome of all BCG strains derived from the original cultures by Camlette and Guerin, but present in both virulent *M.bovis,* from which BCG is derived, and virulent *Mtb* [99]. The reintroduction of RD1 into BCG creates a protein expression profile almost identical to virulent *M. bovis* and *Mtb* [188]. Animal studies suggest that the proteins encoded by this region are important to the difference in the disease pathologies seen. Lungs from mice

infected with a BCG:RD1 knock in showed an increased bacterial burden and greater inflammatory cell infiltration with granuloma formation on histopathological analysis, that was absent with control BCG [189].

RD1 encompasses nine genes which encode the proteins ESAT-6 and culture filtrate protein 10 (CFP-10) and the secretion apparatus to transport these proteins across the hydrophobic, impermeable *Mtb* cell wall [88]. *In vitro* and *in vivo* studies implicate ESAT-6 and CFP-10 in *Mtb* virulence, with a specific role in membrane cytolysis leading on to mycobacterial dissemination proposed. Using fluorescent microscopy, it was shown that macrophages infected with an *M. marinum* CFP-10/ESAT-6 knockout exhibited less cytolysis and cytotoxicity compared to wild type, and this was restored by the insertion of CFP-10/ ESAT-6 from *Mtb* [190] .Electron microscopy of human dendritic cells showed that *Mtb* but not vaccine BCG translocated from the phagolysosome to the cytosol, but that this was absent in *Mtb* ESAT-6 and CFP-10 deletion mutants [191].

ESAT-6 also modulates the host immune response as a consequence of its membrane lysing activity [182, 183]. One study showed that stimulation of THP-1 cells with the full length ESAT-6 protein activated caspases and drove IL-1 beta secretion. Using fluorescent microscopy it was shown that this effect was because ESAT- 6 facilitated translocation of the immunostimulatory agent AG85 into the cell cytosol [183].

However, the hypothesis that ESAT-6 may be in part driving pathology by upregulating metalloproteinase secretion from macrophages has not been investigated. I therefore chose to investigate the role of the ESAT-6 amino acid sequence, independent of its membrane lysing activity, via interactions with cell surface receptors triggering downstream signalling cascades in stimulating MMP-10 secretion. We did this by employing an approach where we used peptide pools spanning the entire ESAT-6 sequence to stimulate MDMs. We were able to identify a single linear sequence (SAIQGNVTSIHSLLD) which alone was sufficient to drive MMP-10 secretion from MDMs. This confirms for the first time that a virulence factor specific to *Mtb* drives MMP-10 expression from MDMs.

The role of MMP-10 in activating MMP-1 has been alluded to as being potentially important in promoting pulmonary collagen destruction. It is therefore worth noting the similarities and differences identified in their regulation. If MMP-1 and MMP-10 do indeed function synergistically, then it is logical that they are both driven by *Mtb* but not BCG, and that they are both regulated by p38 and ERK MAPK signalling. However, there is a divergence in their control at the level of TLR2/ NF-κB signalling axis, though as mentioned it is possible that this has evolved as host mechanism to limit excessive tissue destruction.

In summary, MMP-10 is elevated in the respiratory secretions of patients with TB, suggesting a role in tissue destruction *in vivo*. In a cellular model of TB, MMP-10 expression was driven by *Mtb* and was regulated by the p38 and ERK MAPK pathways, but not the TLR2/ NF-κB signalling axis. *Mtb* infection drove greater MMP-

10 expression than BCG infection. A specific 15 amino acid sequence from ESAT-6, a *Mtb* virulence factor which is not present in BCG, drove MMP-10 secretion. These data implicate MMP-10 in the immunopathological tissue destruction seen in pulmonary TB. It is of particular interest that ESAT-6 may be driving this process, which in addition to the role it plays in *Mtb* virulence will contribute to the success of the organism by facilitating transmission and promoting drug resistance.

MMP-10 is a secreted protease and through the Luminex profiling, we had investigated the majority of secreted MMPs in TB. However, this approach will not identify the membrane-bound MMPs in TB. The membrane bound collagenase MMP-14 has a particularly important role in cell migration as well as collagen degradation because of its cell surface localisation [116]. We have previously shown increased MMP-14 gene expression in *Mtb* infected monocytes [76], but this initial observation of increased gene expression had not been studied further, I therefore proceeded to investigate MMP-14 regulation and its role in collagen degradation and leukocyte migration in patients with pulmonary TB and a functional monocyte based cellular model of TB. The findings will be presented and discussed in the next chapter.

5. CELL SURFACE MMP-14 DRIVES COLLAGEN DEGRADATION AND LEUKOCYTE MIGRATION

5.1 Introduction

MMP-14 is membrane bound and its chief substrates are type I, II and III collagen [112]. Because of its cell surface localisation it degrades collagen in the immediate pericellular environment. A key role for MMP-14 in driving cell migration, by clearing a path at the leading edge of cells for movement through extracellular matrix, has been identified [116, 118, 192]. Accumulating evidence from a zebrafish embryo model indicates that monocyte/macrophage migration may drive bacterial expansion and dissemination in mycobacterial infection [107, 109, 110]. MMP-14 has been implicated in promoting migration of cells of the monocyte lineage [121-123]

Unbiased approaches implicate MMP-14 in TB pathogenesis. For example, a microarray study showed MMP-14 gene expression to be 28.6 fold greater in human lung TB granulomas than normal lung [80]. Similarly, whole blood gene expression profiling has shown MMP-14 expression to be higher in patients with active TB than healthy controls [193]. However, to our knowledge there has never been a detailed study of the role of MMP-14 in TB pathogenesis.

Therefore we investigated the hypothesis that MMP-14 drives two immunopathological processes in TB; leukocyte migration to foci of *Mtb* infection

and localised collagen degradation at sites of disease, using functional monocyte based cell culture model and samples from TB patients.

5.2 Results

5.2.1 MMP-14 is increased in the sputum of TB patients and correlates with lung infiltration

We investigated MMP-14 gene expression in the sputum of patients with TB (n=15) and controls (n=10) to identify if MMP-14 was expressed in cells *in vivo* from areas of inflammation and tissue destruction.

The patient cohort is described in Table 8. The TB and control group were closely matched for age, but a higher proportion of females were present in the control group which may reflect a difference between the sexes in health seeking behaviour [151]. TB patients had significantly more symptoms (fever, cough, night sweats, weight loss and breathlessness), a lower BMI and higher number of abnormal respiratory examinations, consistent with the underlying diagnosis.

All the controls were smear and culture negative for *Mtb*. Twelve of the TB cases were culture positive and of the 3 remaining cases, one was smear positive. These 3 patients all had clinical and radiological features highly suggestive of TB and had been started on TB treatment by a clinician.

MMP-14 gene expression (normalised to β-actin), was higher in the sputum of patients with TB compared to controls (Fig. 20A $p<0.05$). The median value and interquartile ranges (in brackets) for MMP-14/ β-actin gene expression in arbitrary units was for patients with TB 97.7 (56.7 – 150) and for controls 19.1 (7-97.2). Despite the relatively small sample size, the level of MMP-14 gene expression positively correlated with the degree of lung infiltration on chest radiograph (Fig. 20B, $r=0.483$; $p<0.05$). These data confirm that MMP-14 is present at the site of disease.

Table 8: Induced sputum matrix metalloproteinase analysis - Characteristics of patient cohort

Patient characteristics	Control	TB	
Total no.	10	15	
Male: Female	4:6	10:5	
Median age (range) years	31.5 (21-48)	40 (24-73)	ns
Symptoms (duration in days)			
Any	1	15	
Fever	1	11	
Cough	0	14	
Haemoptysis	0	1	
Night sweats	1	12	
Weight loss	0	8	
Breathlessness	0	6	
Pleuritic pain	1	11	
Anorexia	1	3	
Median duration (range)	0 (0-4)	30 (7-98)	p<0.0001
Examination			
Median BMI (range)	25.4 (17.5 - 55.7)	21.6 (18.5 – 29.1)	p<0.05
Temp>37.5	0	1	ns
Abnormal respiratory system	4	13	
Smear			
Positive	0	8	
Negative	10	7	
Culture			
Positive	0	12	
Negative	10	3 *	

*One of these 3 patients was smear positive and all had clinical features highly suggestive of TB with diagnostic features on chest radiograph

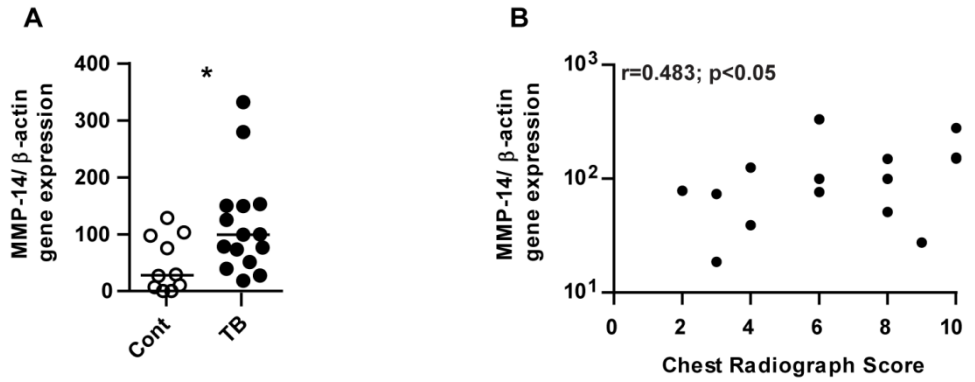

Figure 20: MMP-14 gene expression is increased in the sputum of patients with pulmonary TB and correlates with lung infiltration on chest radiograph

Induced sputum samples were collected prospectively from healthy controls (n=10) and TB patients (n=15) in Cape Town, South Africa. MMP-14 and β-actin gene expression were analysed in the sputum cell pellets by RT-PCR. The degree of lung infiltration on chest radiograph was scored on a scale of 0-10. **A**, MMP-14 gene expression (normalised to β-actin) was increased in the sputum of TB patients compared to healthy controls. Each circle represents one patient and the horizontal line the median value. Statistical analysis was performed using the Mann Whitney U Test (*$p<0.05$). **B**, MMP-14 gene expression in the sputum of TB patients positively correlated with the degree of lung infiltration on chest radiograph by Spearman correlation coefficient ($r=0.483$; *$p<0.05$).

5.2.2 *Mtb* infection of primary human monocytes drives MMP-14 expression

Next, we studied the effect of direct *Mtb* infection on MMP-14 expression in a cellular model. MMP-14 driven degradation of pericellular collagen requires its presence at the cell surface. Flow cytometric analysis showed that *Mtb* infection caused an increase in the MFI for MMP-14 on unpermeabilised monocytes compared to uninfected cells at 24 hours (Fig. 21A). Quantification showed a 31.7 fold increase in MMP-14 surface expression with *Mtb* infection (Fig. 21B, $p<0.05$).

Next, we analysed the kinetics of MMP-14 gene expression in *Mtb* infected monocytes. *Mtb* infection caused a non significant 1.4 fold increase in MMP-14 gene expression (normalised to β-actin) at 3 hours rising to 10.6 fold at 6 hours and 73.4 fold at 24 hours incubation relative to uninfected monocytes (Fig. 22A, $p<0.001$ for 6 and 24 hours). This increased MMP-14 mRNA resulted in higher MMP-14 total protein expression in whole cell lysates of *Mtb* infected monocytes at 48 hours (Fig. 22B). Quantification demonstrated a 14.8 fold increase in the MMP-14 total protein expression compared to uninfected monocytes (Fig. 22C, $p<0.01$).

7H9 alone, which was the growth medium for the *Mtb,* had no greater effect on MMP-14 cell surface expression or gene expression than no stimulus.

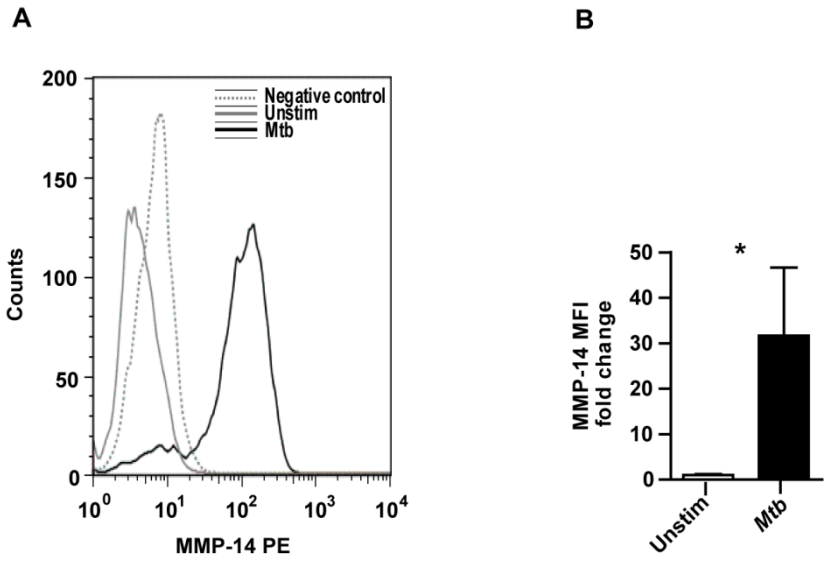

Figure 21: *Mycobacterium tuberculosis (Mtb)* infection of primary human monocytes drives surface MMP-14 expression

Human monocytes were infected with *Mtb* at a MOI of 1 and MMP-14 expression was analysed by flow cytometry. **A**, Surface MMP-14 expression was increased in *Mtb* infected monocytes compared to unstimulated monocytes at 24 hours. **B,** Analysis of MMP-14 median MFI for three separate donors, confirmed increased MMP-14 expression. The mean +/- SD is shown. Statistical analysis was performed using Student's t-test (*$p<0.05$).

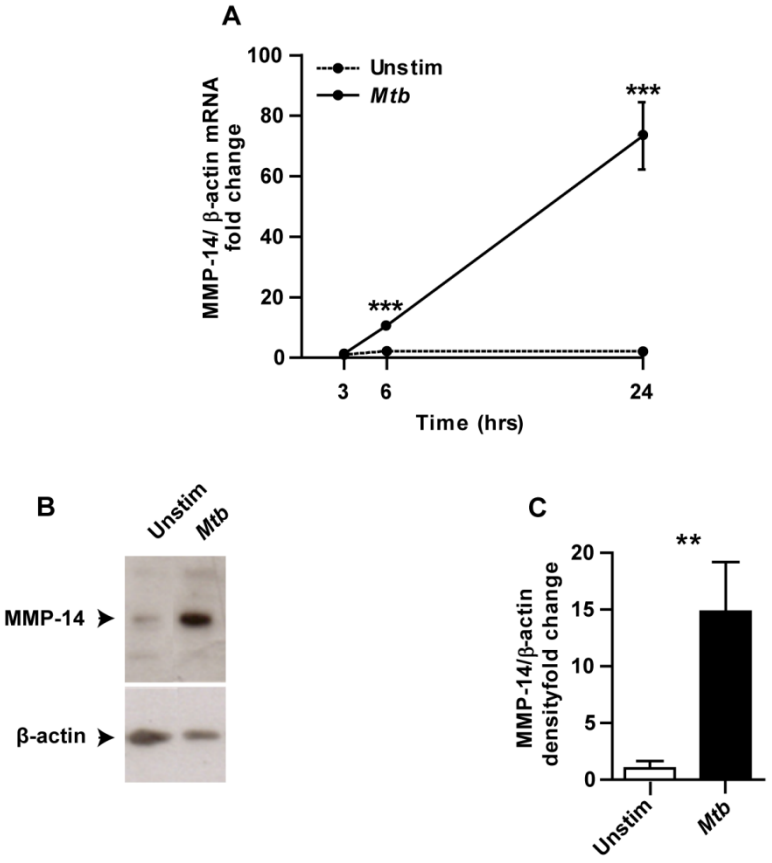

Figure 22: MMP-14 gene expression and total protein expression in monocytes is upregulated by direct *Mtb* infection

Human monocytes were infected with *Mtb* (MOI 1) and MMP-14 expression was analysed by RT-PCR and western blotting. **A,** *Mtb* infection caused increasing MMP-14 mRNA (normalised to β-actin) from 3 hours through to 24 hours, while no change occurred in unstimulated monocytes. Mean +/- SD for an experiment performed in triplicate is shown and is representative of two independent experiments. **B,** *Mtb* infection increased MMP-14 protein at 48 hours compared to unstimulated monocytes. β-actin was probed as a loading control. **C**, Densitometric analysis of MMP-14 and β-actin bands, confirmed increased MMP-14 total protein expression. Mean +/- SD for an experiment performed in triplicate is shown and is representative of two independent experiments. Statistical analysis was performed using Student's t-test (**p<0.01, ***p<0.001).

5.2.3 MMP-14 causes pericellular collagen degradation in *Mtb* infected monocytes

To determine whether MMP-14 was having a proteolytic effect, we performed fluorescent microscopy of cells plated on fluorescent collagen. *Mtb* infection drove surface MMP-14 expression on unpermeabalised monocytes at 24 hours incubation (Fig. 23). *Mtb* infection caused collagen degradation, as indicated by the black zones where fluorescence is absent, which co-localised with areas of MMP-14 expression. Pericellular collagen degradation co-localising with MMP-14 expression was not seen with the unstimulated monocytes.

To determine specificity, we neutralised MMP-14 activity with an inhibitory antibody. A neutralising concentration of 10µg/ml for the MAB3328 antibody is recommended in the data sheet and has been employed in other assays [121]. This downregulated the *Mtb* driven collagen degradation (Fig. 24). The zones of collagen clearance were present in close association with the *Mtb* infected monocytes (Fig. 24B), but were absent in those *Mtb* infected monocytes incubated with the MMP-14 inhibitory antibody (Fig. 24C). The surface area of degraded collagen was quantified, demonstrating that *Mtb* infection drove 42.8 times more collagen degradation by monocytes in comparison to no stimulus and that MMP-14 inhibition resulted in a 73% reduction in this collagen degradation (Fig. 24E $p<0.001$). A matched isotype control antibody had no effect on the collagen degradation driven by *Mtb* infected monocytes. This demonstrates that the *Mtb* driven pericellular collagen degradation is MMP-14 dependent (Fig. 24D and E).

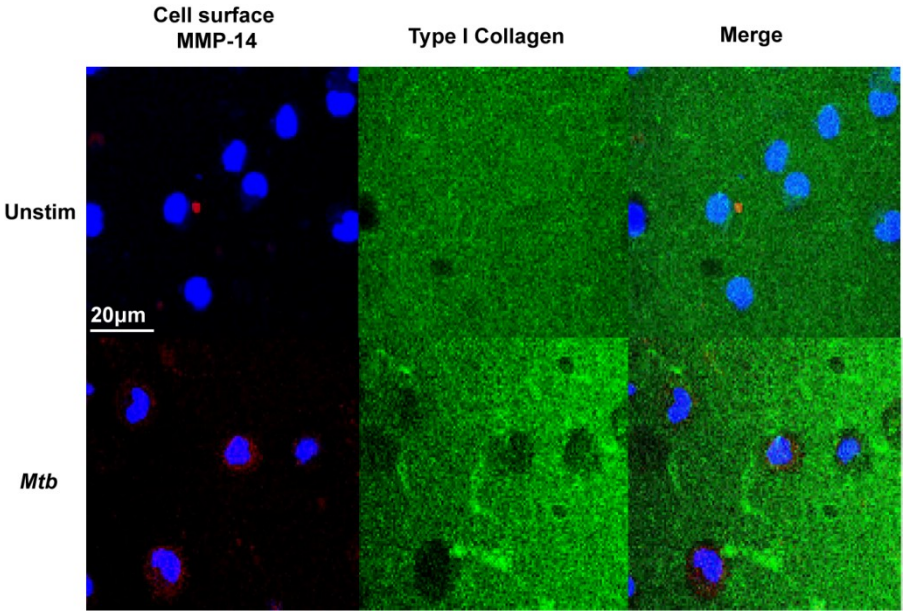

Figure 23: MMP-14 expression co-localises with collagen degradation driven by *Mtb* infected monocytes

Human monocytes were seeded on FITC conjugated Type I Collagen and infected with *Mtb* (MOI 1). MMP-14 surface expression and collagen degradation were analysed by immunofluorescent staining and microscopy. Blue=DAPI nuclear stain, Magenta=MMP-14, Green= Type I Collagen. *Mtb* infection increased surface MMP-14 expression and caused black zones of pericellular collagen degradation that were not seen with unstimulated monocytes at 24 hours incubation. MMP-14 surface expression co-localised with areas of Type I Collagen degradation. The images are representative of 3 independent experiments.

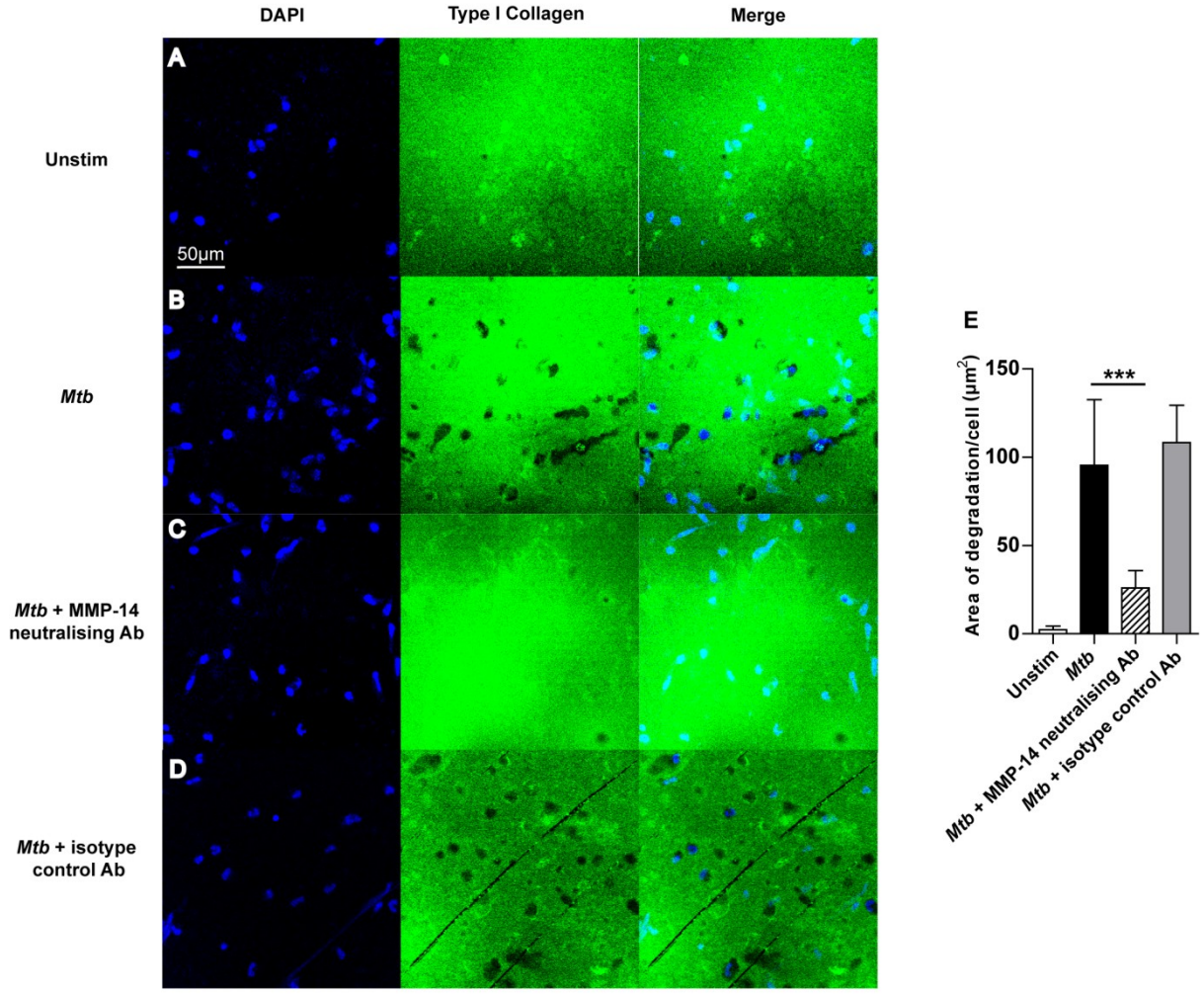

Figure 24: *Mtb* driven collagen degradation is MMP-14 dependent

Human monocytes were seeded on FITC conjugated Type I Collagen and infected with *Mtb* (MOI 1). Collagen degradation was analysed by immunofluorescent microscopy. Blue=DAPI nuclear stain, Green= Type I Collagen. MMP-14 activity was neutralised with an inhibitory anti MMP-14 antibody (Ab, MAB3328, Millipore) at 10µg/ml. **A,** Pericellular collagen was intact around unstimulated monocytes at 24 hours. **B**, *Mtb* infected monocytes degraded pericellular collagen **C,** Neutralisation of MMP-14 activity suppressed pericellular collagen degradation. **D,** A matched isotype control antibody did not suppress pericellular collagen degradation by *Mtb* infected monocytes. **E,** Degraded collagen area was quantified for five images per condition and is expressed as the area of degraded collagen per cell (μm^2). Neutralisation of MMP-14 activity reduced pericellular collagen degradation. The results shown are from a single experiment and are representative of 3 independent experiments. The mean +/- SD is shown. Statistical analysis was performed using a one-way ANOVA with Tukey's post hoc test (***$p<0.001$).

5.2.4 MMP-14 is expressed in granulomas of patients with TB and is upregulated by *Mtb* induced intercellular networks

To further investigate the significance of the cellular data to clinical tuberculosis, biopsies from patients with active TB (n=3) and normal lung tissue at the excision margins of samples from patients with lung cancer (n=3) were immunostained for MMP-14. MMP-14 immunoreactivity was identified diffusely in TB granulomas both in Langerhan's multinucleate giant cells and also in the surrounding epithelioid macrophages (Fig. 25A). In the normal lung tissue of the control patients MMP-14 immunoreactivity was detected only in alveolar macrophages. We have previously shown increased MMP-14 gene expression at the site of disease and this finding confirms the presence of the MMP-14 protein.

MMP-14 was diffusely expressed in the granuloma, but mycobacteria are relatively sparse in granulomas [68]. This lead to investigation of *Mtb* induced intercellular networks and MMP-14 expression, in addition to direct infection. Fluorescent microscopy showed that cell surface MMP-14 expression was increased in CoMTb stimulated unpermeabalised monocytes at 24 hours incubation compared to unstimulated cells (Fig. 25B). Permeabalisation of cells prior to staining demonstrated that MMP-14 was increased intracellularly at 24 hours, as well as on the cell surface. Paraformaldehyde fixation is necessary before permeabalisation of cells with Triton X. We found that it was not possible to detected MMP-14 on the surface of unpermeabalised cells that had been paraformaldehyde fixed prior to immunostaining. This was likely a consequence of antigen cross linking impairing

antibody binding [194]. Therefore the MMP-14 detected in the images of permeabalised monocytes was intracellularly located.

Flow cytometric analysis demonstrated an increase in the MMP-14 MFI for CoMTb stimulated unpermeabalised monocytes compared to unstimulated cells at 24 hours (Fig. 26A). Quantification showed a 17.5 fold increase in MMP-14 surface expression with CoMTb (Fig. 26B, $p<0.05$). These data show that *Mtb* induced intercellular networks, as well as direct infection, drive monocyte surface and intracellular MMP-14 expression.

CoMTb stimulation drove a 5.2 fold increase in MMP-14 gene expression (normalised to β-actin) at 3 hours rising to 22.6 fold at 6 hours and 45.4 fold at 24 hours (Fig. 26C, $p<0.001$ for 6 and 24 hours), indicating that the increased surface expression of MMP-14 protein was secondary to increased gene expression.

In a separate experiment to that shown in Fig. 26A the effect of CoMCont on MMP-14 cell surface expression compared to no stimulus and CoMTb was measured by flow cytometry. The MFI (arbitrary units) for CoMTb stimulated unpermeabalised monocytes was 25.1 compared to CoMCont 12.8 and unstimulated 14.3 (Fig. 26D).

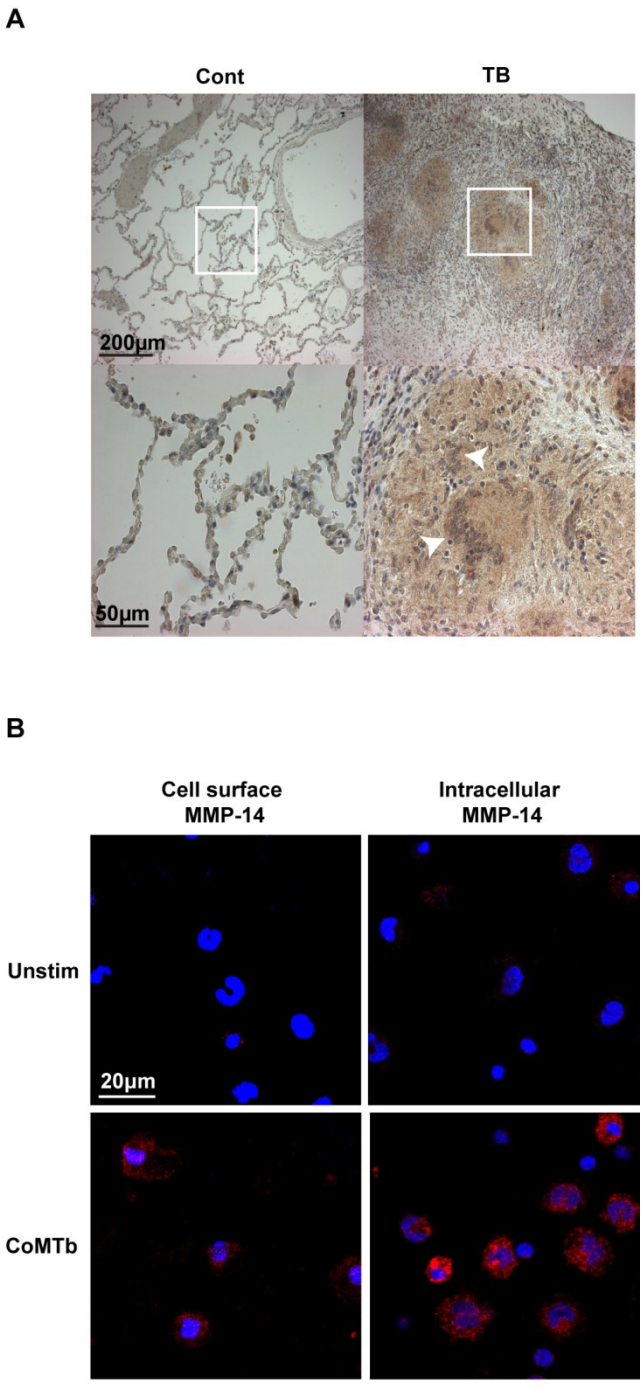

Figure 25: MMP-14 is expressed in granulomas of patients with TB and is upregulated by *Mtb* induced intercellular networks

A, MMP-14 immunohistochemistry was performed on biopsies from patients with culture proven TB (n=3) and normal lung tissue at the excision margins of patients with lung cancer (n=3). MMP-14 immunoreactivity appears brown against the blue haemotoxylin counterstain. MMP-14 was expressed throughout the granuloma within both giant cells and epithelioid macrophages. In control biopsies MMP-14 was expressed only in alveolar macrophages. Boxed areas represent higher magnification image and white arrows indicate Langerhan's multinucleate giant cells which are surrounded by epithelioid macrophages. **B,** Monocytes were stimulated with CoMTb. MMP-14 expression was analyzed by immunofluorescent staining. Blue=DAPI nuclear stain, Magenta=MMP-14. CoMTb stimulation increased both cell surface and intracellular MMP-14 expression at 24 hours compared to unstimulated monocytes. The images are representative of 3 independent experiments.

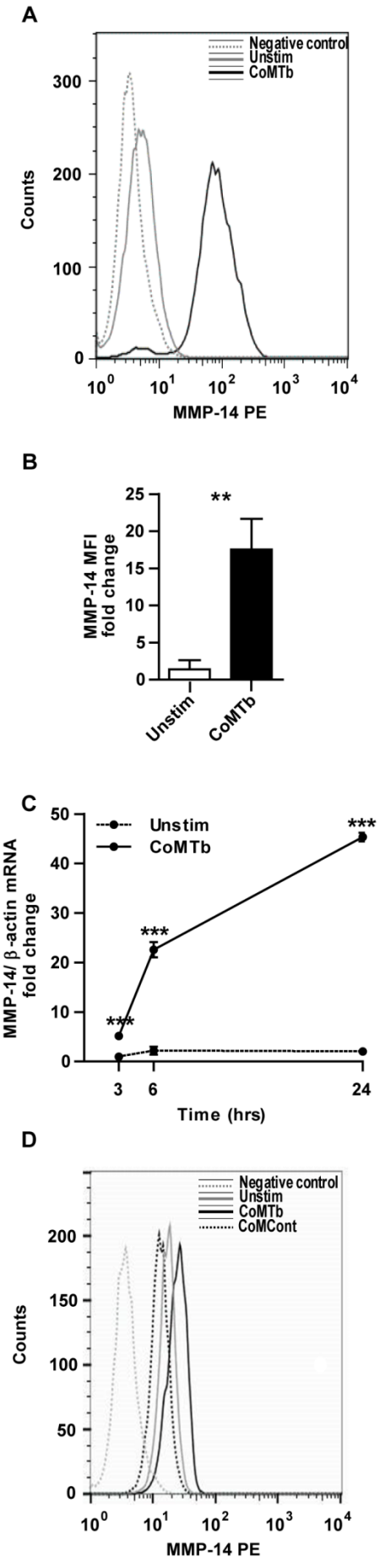

Figure 26: *Mtb* induced intercellular networks drive monocyte MMP-14 expression

Human monocytes were stimulated with CoMTb and MMP-14 expression analysed by flow cytometry (A, B and D) and RT-PCR (C). **A**, Surface MMP-14 expression was increased in CoMTb stimulated monocytes compared to unstimulated monocytes at 24 hours. **B,** Analysis of MMP-14 MFI for three separate donors, confirmed increased MMP-14 expression. The mean +/- SD are shown. **C,** CoMTb caused a progressive increase in MMP-14 mRNA (normalised to β-actin) from 3 hours through to 24 hours incubation, while no change was seen in unstimulated monocytes. Mean +/- SD for an experiment performed in triplicate is shown and is representative of two independent experiments. Statistical analysis was performed using Student's t-test (*p<0.05, ***p<0.001). **D** Surface MMP-14 expression was increased in CoMTb stimulated monocytes compared to unstimulated monocytes at 24 hours, but not in monocytes incubated with CoMCont.

5.2.5 MMP-14 expression driven by *Mtb* induced intercellular networks is regulated by p38 and JNK but not ERK MAPK signalling

MMP-14 expression in TB may be regulated by the MAPK pathways [100, 101] and therefore we investigated regulation of monocyte MMP-14 expression by these pathways. The MAPK pathways are briefly illustrated in Fig. 1.

CoMTb driven phosphorylation of the p38, ERK and JNK MAPK signalling molecules in whole cell lysates was investigated. CoMTb stimulation of monocytes caused a 3 fold increase in p38 phosphorylation (normalised to total p38) compared to unstimulated cells at 30 minutes incubation (Fig. 27A and B, $p<0.05$). A 2.7 fold increase in ERK phosphorylation (normalised to total ERK) was similarly observed (Fig. 27A and C, $p<0.05$). However for JNK, increased levels of not only the phosphorylated but also the total protein were identified (Fig. 27A), therefore densitometric quantification was not performed. The reasons for this unusual finding are unclear, but were consistent across two experiments performed in triplicate. The initial suspicion was that the total JNK antibody was cross reacting with the phosphorylated JNK that has not been fully removed from the membrane by the stripping process. However Cell Signalling Technology advise that the total JNK antibody (9252) does not cross react with phosphorylated JNK, and this antibody has been widely used since 2000, and cited in recent papers where this problem was not experienced [195] .

Specific chemical inhibitors and flow cytometric analysis of MMP-14 MFI on unpermeabalised monocytes were used to investigate the role of the MAPK signalling pathways in controlling MMP-14 expression. The mechanism of action of SB and PD has already been discussed. SP600125 (SP) is a reversible ATP competitive inhibitor of JNK phosphorylation [196]. Inhibition of the p38 MAPK signalling pathway by SB203580 resulted in a 26% reduction in CoMTb driven surface MMP-14 expression on unpermeabalised monocytes at 24 hours incubation (Fig. 28A and B, $p<0.05$). Inhibition of the JNK MAPK signalling pathway by SP produced a 28% reduction (Fig. 28E and F, $p<0.05$) In contrast, inhibition of the ERK MAPK pathway with PD98059 had no effect (Fig. 28C and D). These data showed that monocyte surface MMP-14 expression driven by intercellular networks was regulated by p38 and JNK but not ERK MAPK signalling

PI staining showed that the chemical inhibitors cause no cell death at 24 hours incubation. DMSO, the carrier for the inhibitors, had no effect on MMP-14 surface expression when used at equivalent concentrations alone.

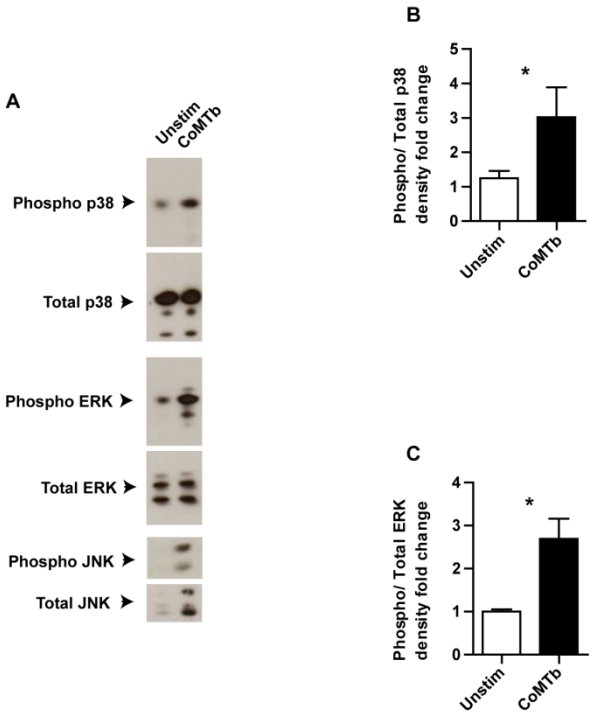

Figure 27: *Mtb* induced intercellular networks drive p38, ERK and JNK MAPK phosphorylation in monocytes

A, p38, ERK and JNK MAPK phosphorylation was analyzed by western blotting. CoMTb stimulation increased phosphorylated p38 and ERK in monocytes compared to unstimulated monocytes at 30 minutes, while total p38 and ERK were unchanged. However CoMTb stimulation increased both phosphorylated and total JNK. **B** and **C,** Densitometric analysis of phosphorylated and total p38 and ERK bands, confirmed increased phosphorylation of p38 and ERK. Mean +/- SD for an experiment performed in triplicate is shown and is representative of two independent experiments. Statistical analysis was performed using Student's t-test (*$p<0.05$).

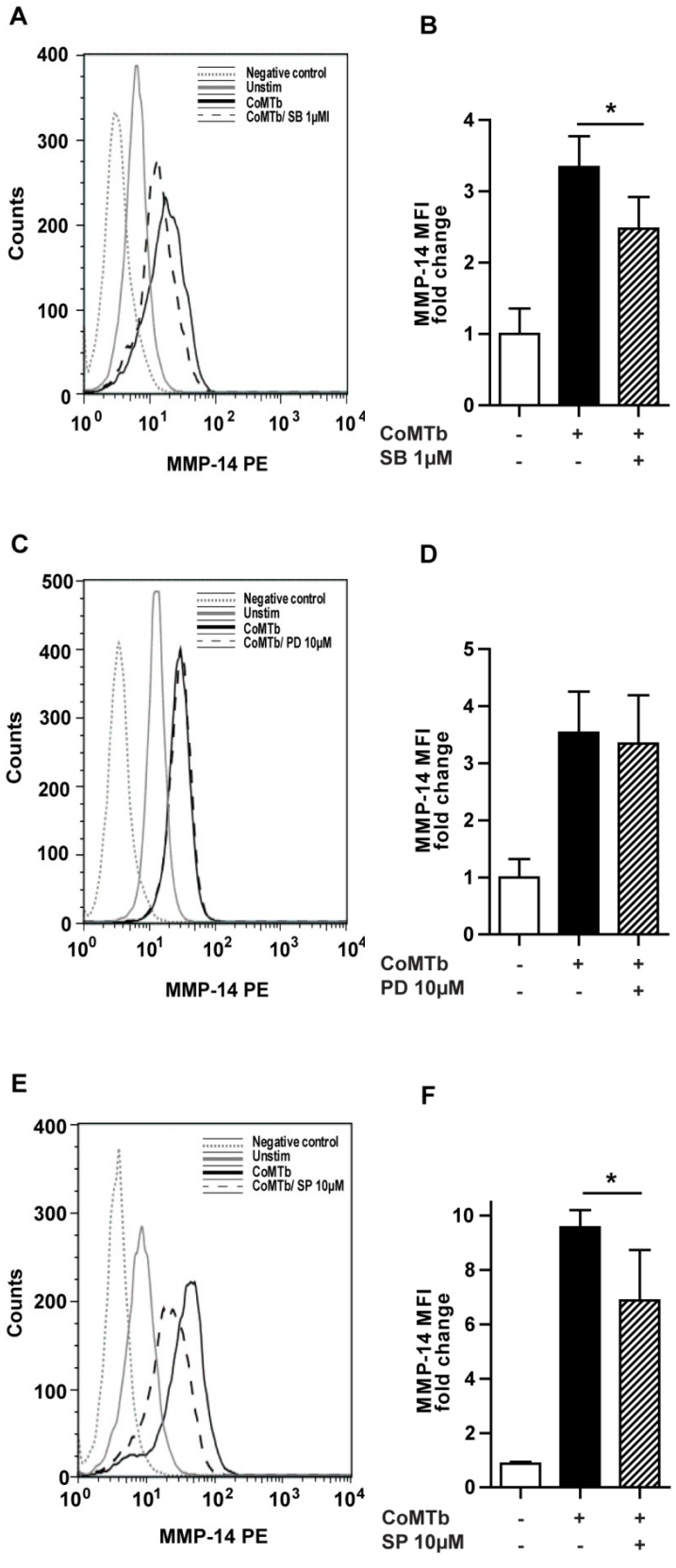

Figure 28: Intercellular network driven monocyte MMP-14 expression is regulated by p38 and JNK but not ERK MAPK signalling

Human monocytes were pre-incubated with the p38 inhibitor SB203580 (SB) 1μM, ERK inhibitor PD98059 (PD) 10μM or JNK inhibitor SP600125 10μM for 1 hour prior to stimulation with CoMTb. MMP-14 surface expression was measured by flow cytometry. **A, C, E** Chemical inhibition of the p38 and JNK but not the ERK MAPK pathway downregulated CoMTb driven surface MMP-14 expression on monocytes at 24 hours. **B, D, F** Analysis of MMP-14 median fluorescence intensity (MFI) for three separate donors, confirmed CoMTb driven surface MMP-14 expression is regulated by the p38 and JNK but not the ERK pathway. The mean +/- SD are shown. Statistical analysis was performed using Student's t-test (*$p<0.05$).

5.2.6 The components of *Mtb* induced intercellular networks

We analyzed cytokines, chemokine and growth factors present in CoMCont and CoMTb from 4 different monocyte donors. Table 9 presents the median values with interquartile ranges for all 4 donors combined. The full list of the thirty cytokines, chemokines and growth factors analysed is detailed in METHODS.

The cytokines IL-1β, IL-6, TNFα, interferon alpha (IFNα), IL-12, interleukin 1 (IL-1) receptor antagonist and interleukin 2 (IL-2) receptor were increased in CoMTb. CCL2 (monocyte chemoattractant protein 1, MCP-1), CCL3 (macrophage inflammatory protein 1 alpha, MIP-1α), CCL4 (macrophage inflammatory protein 1 beta, MIP-1β), CXCL8 (interleukin 8, IL-8) and CXCL9 (monokine induced by gamma interferon, MIG) were the chemokines that were elevated in CoMTb. Finally the growth factors granulocyte macrophage colony stimulating factor (GM-CSF), vascular endothelial growth factor (VEGF), granulocyte colony stimulating factor (G-CSF) and fibroblast growth factor (FGF) were higher in CoMTb.

It was protocol to filter sterilize CoMTb through a 0.2μM pore size Anopore membrane as discussed in METHODS. It has been shown that Anopore (aluminium oxide) filtration removes all MMP -1, -7 and 9 but that Millipore (polyvinylidene fluoride) filtration does not remove MMP -1 [140]. Therefore, I investigated the effect of Anopore *vs.* Millipore filtration on the levels of the above cytokines, chemokines and growth factors in CoMTb.

The mean levels that were found in the four Anopore filtered CoMCont and CoMTb samples are shown in comparison to mean levels in four Millipore filtered CoMCont and CoMTb samples in Table 10. This shows that the Millipore filtration removed IL-1β, IL-6, TNFα, IFNα, IL-2 receptor, CCL3, CCL4, CXCL9, GM-CSF, VEGF, G-CSF and FGF. Anopore filtration removed CCL8, though a large concentration remained. It was therefore appropriate that Anopore filtration was the standard protocol. This resulted in the CoMTb containing a higher concentration of the cytokines, chemokines and growth factors that constitute the *Mtb* induced intercellular network.

Table 9: Cytokines, chemokines and growth factors in CoMCont and CoMTb

	CoMCont	CoMTb
Cytokines		
IL-1β	165 (39-192)	31813 (7994 - 39014)
IL-6	1 (1-1)	50914 (11903 - 63160)
TNFα	1 (1-1)	15369 (1607 - 63755)
IFNα	6 (6-6)	340 (69 - 550)
IL-12	2 (2-2)	752 (167 - 3853)
IL-1 receptor antagonist	628 (144-744)	8893 (3774 - 11242)
IL-2 receptor	2 (2-25)	994 (574 - 1326)
Chemokines		
CCL2 ((MCP-1)	6 (6-10)	1184 (334 - 2780)
CCL3 (MIP-1 α)	4 (4-4)	215660 (19320 - 361100)
CCL4 (MIP-1 β)	2 (2-2)	19799 (5630 -238242)
CXCL8 (IL-8)	34 (9-41)	96439 (7176 - 180980)
CXCL9 (MIG)	47 (8-86)	175 (50 - 217)
Growth factors		
GM-CSF	3 (3-3)	286 (70-1324)
VEGF	35 (7-45)	168 (95 - 192)
G-CSF	3 (3-3)	1394 (245 - 1896)
FGF	256 (64 - 259)	343 (94 - 378)

Median levels and interquartile ranges (in brackets) in pg/ml

Table 10: Anopore *vs*. Millipore filtration of CoMCont and CoMTb

	Filter	CoMCont	CoMTb
Cytokines			
IL-1β	Anopore	132	26274
	Millipore	*3*	*978*
IL-6	Anopore	1	41992
	Millipore	*3*	*978*
TNFα	Anopore	1	26910
	Millipore	*4*	*2430*
IFNα	Anopore	6	319
	Millipore	*6*	*30*
IL-12	Anopore	2	1590
	Millipore	*7*	*1399*
IL-1 receptor antagonist	Anopore	506	7969
	Millipore	*345*	*5042*
IL-2 receptor	Anopore	9	964
	Millipore	*2*	*104*
Chemokines			
CXCL8 (IL-8)	Anopore	28	94865
	Millipore	*32117*	*17977623*
CCL3 (MIP-1 α)	Anopore	4	198693
	Millipore	*40*	*12651*
CCL4 (MIP-1 β)	Anopore	2	87890
	Millipore	*103*	*4481*
CCL2 ((MCP-1)	Anopore	7	1426
	Millipore	*251*	*1016*
CXCL9 (MIG)	Anopore	47	147
	Millipore	*21*	*49*
Growth Factors			
GM-CSF	Anopore	3	560
	Millipore	*3*	*191*
VEGF	Anopore	29	151
	Millipore	*0*	*48*
G-CSF	Anopore	3	1178
	Millipore	*3*	*31*
FGF	Anopore	193	271
	Millipore	*1*	*28*

Median levels and interquartile ranges (in brackets) in pg/ml

5.2.7 Signalling through Gi protein coupled pathways regulates monocyte MMP-14 expression driven by *Mtb* induced intercellular networks

CC chemokines are considered critical to monocyte chemotaxis and migration to sites of infection including *Mtb* [197]. We chemically inhibited signalling through Gi protein coupled pathways using PT [93]. Chemokines signal through Gi proteins and downstream effects of PT include inhibition of chemotaxis [94]. However a range of other ligands signal through G protein coupled receptors, so the effects of PT are not specific to chemokines [93]. PT caused a 35% reduction in CoMTb driven surface MMP-14 expression on unpermeabalised monocytes at 24 hours incubation (Fig 29A and B, $p<0.05$). This shows that the component of the *Mtb* induced intercellular network that signal through Gi protein coupled pathways were driving monocyte surface MMP-14 expression. This component includes but is not limited to chemokines.

Investigation of the individual chemokine in CoMTb which was responsible for driving MMP-14 expression was attempted. The focus was placed on CCL2 given its established role in monocyte chemotaxis [197]. However recombinant CCL2 used at much higher levels than that identified in CoMTb of 100ng/ml did not increase MMP-14 cell surface expression on flow cytometry. When combined as a stimulus with Tb supernatant there was only a very small augmentation of MMP-14 MFI on unpermeabalised monocytes compared to Tb supernatant alone. Therefore the next logical step was to attempt neutralisation of CCL2 in CoMTb using a specific antibody. However the neutralising antibody itself stimulated the cells, making the results uninterpretable.

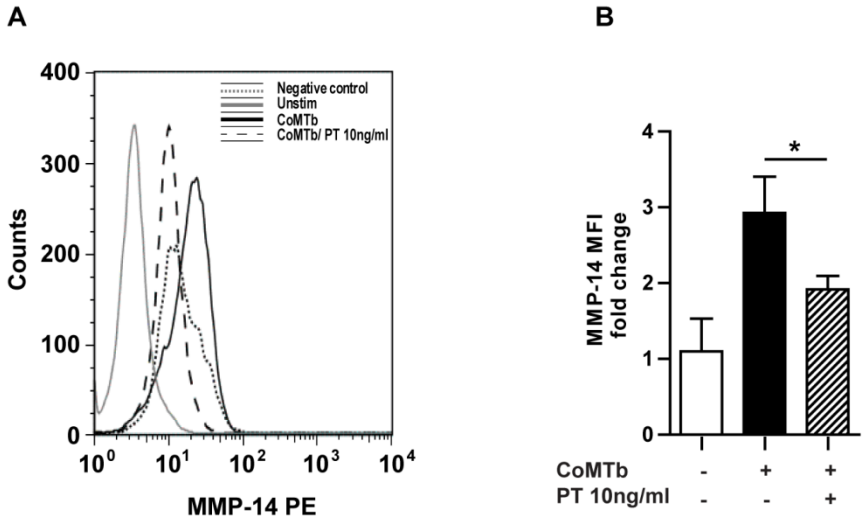

Figure 29: Signalling through Gi protein coupled pathways regulates monocyte MMP-14 expression driven by *Mtb* induced intercellular networks

Human monocytes were pre-incubated with PT 10ng/ml for 1 hour prior to stimulation with CoMTb. MMP-14 surface expression was measured by flow cytometry. A, Chemical inhibition of G-protein coupled receptor signalling downregulated CoMTb driven surface MMP-14 expression on monocytes at 24 hours. B, Analysis of MMP-14 median MFI for three separate donors, confirmed that CoMTb driven surface MMP-14 expression is regulated by G-protein coupled receptor signalling. The mean +/- SD are shown. Statistical analysis was performed using Student's t-test (*$p<0.05$).

5.2.8 Monocyte migration is driven by *Mtb* induced intercellular networks and regulated by MMP-14

We next investigated the role of MMP-14 in promoting monocyte migration using the agarose spot assay for chemotaxis. Monocytes migrated towards CoMTb-impregnated agarose spots, forming clusters around the edge at 24 hours incubation that were not observed in control spots (Fig. 30A and B), demonstrating that CoMTb was a chemotactic stimulus for monocyte migration. Monocytes migrating towards the CoMTb spot expressed higher levels of surface MMP-14 than the cells around the control spot (Fig. 30C and D), indicating that CoMTb drove MMP-14 expression in migrating cells.

Therefore, we investigated if inhibition of MMP-14 activity on monocytes reduced their migration towards CoMTb. MMP-14 inhibition reduced the size of monocyte clusters around spots (Fig. 31C and E). Migration was quantified using the 2 spots per condition with the diameter of monocyte clusters measured at 4 radial points per sphere. The diameter of the monocyte clusters for CoMTb was twice that for the control spots, and inhibition of MMP-14 activity resulted in a 44% reduction in the diameter of the monocyte clusters ($p<0.005$). A matched isotype control antibody had no effect on monocyte migration toward CoMTb (Fig. 31D and E).. These data show that monocyte migration towards *Mtb* induced intercellular networks is MMP-14 dependent.

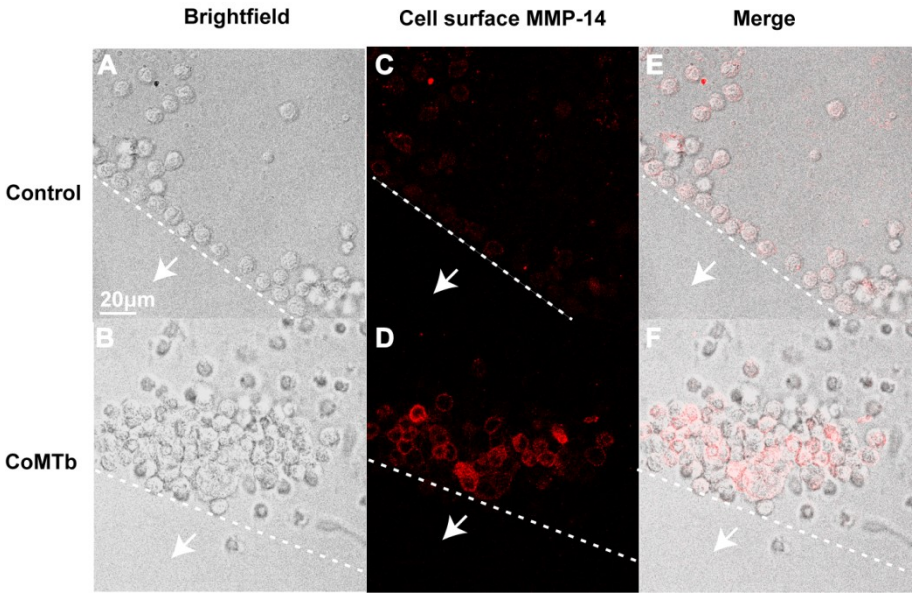

Figure 30: *Mtb* induced intercellular networks induce monocyte migration and concurrent MMP-14 expression

RPMI (Control) or CoMTb-impregnated agarose spots were set on slides coated with Type I collagen. Human monocytes were then added. White arrows indicate the agarose spot and migratory stimulus, while the dashed line indicates the spot edge. Surface MMP-14 expression was measured by immunofluorescent staining, Magenta=MMP-14. **A, B,** Light microscopy images show that monocytes migrated towards the CoMTb spot forming a cluster at 24 hours, which did not occur for the control spot. **C, D,** Surface MMP-14 expression was greater on monocytes migrating towards the CoMTb spot than the control spot at 24 hours incubation. **E, F,** Merged images. Images are representative of 3 independent experiments.

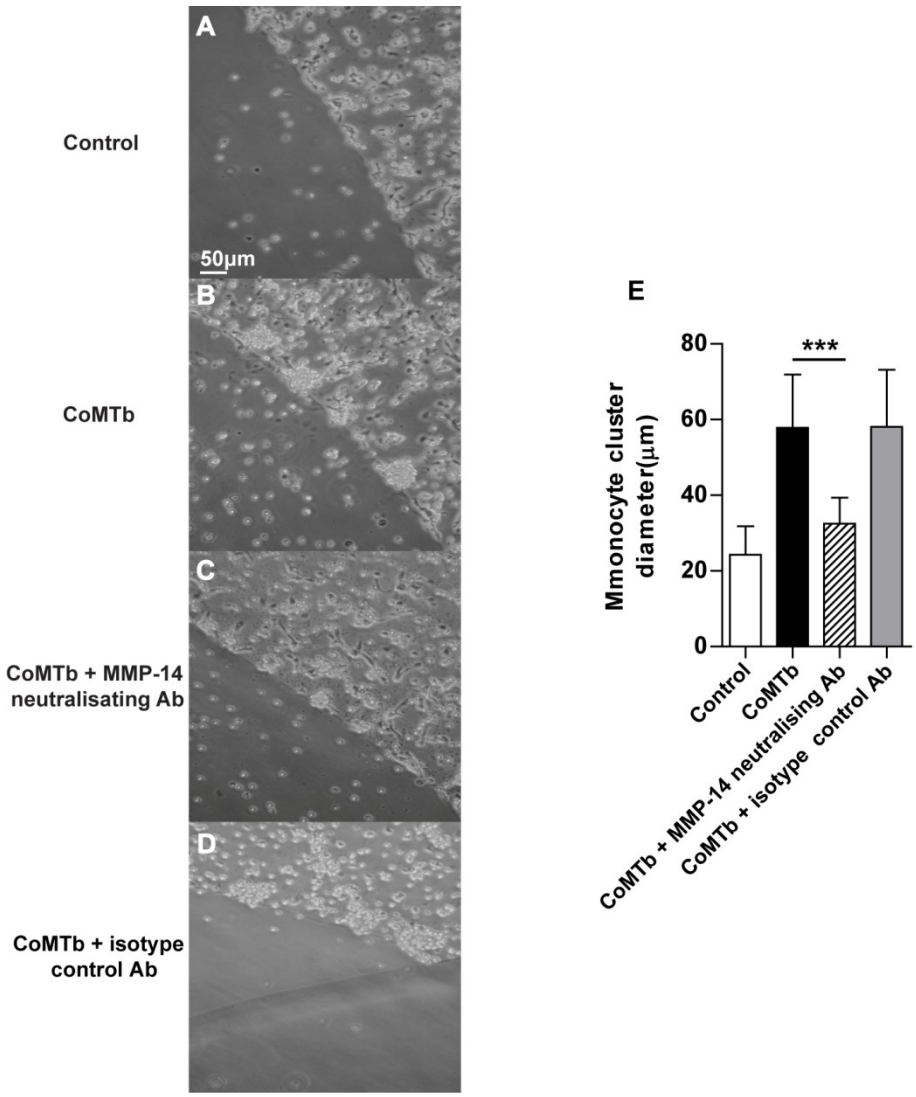

Figure 31: MMP-14 regulates monocyte migration driven by *Mtb* induced intercellular networks

RPMI (Control) or CoMTb-impregnated agarose spots were set on collagen-coated slides. Human monocytes were seeded on these slides. MMP-14 activity was neutralised with an inhibitory anti MMP-14 antibody (MAB3328, Millipore) at 10µg/ml. Light microscopy and image capture was undertaken at 24 hours. **A**, No clustering of monocytes occurred around the control spot. **B**, Monocytes migrated towards CoMTb agarose spots and formed clusters. **C**, Neutralisation of MMP-14 activity reduced the cluster size around CoMTb spots. **D,** A matched isotype control antibody did not reduce the cluster size around CoMTb spots **E,** Monocyte migration was quantified using two spots per condition with images taken at 4 radial points per spot. Maximum diameter of the monocyte clusters was measured, confirming that MMP-14 neutralisation reduced monocyte migration. The results are mean +/- SD from a single experiment and are representative of 2 independent experiments. Statistical analysis was one-way ANOVA with Tukey's post hoc test (***$p<0.001$).

5.3 Discussion

By investigation of patients with TB and functional cell culture models, we demonstrate that TB upregulates MMP-14 expression to cause both collagen destruction and cell migration. MMP-14 gene expression was increased in the sputum of TB patients, positively correlating with the degree of lung infiltration on chest radiograph, and MMP-14 is expressed diffusely in TB granulomas. *Mtb* and monocyte dependent intercellular networks upregulate expression of MMP-14 secondary to increased gene expression. MMP-14 expression causes type I collagen degradation. Monocyte migration was dependent on MMP-14 activity. The MMP-14 expression driven by intercellular networks was mediated by p38 and JNK MAPK and chemokine signalling. These data support the hypothesis that MMP-14 is a central regulator of collagen degradation and leukocyte migration in human pulmonary tuberculosis.

The existing data on MMP-14 in TB was discussed earlier, and the evidence for a role in other destructive lung disease is limited. An early study showed more intense immunoreactivity for MMP-14 in epithelial cells, fibroblasts and alveolar macrophages of emphysematous lung compared to healthy tissue, confirmed by western blotting. Analysis by gelatin zymography showed a higher ratio of the active to the proform of MMP-2 in emphysema, suggesting in situ activation by MMP-14 [198]. Immunohistochemical staining for MMP-14 in lung biopsies from patients with combined idiopathic pulmonary fibrosis/ emphysema and emphysema and controls was performed. This showed higher MMP-14 expression in interstitial fibroblasts

adjacent to areas of parenchymal destruction in diseased compared to healthy lung [199].

There is also some relevant published data on the role of MMP-14 in Toxoplasma infection. *Toxoplasma gondii* is an obligate intracellular parasite, which crosses basal membranes within macrophages and dendritic cells and invades ECM. Toxoplasma infection of THP-1 cells and macrophages upregulated MMP-14 expression measured by western blotting and flow cytometry [200, 201].

We demonstrated that MMP-14 expression on the monocyte surface is driven both by direct *Mtb* infection and the paracrine signalling of *Mtb* induced intercellular networks. This is important because although all monocytes/macrophages have the capacity to phagocytose *Mtb*, the number of intracellular bacilli present at the site of disease is low [68], but because of intercellular signalling networks there is still the potential for high MMP-14 expression. This was confirmed by our *in vivo* findings of increased MMP-14 mRNA in induced sputum, and diffuse MMP-14 expression throughout the granuloma of biopsies form TB patients. *Mtb* induced intercellular network have also previously been shown to drive MMP-9 secretion from monocytes [92].

.

We found that p38 and ERK MAPK signalling regulated the surface MMP-14 expression on monocyte stimulated by intercellular networks. The role of MAPK signalling in controlling MMP-14 monocyte surface expression has not been

previously studied, so the findings are novel though neither p38 nor JNK are a master regulator, as only small changes were noted with inhibition of their activity. We did not demonstrate regulation by ERK MAPK in monocytes, but studies using malignant cells have identified a role for ERK in driving constitutive MMP-14 expression [202, 203], suggesting cell specific regulation.

The *Mtb* driven MMP-14 surface expression was secondary to increased mRNA accumulation. The MMP-14 gene promoter has a NF-κB consensus binding site and we attempted chemical inhibition of NF-κB signalling. Unacceptably high cell death occurred in the presence of SC-514 and Helenalin even at low concentrations therefore it was not possible to pursue this line of enquiry. However NF-κB remains the most likely candidate for the transcriptional regulator driving MMP-14, given its importance in innate immunity and inflammation [103] and the role already identified in other models [204]. A future experimental strategy would be to use siRNA technology to knockdown expression of the NF-κB gene.

We also demonstrated that MMP-14 upregulation was G-protein coupled receptor dependent, implicating chemokine activity. Chemokines are considered critical to leukocyte migration to TB granulomas [96].CCL2 signalling through the CCR2 receptor may be important to monocyte-macrophage migration from studies utilising knockout mice [197]. In our cellular model, chemokine signalling drives expression of MMP-14 on the monocyte surface, which is the critical cell surface MMP for migration [116]. Using fluorescent microscopy MMP-14 clustering has been observed at motility associated protrusions of CCL2 stimulated monocytes

transmigrating through endothelium [121], and CCL2 and CXCL8 promote MMP-14 surface expression, clustering and activity in endothelial cells [205].

Historically, attempts to identify individual chemokines within the *Mtb* induced intercellular network driving MMP expression, by using neutralising antibodies, have proved unsuccessful [72, 92]. This was thought to be a consequence of redundancy within chemokine receptor signalling [206]. I still felt it worthwhile exploring the role of CCL2 specifically in driving monocyte MMP-14 expression, as this chemokine has such a critical role in monocyte migration[197]. However efforts were thwarted by difficulties such as the stimulatory effect of the CCL2 neutralising antibody, as discussed in the results section. As mentioned for investigation of NF-κB signalling a future approach would be to use siRNA technology to knockdown CCL2 gene expression when generating CoMTb.

Unlike the secreted MMPs, MMP-14 is activated intracellularly then inserted at the cell surface [207]. We were able to show that neutralisation of cell surface MMP-14 activity reduced *Mtb* driven pericellular Type I collagen degradation in our fluorescent collagen degradation assay. This is particularly critical to our hypothesis and gives strength to the proposal that the MMP-14 expressed at the site of disease will be driving collagen degradation. Evidence indicates that MMP-14 drives pericellular collagen degradation in other systems. siRNA technology was used to abrogate human gingival fibroblast MMP-14 expression, in a similar assay utilising fluorescently labelled collagen, with almost complete loss of type I collagen degradation [208]. Again it seems that applying siRNA technology to our model may provide data to support the findings with the MMP-14 neutralising antibody.

Although the granuloma has traditionally been viewed as a host strategy to control mycobacterial growth, accumulating evidence suggests that monocyte migration may have deleterious effects to the host. As previously discussed, in the *M. marinum* infected zebrafish model, macrophages migrating into granulomas become newly infected allowing bacterial expansion and then egress the granuloma, disseminating infection to new sites [107, 110]. In mice, intranasal administration of polyinosinic-polycytidylic acid, a type I interferon inducer, caused a CCR2 dependent excessive accumulation of monocytes in the lungs of *Mtb* infected mice, with increased bacterial burden and decreased survival [209].

However, the proteases responsible for driving this leukocyte migration are not considered. We demonstrated that *Mtb* induced intercellular network drove MMP-14 expression in migrating cells, that the monocyte migration in TB was MMP-14 dependent, and that MMP-14 surface expression was potentially upregulated by chemokine signalling.

The background data presented earlier suggesting a critical role for MMP-14 in cell migration, largely pertained to cells invading 3D matrices. The agarose spot assay used in this work was a 2D assay where the cells can migrate on top of the type I collagen layer. This indicates that MMP-14 was promoting the monocyte migration independently of ECM degradation, and therefore three potential mechanisms will be discussed.

There is a body of evidence suggesting that MMP-14 cleaves cell surface proteins to promote the organised cell adhesion-deadhesion required for migration. For example,

syndecan-1 is a transmembrane heparan sulphate proteoglycan which binds extracellular matrix components including collagen, and is cleaved by MMP-14. MMP-14 differs from the secreted MMPs in that its activity is inhibited by TIMP-2 but not TIMP-1. Migration of fibrosarcomatous cells in a wound healing assay was reduced in cells transfected to express a mutant uncleavable syndecan-1, but enhanced in cells transfected with normal syndecan-1 in a process inhibited by TIMP-2 but not TIMP-1 [210]. CD44 is a receptor for haemagglutinin, which is abundant in many tissues, and other ECM components such as Type I collagen. A breast cancer cell line was transfected with plasmids to express CD44 and MMP-14. Using western blotting and a phagokinetic track motility assay, it was shown that MMP-14 cleaves CD44 to produce a soluble fragment. Expression of MMP-14 or CD44 alone did not stimulate cell migration, but co-expression did. Co-expression of a CD44 deletion mutant, which cannot be cleaved by MMP-14, resulted in loss of cell migration [211]. MMP-14 dependent cleavage of other cell surface proteins which interact with ECM components such as integrins and transglutaminase are also considered important to migration of malignant cells [212, 213]

Other evidence suggests internalisation of MMP-14 from the leading cell edge is important in driving migration. A Chinese hamster ovary cell line was transfected with wild-type MMP 14 and varying deletion mutants with different domains absent. Fluorescent microscopy, a matrigel invasion assay and phagokinetic track assay were used. The cytoplasmic tail was required for the internalisation of MMP-14 from the leading edge of the cell in clathrin coated pits, and that this process of internalisation was important to the migration and invasion driven by MMP-14 [214]. Initially it was postulated that this could be because degraded or TIMP-2 inhibited

MMP-14 was not being removed from leading edge and replaced with “fresh” MMP-14. However in a separate study HeLa cells were transfected with wild type MMP-14, MMP-14 with Thr 567 glutamate substituted (permanently phosphorylated) or MMP-14 with Thr 567 alanine substituted (not possible to phosphorylate). Phosphorylation of Thr 567 is required for internalisation of MMP-14. Using fluorescent microscopy, a transwell migration assay and matrigel invasion assay it was shown that the glutamate substitution reduced MMP-14 cell surface expression, but promoted migration and invasion. However the alanine substitution increased cell surface expression, while reducing migration and invasion [215]. This clearly indicates that the MMP-14 internalisation process itself drives cell migration, though the exact underlying mechanism is yet to be elucidated.

It has also been postulated that MMP-14 promotes cell migration by driving ERK MAPK phosphorylation. MMP-14 siRNA technology was employed in a human fibrosarcoma cell line. Western blotting, a Type I collagen coated transwell migration assay, and chemical inhibition of ERK and MMP-14 were used to show that TIMP-2 binding to MMP-14 drove ERK signalling, which increased cell migration independently of the direct enzymatic activity of MMP-14 [216]. TIMP-2 interacts with MMP-14 through its catalytic domain [217].

The antibody used to neutralise MMP-14 activity binds and inhibits the catalytic domain. Therefore it is possible that loss of MMP-14 driven alteration of the cell surface proteome and ERK activation were responsible for the reduced monocyte migration to CoMTb containing agarose spots. It is less clear how the MMP-14 neutralising antibody would impact on internalisation of MMP-14.

Finally the role that matrikines may be playing in this process needs to be considered. Matrikines are protein domains derived from ECM, that act as direct extracellular signals to cells. These signals are frequently cryptic sites revealed to the cells only after cleavage of ECM components. Matrikines may signal via integrins or growth factor receptors to alter cell adhesion to an intermediate promigratory state. ECM proteins that signal to produce this intermediate adhesion state include laminins, tenasicin C, thrombospondin and secreted protein-rich in cysteine [218].

Laminin-332 (previously laminin-5) is an epithelial basement membrane substrate for cell adhesion and migration. Western blotting and a cell migration assay in cell lines for colon and breast carcinomas, hepatomas and hepatocytes showed that migration on Ln-332 correlated with expression of membrane bound MMP-14. The migration was reduced by MMP-14 antisense oligonucleotides. MMP-14 colocalised with laminin-332 in colon and breast cancer tissue. It is the Y2 subunit of laminin-332 that is cleaved and released by MMP-14 [219]. This Y2 subunit carries cryptic sites that are EGF like and stimulate cancer cell migration by signalling through EGF receptors [220]. While laminin-332 was not present in the agarose spot assay I used, it is possible that MMP-14 cleaves and releases matrikines from Type I Collagen, though there is currently no data from other models to support this.

In summary, MMP-14 expression was demonstrated in the sputum and granulomas of TB patients. *Mtb* and intercellular networks upregulated monocytes MMP-14 expression in a p38 / JNK MAPK and chemokine dependent manner. MMP-14 drove collagen degradation and monocyte migration in the functional cellular model

of TB. MMP-14 may be a central regulator of two immunopathological processes in TB, tissue destruction and excessive leukocyte migration.

6. DISCUSSION

In summary, the collagenases MMP-1 and MMP-8 are elevated in active pulmonary TB in the plasma. The increased plasma MMP-8 is specific to TB patients, and is not elevated in controls with other respiratory infections. The stromelysin MMP-10 is elevated in the respiratory secretions of patients with TB and *in vitro* MMP-10 expression is driven by ESAT-6, an *Mtb* specific virulence factor. The membrane bound collagenase MMP-14 is expressed in the induced sputum and granulomas of TB patients, and MMP-14 drives collagen degradation and leukocyte migration in a functional cellular model of TB.

6.1 A model of synergistic MMP activity causing immunopathology in Mtb infection

My data suggest involvement of a range of MMPs in TB immunopathology, and this contrasts with established thinking, which focuses on immune cells, cytokines and lipids driving necrosis in TB [45]. However this model does not take into account the constituents of lung ECM – the primary structural fibril collagen can only be degraded by MMPs at neutral pH [221]. By considering lung ECM structure in conjunction with the complex, diverse and overlapping functions of MMPs, a model comprising activity of at least MMP-1, -8, -10 and -14 involvement in TB immunopathology can be proposed. To consider a single protease dominant in TB may oversimplify the situation *in vivo*.

Though only MMP-1, -8 and -14 can degrade types I, II and III collagen, MMP-10 may be co-operating with these collagenases to degrade the primary structural fibrils of the lung. Destruction of the extracellular matrix will involve a diverse array of proteases, and cannot be performed by a single protease. At a site of pulmonary *Mtb* infection, stromelysin MMP-10 may cleave the proteoglycans crosslinking the collagen fibrils and thereby expose the fibrils, leaving them more vulnerable to the enzymatic activity of the collagenases, MMP-1, -8 and -14. For monocytes entering the pulmonary ECM from capillaries MMP-14 promotes migration not only by cleaving fibrillar collagen at the leading edge of the cell to clear a path, but by altering the cell surface proteome and modulating intracellular signalling. Once the monocytes have arrived at a focus of *Mtb* infection MMP-14 will work alongside MMP-1 and MMP-8, driving localised collagen destruction. The cellular sources and interplay of MMP-1,-8, -10 and -14 are illustrated in Fig. 32.

The role of these individual MMPs in driving TB immunopathology has been discussed in detail in their respective chapters, so now the implications of these findings for TB management must be considered.

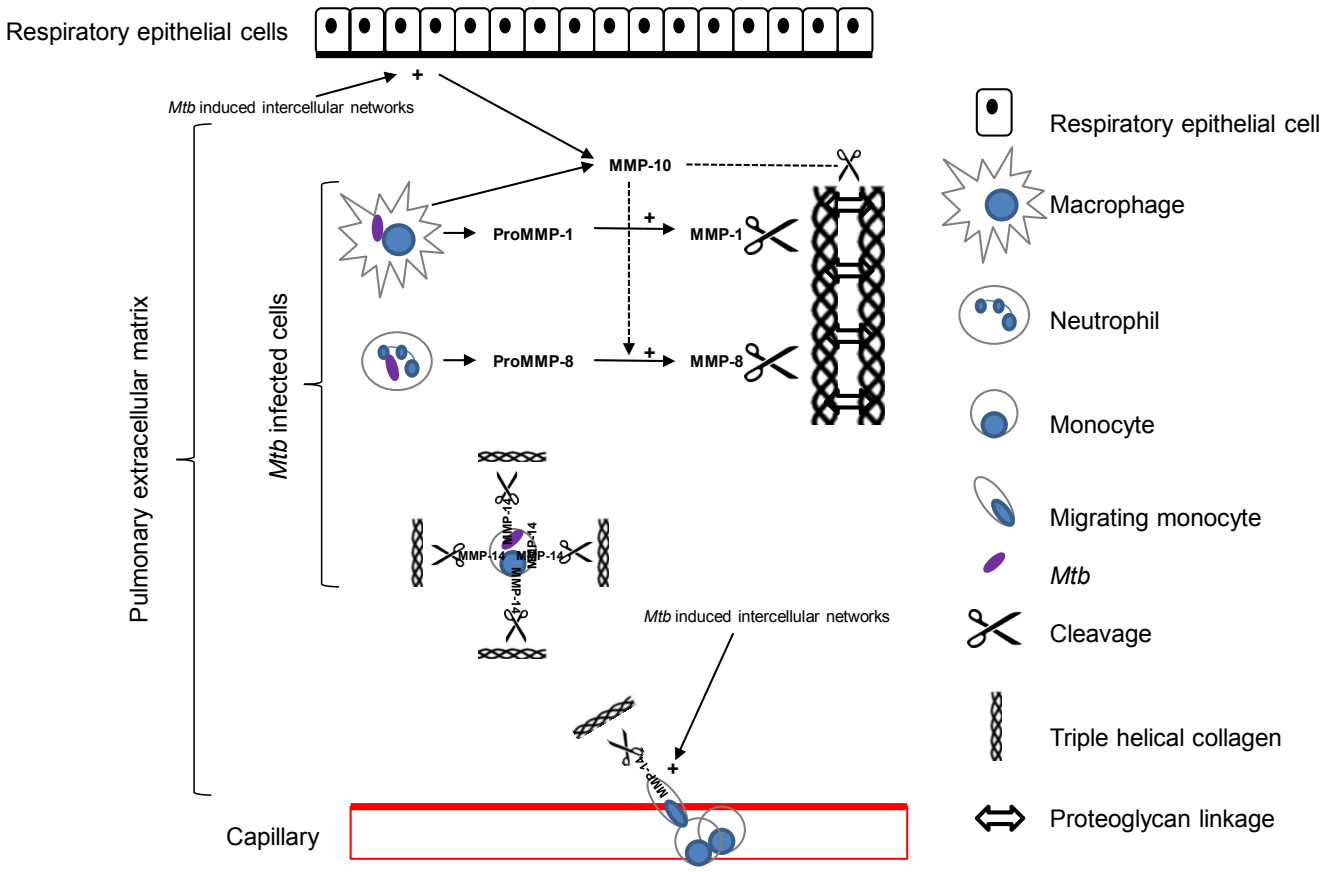

Figure 32: The interaction of MMP-1, -8, -10 and -14 in cell migration and extracellular matrix destruction in pulmonary TB

Mtb infection of macrophages and intercellular network stimulation of respiratory epithelial cells drives secretion of the stromelysin MMP-10. Active MMP-10 directly cleaves proteoglycans cross-linking triple helical collagen fibrils, thus exposing the fibrils to collagenases such as MMP-1 and MMP-8. These are secreted from *Mtb* infected macrophages and neutrophils respectively. MMP-10 converts MMP-1 and MMP-8 from the pro to active forms with greater enzymatic activity against triple helical collagen. Meanwhile *Mtb* induced intercellular networks stimulate MMP-14 expression on monocytes migrating into the ECM from capillaries. MMP-14 cleaves triple helical collagen at the leading edge of the cell to clear a path and also promotes migration by altering the cell surface proteome and modulating intracellular signalling. Once monocytes arrive at the site of *Mtb* infection more generalised cell surface MMP-14 drives local degradation of triple helical collagen, working alongside the secreted collagenases MMP-1 and -8

6.2 MMPs and point of care TB diagnostics

The finding that plasma MMP-8 was specific elevated in TB patients but not controls with other respiratory infections is of particular relevance to TB diagnostics. The need for improved case detection is highlighted in the WHO STOP TB Strategy. A study published in 2011 showed a case detection rate for pulmonary TB of only 56% in HIV infected and 65% in HIV uninfected patients in a rural Western Kenyan community. A large proportion of the unidentified cases were a consequence of cases failing to present to health care services, but it was estimated that 16% could have been detected earlier if case detection facilities were improved [222].

Patients in these settings are assessed in community clinics which have limited or no laboratory facilities, technicians or even electricity. Sputum smear microscopy is the main diagnostic technique in pulmonary TB, but requires some infrastructure to be in place, such as a microscope, centrifuge and perhaps most importantly well trained staff. A centre providing this service may be a considerable distance from the patient's home and consequently logistics of specimen transfer and defaulting from healthcare becomes a major problem. The ideal TB test would be an inexpensive, rapid serological test, which would require minimal training and equipment for implementation, for example a blood or urine dipstick test. This would allow diagnosis and initiation of treatment at the community clinic within hours of presentation [20].

An appropriate point of care test for low and middle income countries has remained elusive. The Xpert MTB/RIF is accurate and easy to use [223] but expensive and requires sophisticated machinery [224]. The existing commercially available serodiagnostic tests, which are used widely in low and middle income countries, have only very low quality data supporting their use, are imprecise and inconsistent and are not endorsed by WHO [225].

Plasma MMP-8 shows significant potential but as an isolated biomarker would lack sensitivity and specificity. However, it may be amenable to a blood dipstick test, combined with other markers as part of a 'biosignature' could be a more accurate diagnostic tool. For example one study showed that a combined detection of antibodies to *Mtb* protein antigens TbF6, DPEP and malate synthase in the serum had 85% sensitivity and 97% specificity [226], and so host-targeted biomarker panels including MMP-8 warrant further investigation.

6.3 Targeting TB immunopathology by MMP inhibition

It is conceivable that in the future tissue destruction in TB could be targeted with specific MMP inhibitors, which function by binding within the catalytic domain. The MMP inhibitor trials in malignancy in the 1990s were thwarted by the inhibitors lacking specificity, and broad spectrum inhibition causing musculoskeletal side effects [227]. Since that time, some effort has been invested in developing more specific inhibitors, with varying levels of success for different MMPs. For example a peptidomimetic inhibitor regasepin1 was synthesized, and showed considerable

specificity for MMP-8 compared to the other secreted collagenases MMP-1 and -13 [228].

Two newly developed MMP-14 inhibitors have been applied to animal models of malignancy. An MMP-14 inhibitory antibody, DX 2400, was identified by Fab library screening. Gelatin zymography showed that it blocked conversion of proMMP-2 to the active form by MMP-14 in fibrosarcoma cells. The antibody impaired invasion and migration of endothelial cells through matrigel. *In vivo* it slowed orthotopic breast cancer progression and reduced metastasis in mice [229]. A selective MMP-14 inhibitor peptide G was developed and demonstrated to inhibit migration and invasion of fibrosarcoma cells through matrigel. It also inhibited tongue squamous carcinoma growth in mice and prolonged survival [230]. Therefore, specific MMP-14 inhibition in the context of disease is a viable prospect, though the approaches above may be difficult to deliver in resource-poor settings. This approach of targeting MMP-14 in TB would require care. While reduction of collagen degradation would have clear benefits, excessive inhibition of leukocyte migration could be deleterious due to inadequate phagocytosis of *Mtb* and effectively cause immunocompromise by preventing cellular recruitment to the site of infection.

6.4 Future work

I have demonstrated that MMP-8 is a potential plasma biomarker of TB and that MMP-10 is another metalloproteinase that is likely to contribute to pathology in TB, working in conjunction with other MMPs to degrade lung matrix. However, in my opinion, the experiments performed pertaining to MMP-14 yielded the most

interesting and intriguing data and it is this area that would be focussed on in the future. MMP-14, being cell surface bound, is relatively difficult to study compared to the secreted MMPs, but by acting both as a collagenase, a sheddase and also regulating cellular behaviour, it potentially has a diverse range of actions.

6.4.1 Clinical samples

The finding of increased MMP-14 gene expression in the induced sputum of TB patients could be investigated further by looking at MMP-14 cell surface expression in respiratory secretions from TB patients. Historically fluorescent staining of BALF cytospin preparations was favoured for such work. However, it has become apparent that flow cytometric analysis is more accurate in identifying leukocyte subsets and by using dead cell markers non-viable cells can be excluded [231].

One difficulty that arises here is that sputum induction is increasingly being performed on patient with suspected pulmonary TB for diagnostic purposes rather than BAL. This is because it is cheaper and less invasive and in large studies of pulmonary TB patients of mixed HIV seroprevalence has been shown to have an equivalent diagnostic yield to BAL [232].

Sputum was always considered a difficult sample for flow cytometric analysis due to the large amount of mucus in addition to squamous epithelial cell and dead cell debris contamination, which causes autofluorescence and non-specific staining. However, recent studies have shown with good induction technique, quick processing and selection of sputum plugs from the surrounding fluid, it is possible to

reduce salivary epithelial cell and dead cell contamination to a minimum [233]. With appropriate antibody panels and careful gating strategies major leukocyte populations can be identified [234]. Therefore, flow cytometric analysis of MMP-14 expression in patients with TB would confirm the initial observation of increased gene expression.

One area in which cytospin could prove useful is to demonstrate functional activity of MMP-14 on the surface of monocytes/ macrophages in induced sputum or BAL. The cells would be spun down on to a slide precoated with fluorescent collagen, and incubated prior to using fluorescent microscopy to look for zones of collagen clearance in the absence and presence of the MMP-14 neutralising antibody. Taken with the flow cytometric data, this would prove a functional collagenolytic effect of MMP-14 expression in TB.

6.4.2 Cellular model

When considering future work in the functional cellular model of TB the most critical area to explore is the role MMP-14 plays in chemoinvasion of monocytes through a 3D collagen matrix. Transwell chamber inserts of varying pore size are commercially available for this type of assay, and can be coated with a layer of collagen. The chemotactic stimulus, in this case CoMTb, would be placed in the lower chamber and the cells seeded on top of the collagen in the upper chamber. The number of cell migrating through the collagen into the lower chamber in the absence and presence of the MMP-14 neutralising antibody would be quantified using flow cytometry or a

haemocytometer, to prove that MMP-14 activity was necessary for cellular migration through the matrix.

To elucidate the role of MMP-14 in driving monocyte migration *in vivo*, the *M. marinum* infected zebrafish embryo model of granuloma formation discussed previously could be utilised. An MMP-14 zebrafish embryo morpholino has already been created [235], meaning this is a feasible line of enquiry. My hypothesis would be that cellular recruitment to mycobacterial granulomas would be suppressed in the MMP-14 morpholino, and since monocytes seem to be a site for mycobacterial proliferation and dissemination, the size and number of granulomas would be lower in the morpholino. The ability to perform real-time imaging as the embryo is translucent would also permit me to study cellular migration in the presence or absence of MMP-14 expression.

Until relatively recently, siRNA transfection of primary cells especially monocytes, macrophages and neutrophils was considered virtually impossible due to high levels of cytotoxicity [236]. However, as technology has advanced and new methods of delivering siRNA to cells have emerged, this picture is changing. For example, a peptide delivery system was recently successfully used to transfect human synovial fluid monocytes and macrophages [237]. In the context of the cellular TB model, there were concerns that *Mtb* infection would cause excessive cell death in the context of siRNA transfection. However our group has recently successfully siRNA transfected Mtb infected human MDMs using a lipid delivery system without unacceptable levels of cell death (unpublished data). Therefore, siRNA technology would be a useful method to establish the role of MMP-14 in monocyte migration and

collagen degradation in the cellular TB model. I have also alluded to using it for investigating signalling pathways in previous chapters.

In conclusion, my data support a role for MMP-1, -8, -10 and -14 in driving collagen degradation and leukocyte migration in TB. A model of multiple MMPs contributing to immunopathology is emerging, with the collagenases being the final effectors of matrix destruction, while the stromelysins may not only cleave cross-linking fibrils to expose cleavage sites but also proteolytically activate the collagenases, and membrane bound MMP-14 regulates cellular recruitment to the granuloma. Further studies in man and in appropriate model systems will be required to establish the true diagnostic and therapeutic potential of these MMPs. In particular those which are true targets need to be identified, as opposed to those which are physiologically required and may lead to poorer outcomes if inhibited inappropriately.

7. REFERENCES

1. WHO, *Global Tuberculosis Report 2012.* 2012.

2. Velayati, A.A., et al., *Emergence of new forms of totally drug-resistant tuberculosis bacilli: super extensively drug-resistant tuberculosis or totally drug-resistant strains in iran.* Chest, 2009. 136(2): p. 420-5.

3. Udwadia, Z.F., et al., *Totally drug-resistant tuberculosis in India.* Clin Infect Dis, 2012. 54(4): p. 579-81.

4. Klopper, M., R.M. Warren, and N.C.G.v.P. Cindy Hayes, Elizabeth Maria Streicher, Borna Müller, Frederick Adriaan Sirgel, Mamisa Chabula-Nxiweni, Ebrahim Hoosain, Gerrit Coetzee, Paul David van Helden, Thomas Calldo Victor, and André Phillip Trollip, *Emergence and Spread of Extensively and Totally Drug-Resistant Tuberculosis, South Africa.* Emerging Infectious Diseases, 2013. 19(3): p. 449=455.

5. HPA, *Tuberculosis in the UK: 2012 report.* 2012.

6. WHO, *Treatment of tuberculosis: guidelines for national programmes.* 2012.

7. Gandhi, N.R., et al., *Multidrug-resistant and extensively drug-resistant tuberculosis: a threat to global control of tuberculosis.* Lancet, 2010. 375(9728): p. 1830-43.

8. Lawn, S.D. and A.I. Zumla, *Tuberculosis.* Lancet, 2011. 378(9785): p. 57-72.

9. Philips, J.A. and J.D. Ernst, *Tuberculosis pathogenesis and immunity.* Annu Rev Pathol, 2012. 7: p. 353-84.

10. Flynn, J.L. and J. Chan, *Immunology of tuberculosis.* Annu Rev Immunol, 2001. 19: p. 93-129.

11. Ernst, J.D., *The immunological life cycle of tuberculosis.* Nat Rev Immunol, 2012. 12(8): p. 581-91.

12. Flynn, J.L., et al., *Tumor necrosis factor-alpha is required in the protective immune response against Mycobacterium tuberculosis in mice.* Immunity, 1995. 2(6): p. 561-72.

13. Cooper, A.M., et al., *Interleukin 12 (IL-12) is crucial to the development of protective immunity in mice intravenously infected with mycobacterium tuberculosis.* J Exp Med, 1997. 186(1): p. 39-45.

14. Ottenhoff, T.H., D. Kumararatne, and J.L. Casanova, *Novel human immunodeficiencies reveal the essential role of type-I cytokines in immunity to intracellular bacteria.* Immunol Today, 1998. 19(11): p. 491-4.

15. Cooper, A.M., et al., *Disseminated tuberculosis in interferon gamma gene-disrupted mice.* J Exp Med, 1993. 178(6): p. 2243-7.

16. Ramakrishnan, L., *Revisiting the role of the granuloma in tuberculosis.* Nat Rev Immunol, 2012. 12(5): p. 352-66.

17. Horsburgh, C.R., Jr., *Priorities for the treatment of latent tuberculosis infection in the United States.* N Engl J Med, 2004. 350(20): p. 2060-7.

18. Kline, S.E., L.L. Hedemark, and S.F. Davies, *Outbreak of tuberculosis among regular patrons of a neighborhood bar.* N Engl J Med, 1995. 333(4): p. 222-7.

19. Davies, P.D. and M. Pai, *The diagnosis and misdiagnosis of tuberculosis.* Int J Tuberc Lung Dis, 2008. 12(11): p. 1226-34.

20. Reid, B.C., *Towards Lab Free Tuberculosis Diagnosis.* 2011.

21. Boehme, C.C., et al., *Rapid molecular detection of tuberculosis and rifampin resistance.* N Engl J Med, 2010. 363(11): p. 1005-15.

22. WHO, *STOP TB Strategy.* 2006.

23. Farman, D.P. and W.A. Speir, Jr., *Initial roentgenographic manifestations of bacteriologically proven Mycobacterium tuberculosis. Typical or atypical?* Chest, 1986. 89(1): p. 75-7.

24. Gandhi, N.R., et al., *Extensively drug-resistant tuberculosis as a cause of death in patients co-infected with tuberculosis and HIV in a rural area of South Africa.* Lancet, 2006. 368(9547): p. 1575-80.

25. Zumla, A., et al., *Tuberculosis.* N Engl J Med, 2013. 368(8): p. 745-55.

26. Rodrigo, T., et al., *Characteristics of tuberculosis patients who generate secondary cases.* Int J Tuberc Lung Dis, 1997. 1(4): p. 352-7.

27. Hunter, R.L., *Pathology of post primary tuberculosis of the lung: an illustrated critical review.* Tuberculosis (Edinb), 2011. 91(6): p. 497-509.

28. Perrin, F.M., et al., *Radiological cavitation, sputum mycobacterial load and treatment response in pulmonary tuberculosis.* Int J Tuberc Lung Dis, 2010. 14(12): p. 1596-602.

29. Kaplan, G., et al., *Mycobacterium tuberculosis growth at the cavity surface: a microenvironment with failed immunity.* Infect Immun, 2003. 71(12): p. 7099-108.

30. Erdogan, A., et al., *Surgical management of tuberculosis-related hemoptysis.* Ann Thorac Surg, 2005. 79(1): p. 299-302.

31. Knott-Craig, C.J., et al., *Management and prognosis of massive hemoptysis. Recent experience with 120 patients.* J Thorac Cardiovasc Surg, 1993. 105(3): p. 394-7.

32. van den Heuvel, M.M. and J.J. van Rensburg, *Images in clinical medicine. Rasmussen's aneurysm.* N Engl J Med, 2006. 355(16): p. e17.

33. Rhee, C.K., et al., *Clinical characteristics of patients with tuberculosis-destroyed lung.* Int J Tuberc Lung Dis, 2013. 17(1): p. 67-75.

34. Jeon, D.S., et al., *Survival and predictors of outcomes in non-HIV-infected patients with extensively drug-resistant tuberculosis.* Int J Tuberc Lung Dis, 2009. 13(5): p. 594-600.

35. Telzak, E.E., et al., *Factors influencing time to sputum conversion among patients with smear-positive pulmonary tuberculosis.* Clin Infect Dis, 1997. 25(3): p. 666-70.

36. Benator, D., et al., *Rifapentine and isoniazid once a week versus rifampicin and isoniazid twice a week for treatment of drug-susceptible pulmonary tuberculosis in HIV-negative patients: a randomised clinical trial.* Lancet, 2002. 360(9332): p. 528-34.

37. Zhang, Y. and W.W. Yew, *Mechanisms of drug resistance in Mycobacterium tuberculosis.* Int J Tuberc Lung Dis, 2009. 13(11): p. 1320-30.

38. Kempker, R.R., et al., *Additional drug resistance in Mycobacterium tuberculosis isolates from resected cavities among patients with multidrug-resistant or extensively drug-resistant pulmonary tuberculosis.* Clin Infect Dis, 2012. 54(6): p. e51-4.

39. Laennec, R., *A treatise on diseases of the chest.* London: T. and G. Underwood, 1821.

40. Helke, K.L., J.L. Mankowski, and Y.C. Manabe, *Animal models of cavitation in pulmonary tuberculosis.* Tuberculosis (Edinb), 2006. 86(5): p. 337-48.

41. Yamamura, Y., et al., *Experimental formation of the tuberculous cavity in the rabbit's lung; experimental study on the tuberculous allergy. I.* Kekkaku, 1954. 29(4): p. 143-6; English abstract, 153-4.

42. Brindle, R.J., et al., *Quantitative bacillary response to treatment in HIV-associated pulmonary tuberculosis.* Am Rev Respir Dis, 1993. 147(4): p. 958-61.

43. Perez-Guzman, C., et al., *Does aging modify pulmonary tuberculosis?: A meta-analytical review.* Chest, 1999. 116(4): p. 961-7.

44. Yamamura, Y., Y. Ogawa, and H. Yamagata, *Prevention of tuberculous cavity formation by immunosuppressive drugs.* Am Rev Respir Dis, 1968. 98(4): p. 720-3.

45. Russell, D.G., et al., *Foamy macrophages and the progression of the human tuberculosis granuloma.* Nat Immunol, 2009. 10(9): p. 943-8.

46. Davidson, J.M., *Biochemistry and turnover of lung interstitium.* Eur Respir J, 1990. 3(9): p. 1048-63.

47. Vincenti, M.P. and C.E. Brinckerhoff, *Signal transduction and cell-type specific regulation of matrix metalloproteinase gene expression: can MMPs be good for you?* J Cell Physiol, 2007. 213(2): p. 355-64.

48. Visse, R. and H. Nagase, *Matrix metalloproteinases and tissue inhibitors of metalloproteinases: structure, function, and biochemistry.* Circ Res, 2003. 92(8): p. 827-39.

49. Parks, W.C., C.L. Wilson, and Y.S. Lopez-Boado, *Matrix metalloproteinases as modulators of inflammation and innate immunity.* Nat Rev Immunol, 2004. 4(8): p. 617-29.

50. Kahari, V.M. and U. Saarialho-Kere, *Matrix metalloproteinases in skin.* Exp Dermatol, 1997. 6(5): p. 199-213.

51. Chandler, S., et al., *Matrix metalloproteinases, tumor necrosis factor and multiple sclerosis: an overview.* J Neuroimmunol, 1997. 72(2): p. 155-61.

52. Ashworth, J.L., et al., *Fibrillin degradation by matrix metalloproteinases: implications for connective tissue remodelling.* Biochem J, 1999. 340 (Pt 1): p. 171-81.

53. Webster, N.L. and S.M. Crowe, *Matrix metalloproteinases, their production by monocytes and macrophages and their potential role in HIV-related diseases.* J Leukoc Biol, 2006. 80(5): p. 1052-66.

54. Giambernardi, T.A., et al., *Overview of matrix metalloproteinase expression in cultured human cells.* Matrix Biol, 1998. 16(8): p. 483-96.

55. Janoff, A., et al., *Experimental emphysema induced with purified human neutrophil elastase: tissue localization of the instilled protease.* Am Rev Respir Dis, 1977. 115(3): p. 461-78.

56. D'Armiento, J., et al., *Collagenase expression in the lungs of transgenic mice causes pulmonary emphysema.* Cell, 1992. 71(6): p. 955-61.

57. Foronjy, R.F., et al., *Progressive adult-onset emphysema in transgenic mice expressing human MMP-1 in the lung.* Am J Physiol Lung Cell Mol Physiol, 2003. 284(5): p. L727-37.

58. Selman, M., et al., *Tobacco smoke-induced lung emphysema in guinea pigs is associated with increased interstitial collagenase.* Am J Physiol, 1996. 271(5 Pt 1): p. L734-43.

59. Finlay, G.A., et al., *Matrix metalloproteinase expression and production by alveolar macrophages in emphysema.* Am J Respir Crit Care Med, 1997. 156(1): p. 240-7.

60. Segura-Valdez, L., et al., *Upregulation of gelatinases A and B, collagenases 1 and 2, and increased parenchymal cell death in COPD.* Chest, 2000. 117(3): p. 684-94.

61. Imai, K., et al., *Human collagenase (matrix metalloproteinase-1) expression in the lungs of patients with emphysema.* Am J Respir Crit Care Med, 2001. 163(3 Pt 1): p. 786-91.

62. Foronjy, R., et al., *Transgenic expression of matrix metalloproteinase-9 causes adult-onset emphysema in mice associated with the loss of alveolar elastin.* Am J Physiol Lung Cell Mol Physiol, 2008. 294(6): p. L1149-57.

63. Russell, R.E., et al., *Release and activity of matrix metalloproteinase-9 and tissue inhibitor of metalloproteinase-1 by alveolar macrophages from patients with chronic obstructive pulmonary disease.* Am J Respir Cell Mol Biol, 2002. 26(5): p. 602-9.

64. Omachi, T.A., et al., *Matrix metalloproteinase-9 predicts pulmonary status declines in alpha1-antitrypsin deficiency.* Respir Res, 2011. 12: p. 35.

65. Hautamaki, R.D., et al., *Requirement for macrophage elastase for cigarette smoke-induced emphysema in mice.* Science, 1997. 277(5334): p. 2002-4.

66. Demedts, I.K., et al., *Elevated MMP-12 protein levels in induced sputum from patients with COPD.* Thorax, 2006. 61(3): p. 196-201.

67. Haq, I., et al., *Matrix metalloproteinase-12 (MMP-12) SNP affects MMP activity, lung macrophage infiltration and protects against emphysema in COPD.* Thorax, 2011. 66(11): p. 970-6.

68. Mukhopadhyay, S. and A.A. Gal, *Granulomatous lung disease: an approach to the differential diagnosis.* Arch Pathol Lab Med, 2010. 134(5): p. 667-90.

69. Chang, J.C., et al., *Effect of Mycobacterium tuberculosis and its components on macrophages and the release of matrix metalloproteinases.* Thorax, 1996. 51(3): p. 306-11.

70. Gonzalez, O.Y., et al., *Spectrum of bacille Calmette-Guerin (BCG) infection after intravesical BCG immunotherapy.* Clin Infect Dis, 2003. 36(2): p. 140-8.

71. Elkington, P.T., et al., *Mycobacterium tuberculosis, but not vaccine BCG, specifically upregulates matrix metalloproteinase-1.* Am J Respir Crit Care Med, 2005. 172(12): p. 1596-604.

72. Elkington, P.T., et al., *Mycobacterium tuberculosis up-regulates matrix metalloproteinase-1 secretion from human airway epithelial cells via a p38 MAPK switch.* J Immunol, 2005. 175(8): p. 5333-40.

73. Elkington, P.T., et al., *Synergistic up-regulation of epithelial cell matrix metalloproteinase-9 secretion in tuberculosis.* Am J Respir Cell Mol Biol, 2007. 37(4): p. 431-7.

74. O'Kane, C.M., P.T. Elkington, and J.S. Friedland, *Monocyte-dependent oncostatin M and TNF-alpha synergize to stimulate unopposed matrix metalloproteinase-1/3 secretion from human lung fibroblasts in tuberculosis.* Eur J Immunol, 2008. 38(5): p. 1321-30.

75. O'Kane, C.M., et al., *STAT3, p38 MAPK, and NF-kappaB drive unopposed monocyte-dependent fibroblast MMP-1 secretion in tuberculosis.* Am J Respir Cell Mol Biol, 2010. 43(4): p. 465-74.

76. Elkington, P., et al., *MMP-1 drives immunopathology in human tuberculosis and transgenic mice.* J Clin Invest, 2011. 121(5): p. 1827-33.

77. Walker, N.F., et al., *Doxycycline and HIV infection suppress tuberculosis-induced matrix metalloproteinases.* Am J Respir Crit Care Med, 2012. 185(9): p. 989-97.

78. Ganachari, M., et al., *Host gene-encoded severe lung TB: from genes to the potential pathways.* Genes Immun, 2012.

79. Thuong, N.T., et al., *Identification of tuberculosis susceptibility genes with human macrophage gene expression profiles.* PLoS Pathog, 2008. 4(12): p. e1000229.

80. Kim, M.J., et al., *Caseation of human tuberculosis granulomas correlates with elevated host lipid metabolism.* EMBO Mol Med, 2010. 2(7): p. 258-74.

81. Mehra, S., et al., *Transcriptional reprogramming in nonhuman primate (rhesus macaque) tuberculosis granulomas.* PLoS One, 2010. 5(8): p. e12266.

82. Zuger, A., and F. D. Lowy., *Tuberculosis of the brain, meninges and spinal cord. .* Tuberculosis., 1995. W. N. Rom and S. M. Garay, eds. Little, Brown and Co.,Boston, 3. Dannenberg, A. M., Jr.: p. pp. 541–556.

83. Thwaites, G.E., et al., *Dexamethasone for the treatment of tuberculous meningitis in adolescents and adults.* N Engl J Med, 2004. 351(17): p. 1741-51.

84. Green, J.A., et al., *Mycobacterium tuberculosis upregulates microglial matrix metalloproteinase-1 and -3 expression and secretion via NF-kappaB- and Activator Protein-1-dependent monocyte networks.* J Immunol, 2010. 184(11): p. 6492-503.

85. Harris, J.E., et al., *Monocyte-astrocyte networks regulate matrix metalloproteinase gene expression and secretion in central nervous system tuberculosis in vitro and in vivo.* J Immunol, 2007. 178(2): p. 1199-207.

86. Price, N.M., et al., *Identification of a matrix-degrading phenotype in human tuberculosis in vitro and in vivo.* J Immunol, 2001. 166(6): p. 4223-30.

87. Eisen, J.S. and J.C. Smith, *Controlling morpholino experiments: don't stop making antisense.* Development, 2008. 135(10): p. 1735-43.

88. Abdallah, A.M., et al., *Type VII secretion--mycobacteria show the way.* Nat Rev Microbiol, 2007. 5(11): p. 883-91.

89. Volkman, H.E., et al., *Tuberculous granuloma induction via interaction of a bacterial secreted protein with host epithelium.* Science, 2010. 327(5964): p. 466-9.

90. Clark, I.M., et al., *The regulation of matrix metalloproteinases and their inhibitors.* Int J Biochem Cell Biol, 2008. 40(6-7): p. 1362-78.

91. Mengshol, J.A., M.P. Vincenti, and C.E. Brinckerhoff, *IL-1 induces collagenase-3 (MMP-13) promoter activity in stably transfected chondrocytic cells: requirement for Runx-2 and activation by p38 MAPK and JNK pathways.* Nucleic Acids Res, 2001. 29(21): p. 4361-72.

92. Price, N.M., et al., *Unopposed matrix metalloproteinase-9 expression in human tuberculous granuloma and the role of TNF-alpha-dependent monocyte networks.* J Immunol, 2003. 171(10): p. 5579-86.

93. Carbonetti, N.H., *Pertussis toxin and adenylate cyclase toxin: key virulence factors of Bordetella pertussis and cell biology tools.* Future Microbiol, 2010. 5(3): p. 455-69.

94. Spangrude, G.J., et al., *Inhibition of lymphocyte and neutrophil chemotaxis by pertussis toxin.* J Immunol, 1985. 135(6): p. 4135-43.

95. Andreasen, C. and N.H. Carbonetti, *Pertussis toxin inhibits early chemokine production to delay neutrophil recruitment in response to Bordetella pertussis respiratory tract infection in mice.* Infect Immun, 2008. 76(11): p. 5139-48.

96. Saunders, B.M. and W.J. Britton, *Life and death in the granuloma: immunopathology of tuberculosis.* Immunol Cell Biol, 2007. 85(2): p. 103-11.

97. Comas, I. and S. Gagneux, *The past and future of tuberculosis research.* PLoS Pathog, 2009. 5(10): p. e1000600.

98. Shrikrishna, D., et al., *Human and canine pulmonary Mycobacterium bovis infection in the same household: re-emergence of an old zoonotic threat?* Thorax, 2009. 64(1): p. 89-91.

99. Behr, M.A., et al., *Comparative genomics of BCG vaccines by whole-genome DNA microarray.* Science, 1999. 284(5419): p. 1520-3.

100. Rand, L., et al., *Matrix metalloproteinase-1 is regulated in tuberculosis by a p38 MAPK-dependent, p-aminosalicylic acid-sensitive signaling cascade.* J Immunol, 2009. 182(9): p. 5865-72.

101. Jo, E.K., et al., *Intracellular signalling cascades regulating innate immune responses to Mycobacteria: branching out from Toll-like receptors.* Cell Microbiol, 2007. 9(5): p. 1087-98.

102. Harris, J.E., et al., *Monocytes infected with Mycobacterium tuberculosis regulate MAP kinase-dependent astrocyte MMP-9 secretion.* J Leukoc Biol, 2007. 81(2): p. 548-56.

103. Newton, K. and V.M. Dixit, *Signaling in innate immunity and inflammation.* Cold Spring Harb Perspect Biol, 2012. 4(3).

104. Miller, M.C., et al., *Membrane type 1 matrix metalloproteinase is a crucial promoter of synovial invasion in human rheumatoid arthritis.* Arthritis Rheum, 2009. 60(3): p. 686-97.

105. Jiang, W.G., et al., *Expression of membrane type-1 matrix metalloproteinase, MT1-MMP in human breast cancer and its impact on invasiveness of breast cancer cells.* Int J Mol Med, 2006. 17(4): p. 583-90.

106. Ueda, J., et al., *Sequence-specific silencing of MT1-MMP expression suppresses tumor cell migration and invasion: importance of MT1-MMP as a therapeutic target for invasive tumors.* Oncogene, 2003. 22(54): p. 8716-22.

107. Davis, J.M., et al., *Real-time visualization of mycobacterium-macrophage interactions leading to initiation of granuloma formation in zebrafish embryos.* Immunity, 2002. 17(6): p. 693-702.

108. Puissegur, M.P., et al., *An in vitro dual model of mycobacterial granulomas to investigate the molecular interactions between mycobacteria and human host cells.* Cell Microbiol, 2004. 6(5): p. 423-33.

109. Clay, H., et al., *Dichotomous role of the macrophage in early Mycobacterium marinum infection of the zebrafish.* Cell Host Microbe, 2007. 2(1): p. 29-39.

110. Davis, J.M. and L. Ramakrishnan, *The role of the granuloma in expansion and dissemination of early tuberculous infection.* Cell, 2009. 136(1): p. 37-49.

111. Sato, H., et al., *A matrix metalloproteinase expressed on the surface of invasive tumour cells.* Nature, 1994. 370(6484): p. 61-5.

112. Ohuchi, E., et al., *Membrane type 1 matrix metalloproteinase digests interstitial collagens and other extracellular matrix macromolecules.* J Biol Chem, 1997. 272(4): p. 2446-51.

113. Hernandez-Barrantes, S., et al., *Binding of active (57 kDa) membrane type 1-matrix metalloproteinase (MT1-MMP) to tissue inhibitor of metalloproteinase (TIMP)-2 regulates MT1-MMP processing and pro-MMP-2 activation.* J Biol Chem, 2000. 275(16): p. 12080-9.

114. Remacle, A., G. Murphy, and C. Roghi, *Membrane type I-matrix metalloproteinase (MT1-MMP) is internalised by two different pathways and is recycled to the cell surface.* J Cell Sci, 2003. 116(Pt 19): p. 3905-16.

115. Itoh, Y., *MT1-MMP: a key regulator of cell migration in tissue.* IUBMB Life, 2006. 58(10): p. 589-96.

116. Hotary, K., et al., *Regulation of cell invasion and morphogenesis in a three-dimensional type I collagen matrix by membrane-type matrix metalloproteinases 1, 2, and 3.* J Cell Biol, 2000. 149(6): p. 1309-23.

117. Sabeh, F., et al., *Secreted versus membrane-anchored collagenases: relative roles in fibroblast-dependent collagenolysis and invasion.* J Biol Chem, 2009. 284(34): p. 23001-11.

118. Galvez, B.G., et al., *Membrane type 1-matrix metalloproteinase is activated during migration of human endothelial cells and modulates endothelial motility and matrix remodeling.* J Biol Chem, 2001. 276(40): p. 37491-500.

119. Mimori, K., et al., *Clinical significance of MT1-MMP mRNA expression in breast cancer.* Oncol Rep, 2001. 8(2): p. 401-3.

120. Shankavaram, U.T., et al., *Monocyte membrane type 1-matrix metalloproteinase. Prostaglandin-dependent regulation and role in metalloproteinase-2 activation.* J Biol Chem, 2001. 276(22): p. 19027-32.

121. Matias-Roman, S., et al., *Membrane type 1-matrix metalloproteinase is involved in migration of human monocytes and is regulated through their interaction with fibronectin or endothelium.* Blood, 2005. 105(10): p. 3956-64.

122. Gawden-Bone, C., et al., *Dendritic cell podosomes are protrusive and invade the extracellular matrix using metalloproteinase MMP-14.* J Cell Sci, 2010.

123. Yang, M.X., et al., *Membrane type 1-matrix metalloproteinase is involved in the migration of human monocyte-derived dendritic cells.* Immunol Cell Biol, 2006. 84(6): p. 557-62.

124. Batra, J., et al., *Matrix metalloproteinase-10 (MMP-10) interaction with tissue inhibitors of metalloproteinases TIMP-1 and TIMP-2: binding studies and crystal structure.* J Biol Chem, 2012. 287(19): p. 15935-46.

125. Madlener, M. and S. Werner, *cDNA cloning and expression of the gene encoding murine stromelysin-2 (MMP-10).* Gene, 1997. 202(1-2): p. 75-81.

126. Windsor, L.J., et al., *Cell type-specific regulation of SL-1 and SL-2 genes. Induction of the SL-2 gene but not the SL-1 gene by human keratinocytes in response to cytokines and phorbolesters.* J Biol Chem, 1993. 268(23): p. 17341-7.

127. Brinckerhoff, C.E., et al., *Rabbit procollagenase synthesized and secreted by a high-yield mammalian expression vector requires stromelysin (matrix metalloproteinase-3) for maximal activation.* J Biol Chem, 1990. 265(36): p. 22262-9.

128. Nicholson, R., G. Murphy, and R. Breathnach, *Human and rat malignant-tumor-associated mRNAs encode stromelysin-like metalloproteinases.* Biochemistry, 1989. 28(12): p. 5195-203.

129. Barksby, H.E., et al., *Matrix metalloproteinase 10 promotion of collagenolysis via procollagenase activation: implications for cartilage degradation in arthritis.* Arthritis Rheum, 2006. 54(10): p. 3244-53.

130. Suzuki, K., et al., *Mechanisms of activation of tissue procollagenase by matrix metalloproteinase 3 (stromelysin).* Biochemistry, 1990. 29(44): p. 10261-70.

131. Saunders, W.B., K.J. Bayless, and G.E. Davis, *MMP-1 activation by serine proteases and MMP-10 induces human capillary tubular network collapse and regression in 3D collagen matrices.* J Cell Sci, 2005. 118(Pt 10): p. 2325-40.

132. Wilkins-Port, C.E., et al., *TGF-beta1 + EGF-initiated invasive potential in transformed human keratinocytes is coupled to a plasmin/MMP-10/MMP-1-dependent collagen remodeling axis: role for PAI-1.* Cancer Res, 2009. 69(9): p. 4081-91.

133. Gill, J.H., et al., *MMP-10 is overexpressed, proteolytically active, and a potential target for therapeutic intervention in human lung carcinomas.* Neoplasia, 2004. 6(6): p. 777-85.

134. Deraz, E.M., et al., *MMP-10/stromelysin-2 promotes invasion of head and neck cancer.* PLoS One, 2011. 6(10): p. e25438.

135. Van Lint, P. and C. Libert, *Matrix metalloproteinase-8: cleavage can be decisive.* Cytokine Growth Factor Rev, 2006. 17(4): p. 217-23.

136. Kuropkat, C., et al., *Significant correlation of matrix metalloproteinase and macrophage colony-stimulating factor serum concentrations in patients with head and neck cancer.* Neoplasma, 2004. 51(5): p. 375-8.

137. Moilanen, M., et al., *Expression and regulation of collagenase-2 (MMP-8) in head and neck squamous cell carcinomas.* J Pathol, 2002. 197(1): p. 72-81.

138. Montel, V., et al., *Altered metastatic behavior of human breast cancer cells after experimental manipulation of matrix metalloproteinase 8 gene expression.* Cancer Res, 2004. 64(5): p. 1687-94.

139. Sepper, R., et al., *Human neutrophil collagenase (MMP-8), identified in bronchiectasis BAL fluid, correlates with severity of disease.* Chest, 1995. 107(6): p. 1641-7.

140. Elkington, P.T., J.A. Green, and J.S. Friedland, *Filter sterilization of highly infectious samples to prevent false negative analysis of matrix metalloproteinase activity.* J Immunol Methods, 2006. 309(1-2): p. 115-9.

141. Wiggins, H. and J. Rappoport, *An agarose spot assay for chemotactic invasion.* Biotechniques, 2010. 48(2): p. 121-4.

142. Sandhu, G., et al., *Discriminating active from latent tuberculosis in patients presenting to community clinics.* PLoS One, 2012. 7(5): p. e38080.

143. Lawson, L., et al., *Clinical presentation of adults with pulmonary tuberculosis with and without HIV infection in Nigeria.* Scand J Infect Dis, 2008. 40(1): p. 30-5.

144. Singh, S., *Anti-mycobacterial drugs modulate Matrix Metalloproteinases in Pulmonary Tuberculosis.* Submitted for publication, 2013.

145. Robin, X., et al., *pROC: an open-source package for R and S+ to analyze and compare ROC curves.* BMC Bioinformatics, 2011. 12: p. 77.

146. Youden, W.J., *Index for rating diagnostic tests.* Cancer, 1950. 3(1): p. 32-5.

147. Walzl, G., et al., *Immunological biomarkers of tuberculosis.* Nat Rev Immunol, 2011. 11(5): p. 343-54.

148. Sundararajan, S., S. Babu, and S.D. Das, *Comparison of localized versus systemic levels of Matrix metalloproteinases (MMPs), its tissue inhibitors (TIMPs) and cytokines in tuberculous and non-tuberculous pleuritis patients.* Hum Immunol, 2012. 73(10): p. 985-91.

149. Hrabec, E., et al., *Circulation level of matrix metalloproteinase-9 is correlated with disease severity in tuberculosis patients.* Int J Tuberc Lung Dis, 2002. 6(8): p. 713-9.

150. Seddon, J., et al., *Procollagen III N-terminal Propeptide and Desmosine are Released by Matrix Destruction in Pulmonary Tuberculosis.* J Infect Dis, 2013.

151. Mavhu, W., et al., *Chronic cough and its association with TB-HIV co-infection: factors affecting help-seeking behaviour in Harare, Zimbabwe.* Trop Med Int Health, 2010. 15(5): p. 574-9.

152. Lonnroth, K., et al., *A consistent log-linear relationship between tuberculosis incidence and body mass index.* Int J Epidemiol, 2010. 39(1): p. 149-55.

153. Mattey, D.L., N.B. Nixon, and P.T. Dawes, *Association of circulating levels of MMP-8 with mortality from respiratory disease in patients with rheumatoid arthritis.* Arthritis Res Ther, 2012. 14(5): p. R204.

154. Ringner, M., *What is principal component analysis?* Nat Biotechnol, 2008. 26(3): p. 303-4.

155. Khan, A., et al., *Lack of weight gain and relapse risk in a large tuberculosis treatment trial.* Am J Respir Crit Care Med, 2006. 174(3): p. 344-8.

156. Zachariah, R., et al., *Moderate to severe malnutrition in patients with tuberculosis is a risk factor associated with early death.* Trans R Soc Trop Med Hyg, 2002. 96(3): p. 291-4.

157. Ugarte-Gil, C.A., et al., *Induced sputum MMP-1, -3 & -8 concentrations during treatment of tuberculosis.* PLoS One, 2013. 8(4): p. e61333.

158. De Groote, M.A., et al., *Elucidating novel serum biomarkers associated with pulmonary tuberculosis treatment.* PLoS One, 2013. 8(4): p. e61002.

159. Taggart, C.C., et al., *Elastolytic proteases: inflammation resolution and dysregulation in chronic infective lung disease.* Am J Respir Crit Care Med, 2005. 171(10): p. 1070-6.

160. Gearing, A.J., et al., *Matrix metalloproteinases and processing of pro-TNF-alpha.* J Leukoc Biol, 1995. 57(5): p. 774-7.

161. Borregaard, N. and J.B. Cowland, *Granules of the human neutrophilic polymorphonuclear leukocyte.* Blood, 1997. 89(10): p. 3503-21.

162. Berry, M.P., et al., *An interferon-inducible neutrophil-driven blood transcriptional signature in human tuberculosis.* Nature, 2010. 466(7309): p. 973-7.

163. Eum, S.Y., et al., *Neutrophils are the predominant infected phagocytic cells in the airways of patients with active pulmonary TB.* Chest, 2010. 137(1): p. 122-8.

164. Eruslanov, E.B., et al., *Neutrophil responses to Mycobacterium tuberculosis infection in genetically susceptible and resistant mice.* Infect Immun, 2005. 73(3): p. 1744-53.

165. Chiang, T.Y., et al., *Elevated plasma matrix metalloproteinase-9 protein and its gene polymorphism in patients with community-acquired pneumonia.* Clin Chem Lab Med, 2012. 50(3): p. 449-54.

166. Yang, S.F., et al., *Excessive matrix metalloproteinase-9 in the plasma of community-acquired pneumonia.* Clin Chim Acta, 2005. 352(1-2): p. 209-15.

167. Puljiz, I., et al., *Mycoplasma pneumoniae in adult community-acquired pneumonia increases matrix metalloproteinase-9 serum level and induces its gene expression in peripheral blood mononuclear cells.* Med Sci Monit, 2012. 18(8): p. CR500-505.

168. Hartog, C.M., et al., *Pulmonary matrix metalloproteinase excess in hospital-acquired pneumonia.* Am J Respir Crit Care Med, 2003. 167(4): p. 593-8.

169. Marriott, I. and Y.M. Huet-Hudson, *Sexual dimorphism in innate immune responses to infectious organisms.* Immunol Res, 2006. 34(3): p. 177-92.

170. Schroder, J., et al., *Gender differences in human sepsis.* Arch Surg, 1998. 133(11): p. 1200-5.

171. Smith, J.M., et al., *Effects of menstrual cycle status and gender on human neutrophil phenotype.* Am J Reprod Immunol, 2007. 58(2): p. 111-9.

172. Yamamoto, Y., et al., *Sex differences in host resistance to Mycobacterium marinum infection in mice.* Infect Immun, 1991. 59(11): p. 4089-96.

173. Jimenez-Corona, M.E., et al., *Gender differentials of pulmonary tuberculosis transmission and reactivation in an endemic area.* Thorax, 2006. 61(4): p. 348-53.

174. Coussens, A., et al., *1alpha,25-dihydroxyvitamin D3 inhibits matrix metalloproteinases induced by Mycobacterium tuberculosis infection.* Immunology, 2009. 127(4): p. 539-48.

175. Kumar, S., et al., *Pyridinylimidazole compound SB 203580 inhibits the activity but not the activation of p38 mitogen-activated protein kinase.* Biochem Biophys Res Commun, 1999. 263(3): p. 825-31.

176. Dudley, D.T., et al., *A synthetic inhibitor of the mitogen-activated protein kinase cascade.* Proc Natl Acad Sci U S A, 1995. 92(17): p. 7686-9.

177. Borghaei, R.C., G. Gorski, and M. Javadi, *NF-kappaB and ZBP-89 regulate MMP-3 expression via a polymorphic site in the promoter.* Biochem Biophys Res Commun, 2009. 382(2): p. 269-73.

178. Kishore, N., et al., *A selective IKK-2 inhibitor blocks NF-kappa B-dependent gene expression in interleukin-1 beta-stimulated synovial fibroblasts.* J Biol Chem, 2003. 278(35): p. 32861-71.

179. Lyss, G., et al., *The anti-inflammatory sesquiterpene lactone helenalin inhibits the transcription factor NF-kappaB by directly targeting p65.* J Biol Chem, 1998. 273(50): p. 33508-16.

180. Smith, J., et al., *Evidence for pore formation in host cell membranes by ESX-1-secreted ESAT-6 and its role in Mycobacterium marinum escape from the vacuole.* Infect Immun, 2008. 76(12): p. 5478-87.

181. Hsu, T., et al., *The primary mechanism of attenuation of bacillus Calmette-Guerin is a loss of secreted lytic function required for invasion of lung interstitial tissue.* Proc Natl Acad Sci U S A, 2003. 100(21): p. 12420-5.

182. Koo, I.C., et al., *ESX-1-dependent cytolysis in lysosome secretion and inflammasome activation during mycobacterial infection.* Cell Microbiol, 2008. 10(9): p. 1866-78.

183. Mishra, B.B., et al., *Mycobacterium tuberculosis protein ESAT-6 is a potent activator of the NLRP3/ASC inflammasome.* Cell Microbiol, 2010. 12(8): p. 1046-63.

184. Brown, T., et al., *Associations between Mycobacterium tuberculosis strains and phenotypes.* Emerg Infect Dis, 2010. 16(2): p. 272-80.

185. Brook, M., et al., *Regulation of tumour necrosis factor alpha mRNA stability by the mitogen-activated protein kinase p38 signalling cascade.* FEBS Lett, 2000. 483(1): p. 57-61.

186. Underhill, D.M., et al., *Toll-like receptor-2 mediates mycobacteria-induced proinflammatory signaling in macrophages.* Proc Natl Acad Sci U S A, 1999. 96(25): p. 14459-63.

187. Cui, C., et al., *CRP promotes MMP-10 expression via c-Raf/MEK/ERK and JAK1/ERK pathways in cardiomyocytes.* Cell Signal, 2012. 24(3): p. 810-8.

188. Mahairas, G.G., et al., *Molecular analysis of genetic differences between Mycobacterium bovis BCG and virulent M. bovis.* J Bacteriol, 1996. 178(5): p. 1274-82.

189. Pym, A.S., et al., *Loss of RD1 contributed to the attenuation of the live tuberculosis vaccines Mycobacterium bovis BCG and Mycobacterium microti.* Mol Microbiol, 2002. 46(3): p. 709-17.

190. Gao, L.Y., et al., *A mycobacterial virulence gene cluster extending RD1 is required for cytolysis, bacterial spreading and ESAT-6 secretion.* Mol Microbiol, 2004. 53(6): p. 1677-93.

191. van der Wel, N., et al., *M. tuberculosis and M. leprae translocate from the phagolysosome to the cytosol in myeloid cells.* Cell, 2007. 129(7): p. 1287-98.

192. Sabeh, F., et al., *Tumor cell traffic through the extracellular matrix is controlled by the membrane-anchored collagenase MT1-MMP.* J Cell Biol, 2004. 167(4): p. 769-81.

193. Maertzdorf, J., et al., *Common patterns and disease-related signatures in tuberculosis and sarcoidosis.* Proc Natl Acad Sci U S A, 2012. 109(20): p. 7853-8.

194. Smith-Clerc, J. and B. Hinz, *Immunofluorescence detection of the cytoskeleton and extracellular matrix in tissue and cultured cells.* Methods Mol Biol, 2010. 611: p. 43-57.

195. Hutchins, E.J. and B.G. Szaro, *c-Jun N-terminal kinase phosphorylation of heterogeneous nuclear ribonucleoprotein K regulates vertebrate axon outgrowth via a posttranscriptional mechanism.* J Neurosci, 2013. 33(37): p. 14666-80.

196. Bennett, B.L., et al., *SP600125, an anthrapyrazolone inhibitor of Jun N-terminal kinase.* Proc Natl Acad Sci U S A, 2001. 98(24): p. 13681-6.

197. Shi, C. and E.G. Pamer, *Monocyte recruitment during infection and inflammation.* Nat Rev Immunol, 2011. 11(11): p. 762-74.

198. Ohnishi, K., et al., *Matrix metalloproteinase-mediated extracellular matrix protein degradation in human pulmonary emphysema.* Lab Invest, 1998. 78(9): p. 1077-87.

199. Rogliani, P., et al., *HRCT and histopathological evaluation of fibrosis and tissue destruction in IPF associated with pulmonary emphysema.* Respir Med, 2008. 102(12): p. 1753-61.

200. Buache, E., et al., *Reduced secretion and expression of gelatinase profile in Toxoplasma gondii-infected human monocytic cells.* Biochem Biophys Res Commun, 2007. 359(2): p. 298-303.

201. Seipel, D., et al., *Toxoplasma gondii infection positively modulates the macrophages migratory molecular complex by increasing matrix metalloproteinases, CD44 and alpha v beta 3 integrin.* Vet Parasitol, 2010. 169(3-4): p. 312-9.

202. Takino, T., et al., *Membrane type 1 matrix metalloproteinase regulates collagen-dependent mitogen-activated protein/extracellular signal-related kinase activation and cell migration.* Cancer Res, 2004. 64(3): p. 1044-9.

203. Tanimura, S., et al., *Specific blockade of the ERK pathway inhibits the invasiveness of tumor cells: down-regulation of matrix metalloproteinase-3/-9/-14 and CD44.* Biochem Biophys Res Commun, 2003. 304(4): p. 801-6.

204. Han, Y.P., et al., *TNF-alpha stimulates activation of pro-MMP2 in human skin through NF-(kappa)B mediated induction of MT1-MMP.* J Cell Sci, 2001. 114(Pt 1): p. 131-139.

205. Galvez, B.G., et al., *Membrane type 1-matrix metalloproteinase is regulated by chemokines monocyte-chemoattractant protein-1/ccl2 and interleukin-8/CXCL8 in endothelial cells during angiogenesis.* J Biol Chem, 2005. 280(2): p. 1292-8.

206. Slight, S.R. and S.A. Khader, *Chemokines shape the immune responses to tuberculosis.* Cytokine Growth Factor Rev, 2013. 24(2): p. 105-13.

207. Yana, I. and S.J. Weiss, *Regulation of membrane type-1 matrix metalloproteinase activation by proprotein convertases.* Mol Biol Cell, 2000. 11(7): p. 2387-401.

208. Lee, H., et al., *A critical role for the membrane-type 1 matrix metalloproteinase in collagen phagocytosis.* Mol Biol Cell, 2006. 17(11): p. 4812-26.

209. Antonelli, L.R., et al., *Intranasal Poly-IC treatment exacerbates tuberculosis in mice through the pulmonary recruitment of a pathogen-permissive monocyte/macrophage population.* J Clin Invest, 2010. 120(5): p. 1674-82.

210. Endo, K., et al., *Cleavage of syndecan-1 by membrane type matrix metalloproteinase-1 stimulates cell migration.* J Biol Chem, 2003. 278(42): p. 40764-70.

211. Kajita, M., et al., *Membrane-type 1 matrix metalloproteinase cleaves CD44 and promotes cell migration.* J Cell Biol, 2001. 153(5): p. 893-904.

212. Belkin, A.M., et al., *Matrix-dependent proteolysis of surface transglutaminase by membrane-type metalloproteinase regulates cancer cell adhesion and locomotion.* J Biol Chem, 2001. 276(21): p. 18415-22.

213. Deryugina, E.I., et al., *Processing of integrin alpha(v) subunit by membrane type 1 matrix metalloproteinase stimulates migration of breast carcinoma cells on vitronectin and enhances tyrosine phosphorylation of focal adhesion kinase.* J Biol Chem, 2002. 277(12): p. 9749-56.

214. Uekita, T., et al., *Cytoplasmic tail-dependent internalization of membrane-type 1 matrix metalloproteinase is important for its invasion-promoting activity.* J Cell Biol, 2001. 155(7): p. 1345-56.

215. Williams, K.C. and M.G. Coppolino, *Phosphorylation of membrane type 1-matrix metalloproteinase (MT1-MMP) and its vesicle-associated membrane protein 7 (VAMP7)-dependent trafficking facilitate cell invasion and migration.* J Biol Chem, 2011. 286(50): p. 43405-16.

216. Sounni, N.E., et al., *Timp-2 binding with cellular MT1-MMP stimulates invasion-promoting MEK/ERK signaling in cancer cells.* Int J Cancer, 2010. 126(5): p. 1067-78.

217. Strongin, A.Y., et al., *Mechanism of cell surface activation of 72-kDa type IV collagenase. Isolation of the activated form of the membrane metalloprotease.* J Biol Chem, 1995. 270(10): p. 5331-8.

218. Grahovac, J. and A. Wells, *Matrikine and matricellular regulators of EGF receptor signaling on cancer cell migration and invasion.* Lab Invest, 2014. 94(1): p. 31-40.

219. Koshikawa, N., et al., *Role of cell surface metalloprotease MT1-MMP in epithelial cell migration over laminin-5.* J Cell Biol, 2000. 148(3): p. 615-24.

220. Schenk, S., et al., *Binding to EGF receptor of a laminin-5 EGF-like fragment liberated during MMP-dependent mammary gland involution.* J Cell Biol, 2003. 161(1): p. 197-209.

221. Owen, C.A. and E.J. Campbell, *The cell biology of leukocyte-mediated proteolysis.* J Leukoc Biol, 1999. 65(2): p. 137-50.

222. van't Hoog, A.H., et al., *High prevalence of pulmonary tuberculosis and inadequate case finding in rural western Kenya.* Am J Respir Crit Care Med, 2011. 183(9): p. 1245-53.

223. Steingart, K.R., et al., *Xpert(R) MTB/RIF assay for pulmonary tuberculosis and rifampicin resistance in adults.* Cochrane Database Syst Rev, 2013. 1: p. CD009593.

224. Denkinger, C.M. and M. Pai, *Point-of-care tuberculosis diagnosis: are we there yet?* Lancet Infect Dis, 2012. 12(3): p. 169-70.

225. Steingart, K.R., et al., *Commercial serological tests for the diagnosis of active pulmonary and extrapulmonary tuberculosis: an updated systematic review and meta-analysis.* PLoS Med, 2011. 8(8): p. e1001062.

226. Houghton, R.L., et al., *Use of multiepitope polyproteins in serodiagnosis of active tuberculosis.* Clin Diagn Lab Immunol, 2002. 9(4): p. 883-91.

227. Coussens, L.M., B. Fingleton, and L.M. Matrisian, *Matrix metalloproteinase inhibitors and cancer: trials and tribulations.* Science, 2002. 295(5564): p. 2387-92.

228. Hu, J., et al., *Targeting neutrophil collagenase/matrix metalloproteinase-8 and gelatinase B/matrix metalloproteinase-9 with a peptidomimetic inhibitor protects against endotoxin shock.* Biochem Pharmacol, 2005. 70(4): p. 535-44.

229. Devy, L., et al., *Selective inhibition of matrix metalloproteinase-14 blocks tumor growth, invasion, and angiogenesis.* Cancer Res, 2009. 69(4): p. 1517-26.

230. Suojanen, J., et al., *A novel and selective membrane type-1 matrix metalloproteinase (MT1-MMP) inhibitor reduces cancer cell motility and tumor growth.* Cancer Biol Ther, 2009. 8(24).

231. Barry, S.M., et al., *Determination of bronchoalveolar lavage leukocyte populations by flow cytometry in patients investigated for respiratory disease.* Cytometry, 2002. 50(6): p. 291-7.

232. Conde, M.B., et al., *Comparison of sputum induction with fiberoptic bronchoscopy in the diagnosis of tuberculosis: experience at an acquired immune deficiency syndrome reference center in Rio de Janeiro, Brazil.* Am J Respir Crit Care Med, 2000. 162(6): p. 2238-40.

233. Pizzichini, E., et al., *Measurement of inflammatory indices in induced sputum: effects of selection of sputum to minimize salivary contamination.* Eur Respir J, 1996. 9(6): p. 1174-80.

234. Lay, J.C., D.B. Peden, and N.E. Alexis, *Flow cytometry of sputum: assessing inflammation and immune response elements in the bronchial airways.* Inhal Toxicol, 2011. 23(7): p. 392-406.

235. Williams, B.B., et al., *VANGL2 regulates membrane trafficking of MMP14 to control cell polarity and migration.* J Cell Sci, 2012. 125(Pt 9): p. 2141-7.

236. Whitehead, K.A., R. Langer, and D.G. Anderson, *Knocking down barriers: advances in siRNA delivery.* Nat Rev Drug Discov, 2009. 8(2): p. 129-38.

237. Kurowska-Stolarska, M., et al., *MicroRNA-155 as a proinflammatory regulator in clinical and experimental arthritis.* Proc Natl Acad Sci U S A, 2011. 108(27): p. 11193-8.

8. FUNDING

I would like to thank the Medical Research Council and Scadding-Morriston-Davies Joint Fellowship in Respiratory Medicine for funding this work.

9. ABBREVIATIONS

AAT: alpha 1 antitrypsin

AFB: Acid-fast bacilli

ANOVA: Analysis of variance

AP-1: Activator protein 1

AUC: Area under the curve

β-actin: Beta- actin

BAL: Bronchoalveolar lavage

BALF: Bronchoalveolar lavage fluid

BCG: Bacillus Calmette-Guérin

BEGM®: Bronchial Epithelial Cell Growth Medium

BMI: Body Mass Index

BSA: Bovine serum albumin

CAP: Community acquired pneumonia

CFP-10: Culture filtrate protein 10

CFU: Colony forming unit

CNS: Central nervous system

CoMCont: Conditioned Medium from Control Monocytes

CoMTb: Conditioned Media from *Mtb* infected monocytes

DMSO: Dimethyl Sulfoxide

ECM: Extracellular matrix

EGF: Epidermal growth factor

ELISA: Enzyme-linked Immunosorbent Assay

EMEM: Eagle's Minimal Essential Medium

ERK: Extracellular signal related kinases

ESAT-6: Early secreted antigenic target 6

FCS: Fetal calf serum

FGF: Fibroblast growth factor

FITC: Fluorescein isothiocyanate

G-CSF: Granulocyte colony stimulating factor

GM-CSF: Granulocyte macrophage colony stimulating factor

HBSS: Hanks Balanced Salt Solution

HIV: Human Immunodeficiency Virus

HRP: Horse Radish Peroxidase

IFNα: Interferon alpha

IFNϒ: Interferon gamma

IGRA: IFNϒ release assay

IL-1: Interleukin 1

IL-12: Interleukin 12

IL-1β: Interleukin 1 beta

IL-2: Interleukin 2

IL-6: Interleukin 6

IL-8: Interleukin 8

IQR: Interquartile range

JNK: C-Jun-N-terminal kinases

LAM: Lipoarabinomannan

MAPK: Mitogen activated protein kinase

MCP-1: Monocyte chemoattractant protein 1

MDMs: Monocyte derived macrophages

MDR-TB: Multidrug resistant TB

MFI: Median fluorescence intensity

MIG: Monokine induced by gamma interferon

MIP-1α: Macrophage inflammatory protein 1 alpha

MIP-1β: Macrophage inflammatory protein 1 beta

MMP: Matrix metalloproteinase

MOI: Multiplicity of infection

Mtb: Mycobacterium tuberculosis

MT-MMP: Membrane type matrix metalloproteinase

N/A: Not applicable

NF-κb: Nuclear factor kappa B

NHBE: Normal human bronchial epithelial

PBS: Phosphate buffered saline

PCA: Principal Component Analysis

PD: PD98059

PE: Phycoerythrin

PI: Propidium iodide

PT: Pertussis toxin

RD1: Region of difference 1

ROC: Receiver operating characteristic

RT-PCR: Real time polymerase chain reaction

SB: SB203580

SD: Standard Deviation

siRNA: Small interfering RNA

SP: SP600125

STAT-3: Signal transducer and activator of transcription 3

TB: Tuberculosis

TGF beta: Transforming growth factor beta

TH1: T helper 1

TIMPs: Tissue Inhibitor of Metalloproteinases

TLR-2: Toll-like receptor 2

TNFα: Tumour necrosis factor alpha

TST: Tuberculin skin test

TTP: Time to positivity

VEGF: Vascular endothelial growth factor VEGF

XDR-TB: Extensively drug resistant TB